Charles University
Faculty of Science

Study programme: Biology
Branch of study: Cell and Developmental Biology

Filip Nemčko

Ribosomal protein Rpl22 regulates the splicing of its own transcripts

Ribozomálny proteín Rpl22 reguluje zostrih svojich vlastných transcriptov

Diploma thesis

Supervisor: Mgr. Kateřina Abrhámová, Ph.D.
Prague, 2018

Prohlášení

Prohlašuji, že jsem závěrečnou práci zpracoval samostatně a že jsem uvedl všechny použité informační zdroje a literaturu. Tato práce ani její podstatná část nebyla předložena k získání jiného nebo stejného akademického titulu.

V Praze, 23.04.2018

Filip Nemčko

Acknowledgements

I would like to sincerely thank my supervisor Katka Abrhámová for her support. Without her guidance this work would not have become a reality. I would like to thank all former and present members of the Laboratory of Gene Expression Regulation for providing a pleasant working atmosphere. A special thank goes to Doc. Folk and Jirka Libus for many scientific discussions and advice, Míša Oplová for the construction of reporter plasmids. I would also like to thank Julie Parenteau (University of Sherbrooke) for yeast strains and Wickens Laboratory (University of Wisconsin-Madison) for plasmids and the yeast strain. This work was supported by the grant from the Czech Science Foundation (14- 19002S).

Many thanks to my family and friends for their care and support.

Abstract

Saccharomyces cerevisiae is an intron-poor organism with introns present in only 5% of its genes. The most prominent group of intron-containing genes are ribosomal protein (RP) genes. They are highly expressed and most of them are present as two paralogs. Parenteau et al. described the existence of intron-dependent intergenic regulatory circuits controlling expression ratios of RP paralogs. In this project, we did not confirm the regulation in 6 out of 7 tested regulatory circuits. We validated the regulation between *RPL22* paralogs. We further showed that Rpl22 protein blocks the pre-mRNA splicing of both paralogs, with *RPL22B* paralog being more sensitive. Rpl22 protein binds to the stem-loop of *RPL22B* intron - disruption of the binding domain of Rpl22 proteins leads to loss of interaction. Moreover, the regulation seems to be working the same way in yeast *Kluyveromyces lacti*s, which has only a single *RPL22* copy. Overall, these results lead to better understanding of intergenic regulation, which adjusts the expression ratio between functionally different *RPL22* paralogs.

Key words

introns, ribosomal protein genes, Rpl22, *RPL22* paralogs, pre-mRNA splicing, *Saccharomyces cerevisiae*

Abstrakt

Kvasinka *Saccharomyces cerevisiae* patrí medzi organizmy s malým počtom intrónov, ktoré sa nachádzajú v približne 5% jej génov. Najdôležitejšou skupinou takýchto génov sú gény kódujúce ribozomálne proteíny. Tie sú okrem iného vysoko exprimované a častokrát kódované dvoma paralógmi. Parenteau s kolegami popísala intrón-dependentné intergénové regulačné obvody, ku ktorým dochádza medzi ribozomálnymi paralógmi a ktoré kontrolujú pomery ich expresie. V tejto práci sa nám nepodarilo potvrdiť prítomnosť takýchto obvodov u 6 zo 7 testovaných párov paralógov. Jedinou funkčnou je regulácia u *RPL22* paralógov. Ukázali sme, že Rp22 proteín blokuje pre-mRNA zostrih oboch *RPL22* paralógov, avšak prednostne *RPL22B*. Proteín Rpl22 to sprostredkováva väzbou na sekundárnu štruktúru v *RPL22B* intróne, pričom mutácia RNA-väzbovej domény proteínu Rpl22 vedie k strate väzby. Takáto sekundárna štruktúra a väzba na ňu je zachovaná aj v kvasinke *Kluyveromyces lactis*, ktorá obsahuje iba jednu kópiu *RPL22* génu. Výsledky tejto práce vedú k lepšiemu porozumeniu intergénovej regulácie, ku ktorej dochádza medzi funkčne odlišnými *RPL22* paralógmi.

Kľúčové slová

intróny, gény ribozomálnych proteínov, Rpl22, *RPL22* paralógy, zostrih pre-mRNA, *Saccharomyces cerevisiae*

List of abbreviations

mRNA	messenger RNA
bp	base pairs
RP	ribosomal protein
OD600	optical density at 600 nm
SD	synthetic defined medium
PEG	polyethylene glycol
U	Uracil
L	Leucin
H	Histidine
3-AT	3-aminotriazole
dNTP	deoxynucleotide triphosphate
EDTA	ethylenediaminetetraacetic acid
PNK	polynucleotide kinase
PCR	polymerase chain reaction
qPCR	quantitative PCR
SDS	sodium dodecyl sulfate
SDS-PAGE	denaturing polyacrylamide gel electrophoresis
wt	wild type
Δi	Intron deletion
Δ	deletion
3-H system	three-hybrid system
IRE	iron-responsive element
IRP	iron regulatory protein
C_T	threshold cycle
s.d.	standard deviation
cDNA	complementary DNA
TAE buffer	Tris-acetate-EDTA buffer
TBE buffer	Tris-borate-EDTA buffer
TE buffer	Tris-EDTA buffer
APS	Ammonium Persulfate
ORF	open reading frame

Table of contents

Preface

Hemiascomycetous yeasts including *Saccharomyces cerevisiae* have lost majority of introns, which were present in intron-rich fungal ancestors. It is believed that only introns that provide a selective advantage, survived. Surprisingly, majority of *S.cerevisiae* introns reside in ribosomal protein genes. Therefore, there has been an intention to understand what is the functional role of introns in this specific group of highly expressed genes.

It has been proposed that introns in ribosomal protein genes provide a global regulatory platform to deal with environmental stress. For example, amino acid starvation leads to the inhibition of pre-mRNA splicing in transcripts derived from ribosomal protein genes only. On the other side, there are studies showing the role of introns in fine-tuning expression through autoregulatory feedback loops.

Recently, distinct functional roles of duplicated ribosomal protein genes emerged. There are 78 ribosomal proteins in the ribosome, however they are encoded by 137 genes. It was already shown in different model organisms that different paralogs/isoforms of ribosomal proteins have distinct functions, both inside ribosomes (called specialized ribosomes) and outside of them (extra-ribosomal functions). There is an indication that introns might have roles in regulating the expression of these functionally different ribosomal protein paralogs in yeast.

Therefore, studying roles of introns in the expression of duplicated ribosomal protein genes might help us to understand why cells maintained and how they utilize the regulatory potential encoded with introns.

1 Literature review

1.1 Introns and pre-mRNA splicing

Although our view of genes is constantly changing (Gerstein et al. 2007), discoveries made in 1970s were shocking and unexpected - most eukaryotic genes are discontinuous with stretches of non-coding sequences (called *introns*) interrupting coding regions (called *exons*) (Berget et al. 1977, Chow et al. 1977, Gilbert 1978). Introns must be precisely removed and exons ligated together to form messenger RNA (mRNA) before being translated. This process, called pre-mRNA splicing, is catalyzed by the spliceosome, a large ribonucleoprotein machinery composed of five small nuclear RNAs and more than 100 proteins (reviewed in Will and Luhrmann 2011).

Presence of introns (note that the thesis is focus on spliceosomal introns only) seems to be a universal feature of all eukaryotic organisms (Collins and Penny 2005). Even though various models of intron origin have been proposed, there is a general agreement that an eukaryotic ancestor had already been intron-rich and since then have gained or lost introns independently in different organisms (e.g. reviewed in Rogozin et al. 2012). While introns have been found in all studied eukaryotes, their organisation shows divergence across species. The only common features of introns seem to be conserved 5' splice site, branch point site and 3' splice site, which are involved in intron recognition and pre-mRNA splicing (reviewed in Will and Luhrmann 2011).

Length of introns varies markedly. While the ciliate *Stentor coeruleus* has tiny introns of the median size 15 bp (base pairs), the axolotl *Ambystoma mexicanum* has gigantic introns of the median size 22 759 bp (Slabodnick et al. 2017, Nowoshilow et al. 2018). In contrast, the median size of introns in the human genome is 1 750 bp (Lander et al. 2001).

Number of introns per genome also varies dramatically, from only 27 introns in the algae *Cyanidioschyzon merolae* (Matsuzaki et al. 2004) to more than 200 000 introns in the human genome (Lander et al. 2001). Interestingly, all known intron-poor organisms are unicellular with a bias in the position of introns more towards the 5' end of their genes (Mourier 2003, Irimia and Roy 2008, Irimia et al. 2007). It is believed that this is because small unicellular organisms have a large effective population size and therefore can easily (compared to organisms with smaller effective populations) eliminate all deleterious introns inherited from their ancestors (Lynch 2002). Introns have been eliminated most probably via homologous recombination with reversely transcribed mRNA molecules, which could explain the bias in the position of maintained introns on the 5' ends of genes (Fink 1987, Mourier 2003).

1.2 Introns of *Saccharomyces cerevisiae*

Compared to higher eukaryotes, which genes are split by many introns and often undergo alternative splicing with multiple splice variants, yeast *S.cerevisiae* contains predominantly one intron per gene with rare alternative splicing events (Schreiber et al. 2015). In general, *S.cerevisiae* is an intron-poor organism with introns present in only 5% of its genes. However, fungal ancestors had a high density of introns in their genomes (Stajich et al. 2007). It implies that all deleterious introns were erased and only the ones, which provide a selective advantage, were maintained in today's *S.cerevisiae* genome.

Overall, there are 287 intron-containing genes annotated in the yeast genome - 278 genes with a single intron and 9 genes with two introns (Spingola et al. 1999, Neuveglise et al. 2011). Note that deep sequencing experiments often find more splicing events, however, they are often supported by a small number of reads (Aslanzadeh et al. 2018).

Introns are not randomly distributed through the genome, but rather reside in a specific group of genes. They are present in highly expressed genes - it was estimated that while representing only 5% of genes in the genome, they produce around 26% of cellular mRNA (Ares et al. 1999). The most prominent group of intron-containing genes are genes involved in translation (Gene Ontology ID GO:0006412). They represent 37.8% of all intron-containing genes in yeast (measurement based on the sacCer3 genome assembly and GO::TermFinder, Boyle et al. 2004). Out of them, ribosomal protein (RP) genes are the most distinguished class with 104 introns present in 101 genes (Parenteau et al. 2011, Spingola et al. 1999). Intron-containing RP genes produce around 24% of cellular mRNA in yeast and 90% of mRNA derived from intron-containing genes (Ares et al. 1999).

Interestingly, introns in RP genes tend to be longer (median size of 408 bp) than other, non-RP genes (median size of 141 bp). Therefore the distribution of *S.cerevisiae* intron lengths is bimodal (Figure 1), the phenomenon shown already before (Neuvéglise et al. 2011, Spingola et al. 1999). This and many other observations are the reason why we discuss the distinct group of RP-gene introns separately.

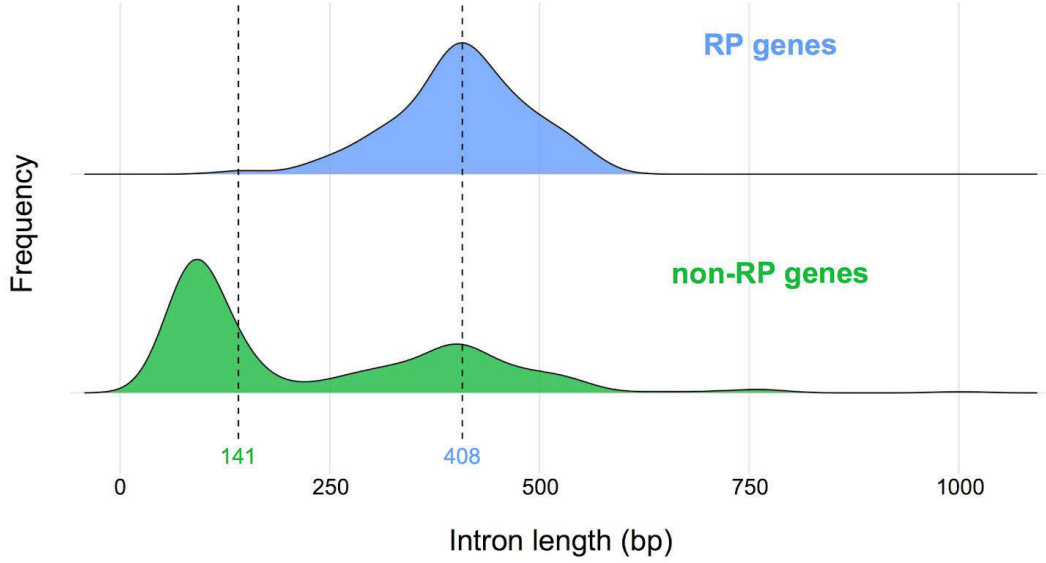

[Figure 1] Distribution of *S.cerevisiae* intron lengths is bimodal. Shown is the frequency of lengths in base pairs for ribosomal protein genes (RP genes) and all other intron-containing genes, marked as non-RP genes. The distribution was made based on the sacCer3 genome assembly.

1.2.1 Introns of non-RP genes

There are 186 intron-containing non-RP genes. They reside in genes of various categories, the most enriched gene ontology term is the meiotic cell cycle (GO:0051321) with 14.1% of intron-containing non-RP genes (measurement based on the sacCer3 genome assembly and GO::TermFinder, Boyle et al. 2004).

Juneau with colleagues showed that intron-containing genes in yeast produce on average 3.9 and 3.3-fold more RNA and protein, respectively, than genes without introns. This is however not true for ribosomal protein genes, as they have to achieve the equimolar amount of ribosomal proteins irrespective of introns presence (Juneau et al. 2006; Zeevi et al. 2011, Yu 2002). Early studies of few intron-containing genes supported the hypothesis that introns positively influence the expression of genes. Using run-on experiments, Furger with colleagues demonstrated that the transcription of *DYN2* and *ASC1* genes is diminished upon deletion of their introns. Interestingly, *DYN2* gene contains two introns and only the deletion of first, promoter-proximal intron leads to its reduced transcription (Furger et al. 2002). Similarly, deletion of introns in *GLC7*, *ACT1* and *PRE3* led to the decrease in their mRNA expression (Juneau et al. 2006).

Despite altering mRNA levels, the manipulation with *ACT1* and *PRE3* genes did not affect growth in rich media. However, the selective advantage of *ACT1* intron appeared when exposed to latrunculin − the strain with *ACT1* intron deletion exhibit an increased sensitivity compared to *wild type* strain (Juneau et al. 2006, Ng et al. 1985). Similarly, expanded experiments with set of 87 non-ribosomal protein genes with intron deletions revealed that absence of introns in only 3 genes influenced the cell fitness under normal conditions. However, deletion of introns in 48 out of 87 genes affected the growth under other than normal conditions, e.g. in the presence of different carbon sources or drugs altering the metabolism of cells (Parenteau et al. 2008). Phenotypic profiling of the yeast with synthetic chromosome II lacking (among other elements) introns in 22 non-RP

genes also shows no apparent defects compared to *wild type* cells under normal conditions (Shen et al. 2017).

All these experiments imply that while not being important under normal conditions, introns of non-ribosomal protein genes provide benefit under stress. Juneau with colleagues proposed (based on experiments with 5 genes, see above) that this is achieved by a slightly higher expression of intron-containing genes under all conditions − the phenotype dispensable under normal conditions, but essential to deal with challenging situations (Juneau et al. 2006).

Furthermore, introns have crucial role in the meiotic regulation. It was shown that many meiosis-specific intronic genes are already expressed in vegetative cells, however, their pre-mRNA splicing is inefficient to start the meiotic program. They become spliced out efficiently upon induction of sporulation (Engebrecht et al. 1991, Davis et al. 2000, Juneau et al. 2007).

1.3 Ribosomal protein genes

There are 79 ribosomal proteins encoded by 137 genes in the yeast *S.cerevisiae*. While 19 of them are encoded by a single gene, 59 ribosomal proteins are expressed from a pair of ribosomal protein genes (aka two paralogs). This is most likely a result of the whole-genome duplication of *S.cerevisiae* ancestor (Planta and Mager 1998; Wolfe and Shields 1997). Interestingly, most of the duplicated genes in yeast were lost and only 551 pairs were retained with RP genes being the most prominent group (Byrne and Wolfe 2005; Evangelisti and Conant 2010).

Ribosomal proteins encoded by duplicated genes were not just retained in the genome, but there is also a selection pressure to maintain their high sequence similarity - 35 out of 59 pairs differ in maximally 1 amino acid, the phenotype not observed for duplicated non-RP genes (Evangelisti and Conant 2010; Steffen et al. 2012). Figure 2A shows the difference in amino acid composition between all RP paralogs.

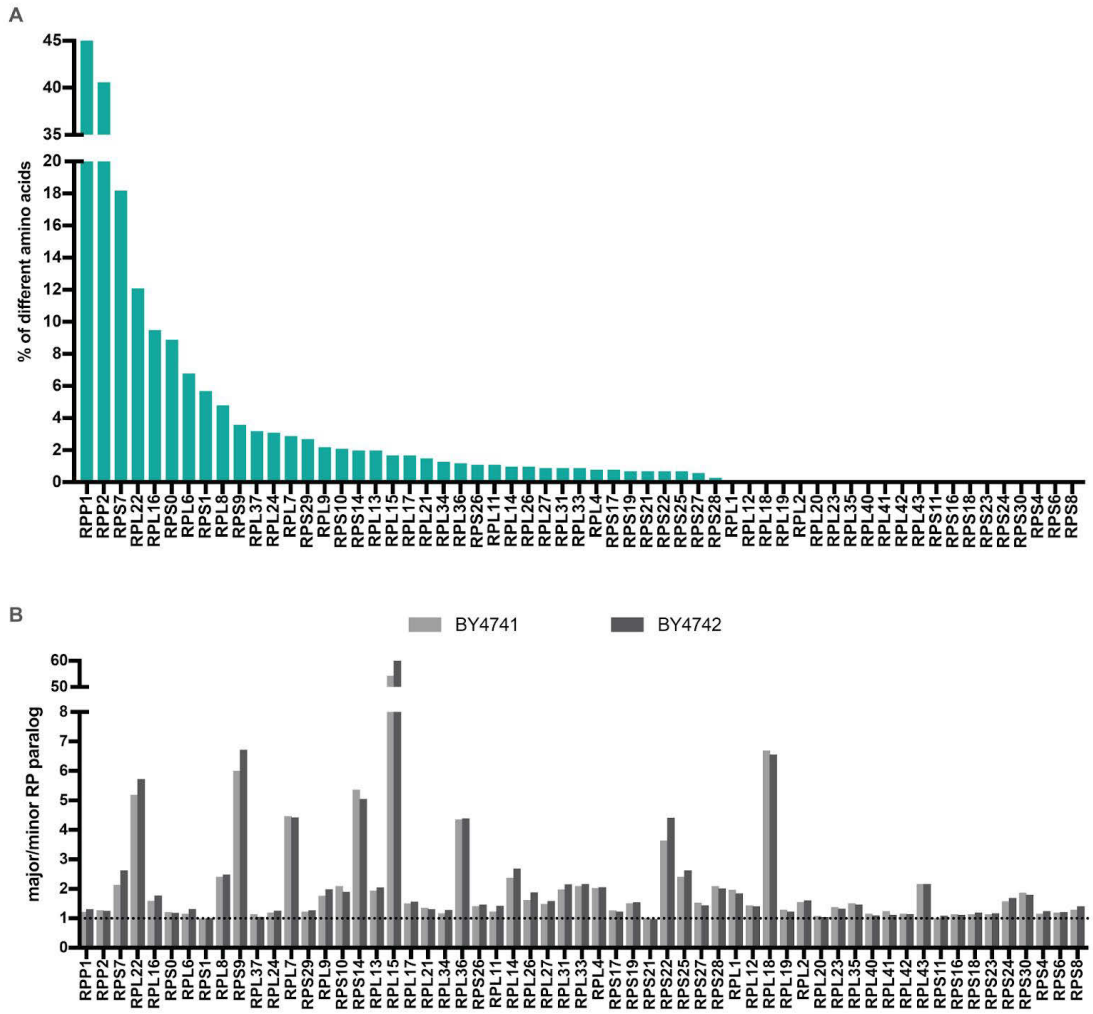

[Figure 2] Paralogous ribosomal proteins are often similar and expressed asymmetrically. (A) Shown is the percentage of different amino acids for every pair of RP genes. In the case of different size of proteins, the length of longer paralog was chosen. Based on data from (Steffen et al. 2012). (B) The expression ratio between major and minor RP paralogs shown for two *wild type* strains, BY4741 and BY4742. The data are extracted from our RNA-seq experiment with 2 biological replicates per strain (Abrhámová et al. 2018).

While the coding sequence is very similar in many RP paralogs, this is not true for the regulatory elements - promoters, untranslated regions as well as introns are dissimilar in RP paralogs (Evangelisti and Conant 2010; Wapinski et al. 2010). This is reflected in the expression of duplicated RP gene - many paralogs are expressed asymmetrically (Parenteau et al. 2011; Parenteau et al. 2015). Based on our RNA-seq data for *wild type* strains, there are 32 pairs of RP genes with one paralog expressed at least 1.5 times more than the other one (Abrhámová et al.

2018). Expression ratios between major and minor paralogs for all pairs of RP genes is shown in the Figure 2B. The differential expression of RP paralogs allows for their sub-functionalization, as discussed later.

1.3.1 Intron-containing RP genes

Approximately 74% of yeast ribosomal protein genes are intron-containing, making them the most abundant class of intronic genes (see above). While there are only 7 out of 19 single-copy RP genes with introns, 94 out of 118 RP paralogs are intronic. Therefore, introns are preferentially present in duplicated RP genes (Parenteau et al. 2011, Spingola et al. 1999). Besides being on average longer (see above), introns of RP genes seem to be lost less frequently compared to non-RP introns, as based on the evolutionary analyses of introns in species of the Saccharomycetaceae family (Plocik and Guthrie 2012, Hooks et al. 2014).

Whole-genome studies of pre-mRNA splicing revealed that the splicing of RP genes is different compared to other, non-RP genes. In general, they are spliced much more efficiently and compared to non-RP transcripts also preferentially during their transcription, i.e. cotranscriptionally (Pleiss et al. 2007; Wallace and Beggs 2017). This notion is also supported but the fact that despite being highly expressed, their pre-mRNA levels are almost undetectable (Pleiss et al. 2007) and they have a high density of U1 small nuclear ribonucleoproteins bound to their transcripts associated with chromatin (Harlen et al. 2016, Tardiff et al. 2006).

Transcripts of ribosomal protein genes also react differently to the presence of mutations in spliceosomal components (Pleiss et al. 2007). Amino acid starvation leads to the specific inhibition of pre-mRNA splicing of RP-genes without noticeable effects on the splicing of other transcripts (Pleiss et al. 2007, Bergkessel et al. 2011). Despite not knowing what are the specific properties of RP transcripts/introns, which can be distinguished by the spliceosomal machinery, it is generally believed that introns of RP genes are dissimilar to the introns of other, non-RP transcripts, as shown above.

Parenteau with colleagues systematically studied introns in all 101 intronic RP genes. They showed that deletion of none of RP introns affected cell growth in rich media, the findings similar to non-RP genes, as discussed above (Parenteau et al. 2008; Parenteau et al. 2011). Strikingly, the deletion of any RP introns did not affect the growth in neither alternative carbon sources nor different cultivation temperatures. However, when tested the fitness of mutants by co-cultivation with *wild type* cells, 25% of intron deletions led to the increase in cell fitness, while the fitness decreased in 17% of intron deletants. Not just affecting fitness of cells, deletion of introns in 84% of intron-containing RP genes led to the deregulation of respective genes, suggesting the presence of intron-dependent intragenic regulation. In 43% of cases, the deletion of intron led to an upregulation of host genes, i.e. presence of introns inhibited their expression. In contrast, deletion of introns in 41% of RP genes resulted in their downregulation, arguing that their introns could enhance the expression of host genes (Parenteau et al. 2011).

More interestingly, Parenteau et al. looked closely on paralogous RP genes and measured the impact of intron removal on the expression of not only the host gene, but also its paralog *in trans*. They found intron-dependent intergenic regulatory circuits - removal of introns affected the expression of paralogs as well. Overall, they proposed that these intron-dependent intergenic regulation loops adjust the expression ratios between RP paralogs in 36 pairs, the phenomenon potentially explaining asymmetrical expression of at least some RP paralogs (Parenteau et al. 2011). Unexpectedly though, deletion of introns in host RP genes led to the compensatory adjustment of expression of paralogs *in trans* only in 15 cases, while it did not compensate the amounts of respective RP transcripts (the sum of mRNA levels of both paralogs was higher or lower than in *wild type*) in 56 cases. Out of all 56 non-compensatory changes, 41 changes in the expression of paralogs *in trans* were even simultaneous, i.e. both the host gene and the paralog *in trans* were up/down-regulated (Parenteau et al. 2011). This suggests that the described intergenic circuits might not be simple negative feedback loops, but rather sophisticated RP-specific ways how to maintain the expression patterns of ribosomal protein paralogs.

Deletion of introns in ribosomal protein genes affects the expression of paralogs and leads to distinct phenotypes. Authors demonstrated that removal of introns has impact on the ribosome biogenesis with paralog-specific defects, i.e. accumulation of different ribosomal RNA processing intermediates. This phenomenon cannot be explained by a simple downregulation of particular ribosomal proteins. For example, deletion of intron in *RPS29A* inhibits the processing of 20S pre-rRNA, while removing the *RPS29B* intron leads to the accumulation of 27S pre-rRNA. However, deletion of the whole *RPS29B* gene does not lead to any defects (Parenteau et al. 2011).

Another example of functional roles of these regulatory circuits is the response to stress. Parenteau with colleagues showed that exposing cells to different conditions modulates the expression ratio between RP paralogs, phenotype relying upon their introns. E.g., while osmotic stress favours the expression of *RPS9A*, the exposure to the non specific inhibitor of kinases, staurosporine, leads to the preferential expression of *RPS9B* paralog (Parenteau et al. 2011). Note that these are relative changes compared to *wild type* and there are still more transcripts of *RPS9A* paralog, which represents ~85% of *RPS9* mRNA in *wild type* yeast (Parenteau et al. 2011).

Overall, it is believed that introns provide a platform to set the expression patterns of functionally different ribosomal protein paralogs in yeast. The production of different ribosomal protein isoforms/paralogs leads to ribosomes with a specific composition and therefore function. Indeed, there are several recent publications showing this phenomenon, called specialized ribosomes, in different model organisms (reviewed in Shi and Barna 2015). Therefore, scientists try to explore molecular mechanisms behind these regulatory circuits, as already shown for the regulation between *RPS9* paralogs (Plocik and Guthrie 2012; Petibon et al. 2016), *RPS14* paralogs (Li et al. 1995; Fewell and Woolford 1999) and *RPL22* paralogs (this study and Abrhámová et al. 2018; Gabunilas and Chanfreau 2016). On the other side, there are also studies exploring the distinct functions of ribosomal protein paralogs, as shown for the Rpl22 paralogs below.

1.4 Ribosomal protein Rpl22

Rpl22 is an eukaryotic-specific ribosomal protein of large ribosomal subunit (Toczyski et al. 1994, Ban et al. 2014). Based on the solved yeast ribosome structure, it is an RNA-binding protein interacting with the helices 57 and 59 of 25S rRNA. It is believed that this interaction is based on the shape and charge complementarities with the rRNA, rather than sequence specificity, see the Discussion section for more details (Ben-Shem et al. 2010; Klinge et al. 2011). Rpl22 is in the proximity of polypeptide exit tunnel of ribosomes, being the only eukaryotic-specific element, which could potentially affect or interact with the nascent chain of translated proteins (Ben-Shem et al. 2010; Klinge et al. 2011).

1.4.1 Roles of Rpl22 protein in yeast

Rpl22 protein is encoded by two paralogs, *RPL22A* and *RPL22B*. These paralogs are expressed asymmetrically with *RPL22A* producing ca 5.5-times more mRNA than *RPL22B* (Abrhámová et al. 2018). They differ in 22 out of 122 amino acids, making them the third most divergent ribosomal protein paralogs in yeast (Steffen et al. 2012). Rpl22 is a non-essential protein, however its deletion leads to growth defects, as shown in the Results section and (Costanzo et al. 2010).

While not being essential, Rpl22 protein is required for the meiotic induction (Kim and Strich 2016). Briefly, deprivation of fermentable carbon sources and nitrogen leads to the expression of *IME1*, the master regulator which induces the transcriptional program leading to meiosis (Kassir et al. 1988). Kim and Strich showed, that the presence of Rpl22 protein in ribosomes is required for the efficient translation of *IME1* (but not for translation in general). This Rpl22-dependent translational control most probably targets the 5’ untranslated region of *IME1* (Kim and Strich 2016). Despite showing this phenotype only with a “harsh” Rpl22 deletion, we might speculate that cells could utilize this phenomenon and regulate the meiotic induction by altering Rpl22 in ribosomes translating *IME1* transcripts.

There are studies showing the specific roles of *RPL22* paralogs. For example, it was shown that deletion of paralog *RPL22A*, but not *RPL22B*, leads to the enhanced tolerance to acetic acid (An et al. 2014). Deletion of *RPL22A*, but not *RPL22B*, significantly (>50%) increases replicative lifespan, making it one of the top single-gene mutants with the highest longevity reported in yeast (Steffen et al. 2008, Steffen et al. 2012, Beaupere et al. 2017). We might speculate that the fraction of ribosomes containing Rpl22B paralog is increased, leading to specific changes in translation.

Chan with colleagues found that exposure to oxidative stress (hydrogen peroxide) induces the Trm4 methyltransferase, which methylates the cytosine present in the wobble position of $tRNA^{Leu(\underline{C}AA)}$, changing its specificity. Authors showed that the methylation leads to preferential interaction with UUG codon. It is believed that preferential translation of transcripts with UUG codons might lead to an adaptation to oxidative stress. Interestingly, while only 34% of Leucine codons have UUG sequence in *RPL22B* paralog, all Leucine codons are coded by UUG in *RPL22A* paralog. Indeed, exposure to oxidative stress leads to the preferential translation of *RPL22A* transcripts, while the mRNA levels of both paralogs remain unchanged. Loss of Rpl22A, but not Rpl22B paralog, leads to increased sensitivity to oxidative stress. This implies that *RPL22* paralogs have specialized function in dealing with stress (Chan et al. 2012).

There is a study coupling Swi/Snf chromatin remodelling complex to splicing of meiotic genes. Authors analyzed the transcriptome of cells lacking the core ATPase of complex, Snf2. They showed that the deletion of Snf2 leads to downregulation of RP genes. While not being focus of the study (even not being mentioned), their data shows that *RPL22B* splicing efficiency is improved ~3.66-times upon Snf2 deletion, making it the top improved splicing in the study. The splicing efficiency of *RPL22A* was not changed (Venkataramanan et al. 2017). This might be partially explained by the fact that RP genes were downregulated and thus Rpl22A could not block the splicing of *RPL22B*, as shown in the Results. However, it remain unclear why the splicing efficiency of other *RP* paralogs such

as *RPS14B* or *RPS9A*, for which we know that their splicing is blocked by the expression of *RPS14A* and *RPS9B* paralogs, respectively, did not change (Venkataramanan et al. 2017; Petibon et al. 2016; Li et al. 1995).

Ash1 protein is exclusively localized to daughter cells in yeast. Its role is to suppress the mating-type switching of newly emerged cells (Sil and Herskowitz 1996). It has been revealed that the *ASH1* mRNA is specifically targeted to the bud tip of daughter cell before split of cells. Surprisingly, the localization of *ASH1* is mediated by ribosomes containing specific set of RP paralogs. Presence of Rpl7A, Rps18B, Rpl12B and Rpl22A in ribosomes translating *ASH1* mRNA is necessary for its proper localization. Authors showed that deletion of *RPL22A* abolish the targeting. To confirm that it is not because of the lack of Rpl22, authors overexpressed the *RPL22B* and found that the localization of *ASH1* does require the Rpl22A paralog (Komili et al. 2007).

All these experiments suggest that Rpl22A and Rpl22B proteins, despite sharing 82% of their amino acid sequence, have distinct function in cells. Interestingly, they do differ in their nucleic acid sequence. As discussed above, they employ different codons for Leucine (Chan et al. 2012). Lin with colleagues attempted to train the algorithm (supervised machine learning approach), which would be able to discriminate between ribosomal protein genes and other, non-RP genes based on their amino acid composition and codon usage bias. While the algorithm was able to accurately discriminate between these two classes, it always failed with the categorization of *RPL22B* paralog. The codon adaptation index (e.g. value 1 means no codon usage bias) of RP genes is usually high, ranging between 0.6 - 0.9. While to codon adaptation index of *RPL22A* is 0.86, it is only 0.29 for *RPL22B*. This makes *RPL22B* the most dissimilar from all other ribosomal proteins (Lin 2002).

1.4.2 Roles of Rpl22 protein in other organisms

Rpl22 protein is nonessential in mouse, Rpl22-deficient mice do not differ in growth rate or size from *wild type*. However, they do exhibit defects in development of alpha-beta (but not gamma-delta) T lymphocytes (Anderson et al. 2007). Rpl22 deficiency also leads to the reduction of peripheral B lymphocytes due to the defects in early B cell development (O'Leary et al. 2013, Fahl et al. 2014). Both defects can be explained by the p53-dependent induction of apoptosis in precursors of affected cells (Anderson et al. 2007, Fahl et al. 2014). How Rpl22 deletion can lead to the apoptosis in specific cells remains unclear. Rashkovan with colleagues showed that Rpl22 protein negatively regulates the translation of p53 mRNA. They propose that Rpl22 does it by binding to p53 transcripts (Rashkovan et al. 2014). On the other hand, Solanki with colleagues proposed that it is the dysregulation of endoplasmic reticulum stress signalling induced by Rpl22 loss, which lead to the upregulation of p53. Their experiments suggest that stress signalling is unable to attenuate the protein synthesis in the absence of Rpl22, therefore extensive production of unfolded proteins leads to the induction of p53 (Solanki et al. 2016).

O'Leary with colleagues found that upon deletion of Rpl22, Rpl22-like1 gene was induced ~3-fold in different tissues compared to *wild type* mice. Interestingly, while having very limited expression in most of the tissues, Rpl22-like1 is highly expressed in pancreas of *wild type* mice too. Rpl22-like1 shares 73% of amino acid sequence with mouse Rpl22 protein and is conserved from human to zebrafish. Authors found that in most of the tissues, Rpl22 influences the stability of Rpl22-like1 mRNA by direct binding to the hairpin structure present in the exon 2 of Rpl22-like1 mRNA. The hairpin structure alone is sufficient for the regulation, since Rpl22 can inhibit the expression of GFP fused with the hairpin. Overall, authors found that similarly to yeast, mice and zebrafish have two Rpl22 homologs. The deletion of Rpl22 leads to the compensatory overexpression of its homolog Rpl22-like1, therefore making Rpl22-deficient mice phenotypically (almost) comparable to *wild type* mice. Authors also showed that knock-down of

Rpl22-like1 in Rpl22-deficient cells leads to the growth defects (O'Leary et al. 2013). Moreover, Rpl22-like1 deficiency is embryonically lethal in mice (Zhang et al. 2017).

Discovery that Rpl22 has the homolog, Rpl22-like1, prompted authors of the study focusing on effects of Rpl22 deficiency in mice to examine the Rpl22-like1 deletion. They employed zebrafish as a model organism. Interestingly, while Rpl22 deficiency led to the blockage of alpha-beta T cells developmental as in mice, the Rpl22-like1 loss diminished the development of both alpha-beta and gamma-delta T cells. Overall, the two homologs influence different progenitors of T cells. Authors showed that both Rpl22 and Rpl22-like1 proteins bind the mRNA of transcription factor Smad1 and repress and activate its translation, respectively. The distinct roles of Rpl22 and Rpl22-like1 in regulation of Smad1 expression lead to different effects on haematopoiesis (Zhang et al. 2013). Later on, Zhang with colleagues showed that the knock-down of Rpl22-like1 additionally leads to defects in anterior-posterior extension during zebrafish gastrulation, the phenotype being a consequence of affected TGF-β/Smad signalling pathway. Indeed, they confirmed that both paralogs directly bind to the exon 8 of Smad2 mRNA. While binding of Rpl22 leads to the skipping of exon 9 during the pre-mRNA splicing, binding of Rpl22-like1 leads to its inclusion. This phenotype is conserved from zebrafish to mice (Zhang et al. 2017).

Besides having role in haematopoiesis, it was e.g. shown that Rpl22 associates with the human telomerase RNA. Its role in telomerase remains unknown (Le et al. 2000). Drosophila Rpl22 interacts with the histone H1 in condensed chromatin and their association is essential for the transcriptional repression (Ni et al. 2006). Additionally, human Rpl22 directly binds to the region of hepatitis C virus RNA genome and stimulates its internal ribosome entry site-mediated translation (Wood et al. 2001). Most interestingly, human Rpl22 binds to the small RNA produced by Epstein-Barr virus, EBER-1, in B cells (Toczyski and Steitz 1991; Toczyski et al. 1994). It was shown that the role of EBER-1 RNA is to sequestrate Rpl22 by binding to up to three Rpl22 molecules and to relocalize them from nucleoli to

nucleoplasm (Fok et al. 2006; Toczyski et al. 1994). The sequestration of Rpl22 is critical for tumorigenic potential of Epstein-Barr virus (Houmani et al. 2009).

Overall, all these experiments demonstrate that Rpl22 paralogs have distinct functions, the phenomenon conserved in different organisms. Knowing the molecular mechanisms of their regulation might help us to understand how cells utilize their different roles. This project aims to bring an insight into regulation between *RPL22* paralogs in yeast.

2 Thesis aims and objectives

The general objective of this project is to investigate a role of introns in the regulation of duplicated ribosomal protein (RP) genes. The project aims to extend work of Parenteau and colleagues (Parenteau et al., 2011) and to bring an additional insight into described intergenic regulatory circuits, which define the expression ratio of RP paralogs.

We firstly intended to identify candidate paralogous RP genes with intron-dependent intergenic regulation. Identification of *RPL22* pair led as to more specific aims, such as addressing the following questions: Which step of Rpl22 expression is regulated? What is the molecular mechanism of regulation? Which part of the *RPL22B* intron is responsible for the regulation? Is the regulation evolutionarily conserved?

3 Material & Methods

3.1 Microbiological techniques

3.1.1 Strains used in this study

Tables 1 and 2 contain description of all bacterial and yeast strains used in this study, respectively.

[Table 1] List of used *Escherichia coli* strains

Name	Description	Source
DH5α	F- Φ80lacZΔM15 Δ(lacZYA-argF) U169 recA1 endA1 hsdR17 (rk-, mk+) phoAsupE44 λ-thi-1 gyrA96 relA1	Stratagene

[Table 2] List of used *Saccharomyces cerevisiae* strains

Name	Description	Source
JPY166B2	*MATa/α ura3Δ0/ura3Δ0 lys2Δ0/lys2Δ0 leu2Δ0/leu2Δ0 his3Δ200/HIS3 ade2Δ::hisG/ADE2 rpl16aΔi/RPL16A rpl16bΔi/RPL16B* (pRS425-SCE)	(Parenteau et al. 2011)
JPY156B8	*MATa/α ura3Δ0/ura3Δ0 lys2Δ0/lys2Δ0 leu2Δ0/leu2Δ0 his3Δ200/HIS3 ade2Δ::hisG/ADE2 rpl22aΔi/RPL22A rpl22bΔi/RPL22B* (pRS425-SCE)	(Parenteau et al. 2011)
JPY156A9	*MATa/α ura3Δ0/ura3Δ0 lys2Δ0/lys2Δ0 leu2Δ0/leu2Δ0 his3Δ200/HIS3 ade2Δ::hisG/ADE2 rpl37aΔi /RPL37A rpl37bΔi/RPL37B* (pRS425-SCE)	(Parenteau et al. 2011)
JPY165I5	*MATa/α ura3Δ0/ura3Δ0 lys2Δ0/lys2Δ0 leu2Δ0/leu2Δ0 his3Δ200/HIS3 ade2Δ::hisG/ADE2 rps0aΔi/RPS0A rps0bΔi/RPS0B* (pRS425-SCE)	(Parenteau et al. 2011)
JPY156A5	*MATa/α ura3Δ0/ura3Δ0 lys2Δ0/lys2Δ0 leu2Δ0/leu2Δ0 his3Δ200/HIS3 ade2Δ::hisG/ADE2 rps18aΔi/RPS18A rps18bΔi/RPS18B* (pRS425-SCE)	(Parenteau et al. 2011)

JPY156C3	*MATa/α ura3Δ0/ura3Δ0 lys2Δ0/lys2Δ0 leu2Δ0/leu2Δ0 his3Δ200/HIS3 ade2Δ::hisG/ADE2 rpl2aΔi/RPL2A rpl2bΔi/RPL2B* (pRS425-SCE)	(Parenteau et al. 2011)
JPY166B7	*MATa/α ura3Δ0/ura3Δ0 lys2Δ0/lys2Δ0 leu2Δ0/leu2Δ0 his3Δ200/HIS3 ade2Δ::hisG/ADE2 rpl17aΔi/RPL17A rpl17bΔi/RPL17B* (pRS425-SCE)	(Parenteau et al. 2011)
BY4741	*MATa his3Δ1 leu2Δ0 met15Δ0 ura3Δ0*	EUROSCARF
BY4742	*MATα his3Δ1 leu2Δ0 lys2Δ0 ura3Δ0*	EUROSCARF
KAY60	*MATa his3Δ1 leu2Δ0 met15Δ0 ura3Δ0 RPL22a*Δi	(Abrhámová et al. 2018)
KAY61	*MATα his3Δ1 leu2Δ0 lys2Δ0 ura3Δ0 RPL22a*Δi	(Abrhámová et al. 2018)
KAY67	*MATα his3Δ1 leu2Δ0 lys2Δ0 ura3Δ0 RPL22b*Δi	(Abrhámová et al. 2018)
KAY139	*MATa his3Δ1 leu2Δ0 met15Δ0 ura3Δ0 RPL22a*Δi *RPL22b*Δi	(Abrhámová et al. 2018)
KAY140	*MATα his3Δ1 leu2Δ0 lys2Δ0 ura3Δ0 RPL22a*Δi *RPL22b*Δi	(Abrhámová et al. 2018)
rpl22aΔ	*MATa his3Δ1 leu2Δ0 met15Δ0 ura3Δ0 rpl22a::kanMX4*	EUROSCARF
rpl22bΔ	*MATa his3Δ1 leu2Δ0 met15Δ0 ura3Δ0 rpl22bΔ::kanMX4*	EUROSCARF
FNY33	*MATa his3Δ1 leu2Δ0 met15Δ0 ura3Δ0 rpl22aΔ RPL22b*Δi	this study
FNY34	*MATa his3Δ1 leu2Δ0 met15Δ0 ura3Δ0 RPL22a*Δi *rpl22bΔ*	this study
FNY35	*MATα his3Δ1 leu2Δ0 met15Δ0 ura3Δ0 rpl22aΔ rpl22bΔ*	this study
YBZ1	*MATa ura3-52 leu2-3, 112 his3-200 trp1-1 ade2 LYS2::(LexA$_{op}$)-HIS3, ura3::(lexA-op)-lacZ LexA-MS2 coat (N55K*	(Hook et al. 2005)

3.1.2 S.cerevisiae growth and maintenance

Using aseptic technique, a small quantity of a frozen glycerol stock was plated on an appropriate agar plate and stock quickly returned to -80°C. Plates were incubated for 1-3 days at 30°C. Grown yeast mass was used in further experiments or to inoculate pre-culture (usually 5 ml of liquid media in 50 ml Erlenmeyer flask). After about 12 hours of growing at 30°C with shaking (180 rpm, Thermo Scientific 4520 Orbital Shaker or Ecotron, Infors HT), the optical density (OD600) of pre-culture was measured with Spekol 20 (Carl Zeiss) or CO8000 Cell Density Meter* (WPA Biowave) against medium as blank (used dilutions to stay in the linear range of spectrophotometer). Adequate volume of pre-culture was used to inoculate a main culture (usually initial OD600 of 0.075 in 10 ml of liquid media). Main culture was grown for at least three generations to mid-exponential phase of growth (usually OD600 of 0.6), harvested and used in subsequent experiments.

**Note that CO8000 Cell Density Meter (WPA Biowave) shows 3-times higher values than Spekol 20 (Carl Zeiss) or Varioskan Flash reader. Therefore all OD600 values measured by the CO8000 Cell Density Meter are shown as ⅓ of the actual value. This allows us to compare OD600 values between all readers used in the lab.*

For long-term (indefinite) storage, yeast culture mass was resuspended in 30% (v/v) sterile glycerol solution, incubated 30 minutes at room temperature and then stored at -80°C. Yeast strains could be stored on plates at 4°C for up to 3 weeks.

3.1.3 Growth media

3.1.3.1 S.cerevisiae growth media

All media were sterilized at 119°C for 20 minutes (autoclave Tuttnauer 2840EL-D). Ampicillin (1000x, Biotika) was added to media to a final concentration of 100 µg/ml. If needed, agar (Agar No.1, Oxoid) was added to media prior to sterilization to a final concentration of 2% (20 g/l).

YPAD (rich medium)

10 g/l	Yeast Extract (Formedium)
20 g/l	Universal peptone M 66 (Merck)
100 mg/l	Adenine hemisulfate salt (Sigma)

Components were dissolved in deionized water (nine-tenth volume of the medium) and autoclaved. Then, one-tenth of the medium volume of 20% glucose solution (autoclaved separately) was added to a final concentration of 2%. If required for a selection, antibiotics G418 (Life Technologies) or nourseothricin (Jena Bioscience) were added to a final concentration of 200 µg/ml and 90 µg/ml, respectively.

2x YPAD

20 g/l	Yeast Extract (Formedium)
40 g/l	Universal peptone M 66 (Merck)
100 mg/l	Adenine hemisulfate salt (Sigma)

Components were dissolved in deionized water (four-fifth volume of the medium) and autoclaved. Then, one-fifth of the medium volume of 20% glucose solution (autoclaved separately) was added to a final concentration of 4%.

SD (synthetic defined medium)

6.7 g/l	Yeast Nitrogen Base without Amino Acids (Difco)
1.394 g/l	Synthetic Complete Amino Acid (Kaiser) drop-out: -His, -Leu, -Trp, -Ura (Formedium)

Components were dissolved in deionized water (nine-tenth volume of the medium) and autoclaved. In the case of SD-Lys/SD-Met/SD-Lys-Met media, only Yeast Nitrogen Base without Amino Acids (Difco) was dissolved in deionized water and autoclaved. Then, one-tenth of the medium volume of 20% glucose solution (autoclaved separately) was added to a final concentration of 2%. If required for a selection, antibiotics nourseothricin (Jena Bioscience) was added to a final

concentration of 90 µg/ml. Depending on auxotrophic requirements, SD medium was supplemented with missing constituents from separately autoclaved 100x stock solutions.

Pre-sporulation medium

1 g/100 ml	Universal peptone M 66 (Merck)
0.5 g/100 ml	Yeast Extract (Formedium)

Components were dissolved in 50 ml of deionized water and autoclaved. Then, 50 ml of 20% glucose solution was added to a final concentration of 10%.

Sporulation medium

0.5 g/100 ml	KAc (Sigma)
0.23 g/100 ml	KCl (Penta)

Components were dissolved in 100 ml of deionized water and autoclaved. Depending on requirements, the medium was supplemented with missing constituents from separately autoclaved 100x stock solutions.

3.1.3.2 E. coli growth media

Bacterial cultures were grown in liquid media at 37°C with shaking (180 rpm, Thermo Scientific 4520 Orbital Shaker) or on the surface of agar plates at 37°C. Agar (Agar No.1, Oxoid) was added to the media prior to the sterilization to a final concentration of 2% (20 g/l). Media were sterilized at 119°C for 20 min (autoclave Tuttnauer 2840EL-D).

LB medium

5 g/l	Yeast Extract (Formedium)
10 g/l	Universal peptone M 66 (Merck)
5 g/l	NaCl (Lach-Ner)

Components were dissolved in deionized water and autoclaved. If required for a selection, 1000x stock solution of ampicillin (Biotika) was added to a final concentration of 100 µg/ml once the medium has cooled to about 50-60°C.

3.1.3.3 Media supplements

1000x Ampicillin

1000x stock solution of ampicillin (Biotika) was prepared by dissolving the powder aliquot (0.5 g) in 4 ml of deionized water and 1 ml of 96% ethanol.

100x solutions to supplement SD media

2 g/l	L-Histidine monohydrochloride monohydrate (Sigma)
10 g/l	L- Leucine (Sigma)
2 g/l	L- Tryptophan (Sigma)
2 g/l	Uracil (Sigma)
3 g/l	L-Lysine monohydrochloride (Sigma)
2 g/l	L-Methionine (Sigma)
10 g/l	Adenine hemisulfate salt (Sigma)

Supplements were dissolved in deionized water and autoclaved.

3.1.4 Yeast mating

Two haploid strains with opposite mating type (*MATa* and *MATα*) were grown on YPAD plates. Small amount of yeast mass was resuspended in 100 µl sterile water and 10 µl of the suspension was transferred on an appropriate selective plate as *MATa*, *MATα* and *MATa* + *MATα* spots. Plates were incubated for 1-3 days at 30°C. Diploid cell mass was streaked on a selective plate to ensure purity of the diploid cells.

Diploids could be selected on a selective plate when the haploid parental strains carry complementary genetic markers. Here, all used strains were derived from BY4741 (*MATa his3Δ1 leu2Δ0 met15Δ0 ura3Δ0*) and BY4742 (*MATα his3Δ1 leu2Δ0 lys2Δ0 ura3Δ0*) *wild type* strains, thus selected for mating on SD plates without Lysine and Methionine.

3.1.5 Yeast sporulation and spore isolation

Diploid yeast cells were plated on pre-sporulation plate and incubated overnight at 30°C. The yeast mass was quantitatively transferred to about 30-50 µl of sterile water. A dense suspension of cells was dropped on the sporulation plate and incubated at room temperature for 4-10 days. The presence of asci was checked under a microscope.

A small amount of sporulated cells was transferred into 100 µl of yeast lytic enzyme (1 mg/ml, MP Biomedicals) and incubated overnight at 30°C to break down the cell wall of diploid cells as well as the wall of asci. Next day, the suspension was diluted with 1 ml sterile water and 3-times sonicated at 10% power for 15 sec on a probe sonicator (Sonopuls HD 2070, Bandelin). The tube was cooled on ice between sonication steps. The absence of diploid cells was checked under a microscope and re-sonicated if required. Afterwards, 50 µl of suspension was plated on an appropriate solid medium and cultured. Grown colonies were subsequently tested for a desirable genotype.

3.1.6 Yeast transformation using the Lithium Acetate method

A yeast pre-culture was prepared by inoculation of a yeast mass into 5 ml of 2x YPAD and incubated overnight. Next day, 10 ml of 2x YPAD was inoculated from the pre-culture to OD600 of ca 0.2 and cultured until it reached ca 0.8.

Cell culture was harvested by centrifugation (1500g, 3 min), medium discarded and sediment washed with 10 ml sterile water. Sediment was resuspended in 1 ml

sterile water, transferred to a microtube and centrifuged again (5000g, 1 min). The sediment was resuspended in a transformation mix (described below) and incubated at 42°C for 40 minutes:

40 µl	sterile water
36 µl	Lithium Acetate
10 µl	denatured ssDNA (10 mg/ml salmon sperm DNA, Sigma)
34 µl	DNA (>100 ng of plasmid/oligonucleotides)
240 µl	50% (w/v) PEG 3500 (Sigma)

Afterwards, the suspension was centrifuged (8000g, 3 min) and supernatant quantitatively removed. Cell mass was resuspended in 100 µl sterile deionized water and plated on an appropriate selection media plate.

3.1.8 Measurement of S.cerevisiae growth parameters

A pre-culture of strains of interest has been cultured for about 12 hours at 30°C with shaking.

Manual inspection:
Adequate volume of pre-culture was used to inoculate a culture of 15 ml (in 100 ml Erlenmeyer flask) to the final OD600 of 0.05 and measured with CO8000 Cell Density Meter (WPA Biowave). The culture was grown at 30°C with shaking (180 rpm, Thermo Scientific 4520 Orbital Shaker or Ecotron, Infors HT) and its OD600 measured every 2 hours.

Automatic inspection:
Adequate volume of pre-culture was used to inoculate the culture of total volume of 1.4 ml and OD600 of 0.1 in 12-well culture plate. Culture was cultured in the Varioskan Flash reader (Thermo Fisher) machine at 30°C with orbital shaking of 180 rpm speed and 20 mm diameter. The OD600 of cultures was measured every 10 min.

3.1.8 Yeast three-hybrid system

RNA-protein interactions were assayed using the yeast three-hybrid (3-H) system (SenGupta et al. 1996). We used strain YBZ1, which contains the *HIS3* reporter (expressed only in the case of interaction) and is auxotrophic for Uracil (U) and Leucine (L). The strain was transformed with plasmids expressing protein of interest fused with the *GAL4* activation domain (pACT2 derived, also expressing *LEU2* marker) and RNA of interest fused with two MS2 loops (p3HR2 derived, also expressing *URA3* marker). Single colonies containing both plasmids were selected on the synthetic medium without Leucine and Uracil (SD-U-L).

Three independent colonies were cultured overnight in the liquid SD-U-L medium, their OD600 was measured and an appropriate amount was used to prepare a suspension of the final OD600 of 0.08 (labelled as D1). D1 dilution was used to prepare three 10-fold serial dilutions (D2-D4). All four dilutions were spotted on the SD-U-L plate to assess the presence of both plasmids. They were also spotted on the synthetic medium lacking Histidine (H), SD-U-L-H, to assess expression of the *HIS3* reporter, e.g. RNA-protein interactions. Moreover, to eliminate false-positive interactions, the growth was assessed on SD-U-L-H media in the presence of 1mM and 5mM 3-aminotriazole (3-AT), a competitive inhibitor of the enzymatic function of *HIS3* reporter. The plates were incubated at 30°C for 3-4 days and photographed using DMC-F27 camera (Panasonic).

3.1.9 Electroporation of E.coli

Aliquot (~40 µl) of electrocompetent *DH5α* cells stored in -80°C was slowly thawed on ice, mixed with 1 µl of an inactivated ligation reaction or ~100 ng of a plasmid. Suspension was transferred to a chilled electroporation cuvette (2 mm, Cell Projects) and electroporated (2500 V, 200 Ω; 25 µF) by GenePulser Xcell (Bio-Rad). Suspension was immediately resuspended in 1 ml of LB medium and incubated at 37°C for 1 hour. Afterwards, 100 µl of suspension was plated on an appropriate selection LB media plate. Plates were incubated at 37°C overnight.

3.2 Nucleic acid techniques

3.2.1 Plasmids used in this study

Table 3 contain description of all plasmids used in this study.

[Table 3] List of plasmids

Name	Description	Source
pMO01	p423GPD with *RPL22A*_intron-*CUP1* construct for the primer-extension assay	(Abrhámová et al. 2018)
pMO03	p423GPD with *RPL22B*_intron-*CUP1* construct for the primer-extension assay	(Abrhámová et al. 2018)
pACT2	used to express fusions of protein of interest with the *GAL4* activation domain in the yeast three-hybrid (3-H) system	(SenGupta et al. 1996)
pFN03	pACT2 expressing *RPL22AΔi*	this study
pFN04	pACT2 expressing *RPL22AΔi_mut*	this study
pFN13	pACT2 expressing *RPL22BΔi*	this study
pFN14	pACT2 expressing *RPL22BΔi_mut*	this study
pFN12	pACT2 expressing *K.lactis RPL22Δi*	this study
pFN15	pACT2 expressing *S.pombe RPL22Δi*	this study
pAD-*H.s.RPL22*	pACT2 expressing *H. sapiens RPL22Δi*	J. Libus (unpublished)
pAD-IRP	used to express fusions of iron regulatory protein (IRP) with the *GAL4* activation domain in the 3-H system	(SenGupta et al. 1996)
p3HR2	used to express fusions of RNA of interest with two MS2 loops in the 3-H system	(Stumpf et al. 2008)
pFN05	p3HR2 expressing *RPL22B* intronic region 1 (I1)	this study
pFN06	p3HR2 expressing *RPL22B* intronic region 2 (I2)	this study
pFN07	p3HR2 expressing *RPL22B* intronic region 3 (I3)	this study
pFN08	p3HR2 expressing *RPL22B* intron (I)	this study
pFN09	p3HR2 expressing *K.lactis RPL22* intronic region 1.1 (I1.1)	this study
pFN10	p3HR2 expressing *K.lactis RPL22* intronic region 1.2 (I1.2)	this study
pFN11	p3HR2 expressing *K.lactis RPL22* intronic region 3 (I3)	this study
pIIIA/IRE-MS2	used to express fusion of iron response element (IRE) with two MS2 loops in the 3-H system	(SenGupta et al. 1996)

3.2.2 Plasmid DNA purification

NucleoSpin Plasmid kit (Macherey-Nagel) was used for small-scale preparations of plasmid DNA prior to sequencing or restriction analysis.

- **Cell preparation:** Cells transformed with plasmid of interest were cultivated overnight in 5 ml of LB media supplemented with ampicillin. Culture was centrifuged (11000g, 30 sec) and pellet resuspended in 250 µl Buffer A1.
- **Lysis:** 250 µl of Buffer A2 was added and gently mixed by inverting the tube 8 times. Mixture was incubated for 5 minutes at room temperature.
- **Neutralization:** 300 µl of Buffer A3 was added to the mixture and gently mixed by inverting the tube 8 times.
- **Binding:** Mixture was centrifuged (11000g, 5 min) and supernatant loaded on a NucleoSpin Plasmid Column. Flow-through in a collection tube was discarded after centrifugation (11000g, 1 min).
- **Wash:** Column was washed with 600 µl Buffer A4, centrifuged (11000g, 1 min) and flow-through in a collection tube discarded.
- **Dry:** Column was dried out by centrifugation (11000g, 2 min).
- **Elution:** Column was transferred into a microtube and DNA eluted by adding 50 µl of deionized water. Column was centrifuged (11000g, 1 min) after one minute incubation.

Large-scale preparations of plasmid DNA were performed using alkaline extraction method.

- **Cell preparation:** *E. coli* transformed with plasmid of interest was cultivated overnight in 15 ml of LB media supplemented with ampicillin. Culture was put on ice for 10 min, transferred to a 15 ml tube and centrifuged (3000g, 15 min, 4°C). Pellet was resuspended in 400 µl of pre-cooled solution I (25 mM Tris-HCl (pH 8.0), 10 mM EDTA-NaOH, 1% glucose).
- **Lysis:** Tube was removed from ice, 800 µl of solution II (1% SDS, 0.2 M NaOH; stored at room temperature) was added to the mixture and gently mixed by inverting tube eight times. Mixture was incubated for 5 min at room temperature.

- **Neutralization:** Tube was returned on ice, 600 µl of pre-cooled solution III (3 M potassium acetate, 2 M acetic acid, pH 5.4) was added to the mixture and gently mixed by inverting 8 times. Mixture was incubated for 30 minutes on ice.
- **Cleaning and concentration:** Mixture was transferred to a 15 ml tube and centrifuged (15000g, 15 min). Supernatant was transferred to a clean 15 ml tube, mixed with isopropanol (0.6 volume of supernatant) and centrifuged (15000g, 5 min). Pellet was air dried and dissolved in 300 µl deionized water. RNA was partially removed by adding 350 µl of 10 M LiCl followed by incubation in -80°C for 10 min. Sample was centrifuged (15000g, 5 min) and supernatant transferred to a new microtube. DNA was precipitated by adding 700 µl of 96% ethanol followed by incubation in -80°C for 10 min. Sample was centrifuged (15000g, 5 min), pellet washed with 1 ml of 70% ethanol and air dried.
- **Elution:** DNA was dissolved by adding 100 µl of deionized water.

Quantity of isolated plasmid DNA was measured using NanoDrop 2000 (Thermo Scientific) in the case of small-scale preparations (RNA free samples) or estimated from an electrophoretic gel in the case of large-scale preparations (containing RNA). Its identity was confirmed by a restriction analysis with appropriate restriction enzymes followed by electrophoresis (see later).

3.2.3 Extraction of S.cerevisiae genomic DNA

A small amount of yeast mass (either from single colony or pelleted liquid culture) was resuspended in 100 µl of 200 mM Lithium Acetate solution containing 1% sodium dodecyl sulphate and incubated for 5 min in 70°C. Subsequently, 300 µl of 96% ethanol was added, mixed by vortexing and spun down (15000g, 3 min). Pellet (containing precipitated DNA as well as cell debris) was washed with 700 µl of 70% ethanol, dried and dissolved in 100 µl of deionized water. Cell debris was spun down (15000g, 30 sec) and 1.5 µl of supernatant was used for a PCR reaction (Lõoke et al. 2011).

3.2.4 Polymerase chain reaction (PCR)

Routine PCR (for genotyping, verification of primers) was performed using Taq DNA polymerase (recombinant, Thermo Fisher). Cloning PCR was performed using Q5® High-Fidelity DNA Polymerase (New England BioLabs). The composition of PCR reactions is described in the Table 4.

[Table 4] The composition of PCR reactions

Routine PCR			Cloning PCR	
1 µl	10x Taq Buffer with KCl		5 µl	5x Q5 Reaction Buffer
1 µl	$MgCl_2$ (25 mM)		1.25 µl	forward primer (10 µM)
1 µl	forward primer (10 µMl)		1.25 µl	reverse primer (10 µM)
1 µl	reverse primer (10 µM)		0.5 µl	dNTPs (10 mM each)
1 µl	dNTPs (2.5 mM each)		1.5 µl	DNA
1.5 µl	DNA		0.25 µl	Q5® High-Fidelity DNA Polymerase
0.1 µl	Taq DNA polymerase		15.25 µl	deionized water
3.4 µl	deionized water			

Primers used in this study are listed in the Table 5. The reaction was prepared on ice and PCR performed on the Veriti® 96-well Thermal Cycler (Applied Biosystems) or on the TAdvanced 96 Thermal Cycler (Biometra) with conditions described in the Table 6.

[Table 5] List of primers used in this study

Name	Sequence	Purpose*
KA92	TAGACTTCTCCCTCTGTATCCATGC	*RPL16A*_genotyping_fwd
KA93	CAACAACGGAAGCTAAACGACCTAC	*RPL16A*_genotyping_rev
KA94	TAGAACCTGAAACTGCCCGCTAAAG	*RPL16B*_genotyping_fwd
KA95	CAATACTTGCTTGGCAATAGTGGAG	*RPL16B*_genotyping_rev

KA96	CGCTACTGAGTAAATGTTTAGCTTG	*RPL22A*_genotyping_fwd
KA97	GGCAGTGGAAACAACAGTAACAACG	*RPL22A*_genotyping_rev
KA98	TACCACGATAGGATCGTTTATTTGC	*RPL22B*_genotyping_fwd
KA99	CTACGGCACCATCTACTTTAATATG	*RPL22B*_genotyping_rev
KA100	TTCTCATCACCGTCAATATTACAAG	*RPL37A*_genotyping_fwd
KA101	TCCGGTCATGAATTACGAAACTATC	*RPL37A*_genotyping_rev
KA102	ACATGGCTGGAATAGTAAGCATAGG	*RPL37B*_genotyping_fwd
KA103	AAGCAGAAGTAGCCTTAGCAGAACC	*RPL37B*_genotyping_rev
KA106	AAATAGAGAGCGAAATGTCCTTACC	*RPS0A*_genotyping_fwd
KA107	ATATCACCTTACTTACCACTCGACG	*RPS0A*_genotyping_rev
KA108	CCGAAATAGCACAAGAAGAGATAAG	*RPS0B*_genotyping_fwd
KA109	TCCTTACAATATTCACACACATTGC	*RPS0B*_genotyping_rev
KA110	CTAGTGAACGTATACACAAGAGCGG	*RPS18A*_genotyping_fwd
KA111	AAAGGCAAGTTGAAATTATGGTCAC	*RPS18A*_genotyping_rev
KA112	CTGACACCTTTGCTATCCTAACTGG	*RPS18B*_genotyping_fwd
KA113	AACACGTGTAGTACTTTCTCCTTTG	*RPS18B*_genotyping_rev
KA114	TCTGAGCAAACTAAGAAACCATTAG	*RPL2A*_genotyping_fwd
KA115	CTATAAACGCGTAAGGCAGAAAGCC	*RPL2A*_genotyping_rev
KA116	ATGTTGGATACTAAGCAGTTCCCAG	*RPL2B*_genotyping_fwd
KA117	TATCACTTTATAAGGAACGTTTCGG	*RPL2B*_genotyping_rev
KA118	AAAGAGCAAACAAAGAGTCCTCAAG	*RPL17A*_genotyping_fwd
KA119	ATCTTCTATTTAAGCAGCAATACGC	*RPL17A*_genotyping_rev
KA120	AGTGTAGCTTGTACTCTTTCCCTGC	*RPL17B*_genotyping_fwd
KA121	TTTATCCCATTTCTCTAGATTCGAC	*RPL17B*_genotyping_rev
KA54	CTCTTTGAAAACGGAAGGTGAAGAAC	*RPL16A*_mRNA_qPCR_fwd
KA55	ACGACCTACTAAATGACCCTTACCAT	*RPL16A*_mRNA_qPCR_rev
KA58	CAACCAACCAACCATAAAAGATGTCTC	*RPL16B*_mRNA_qPCR_fwd
KA59	CGACCCAACAAATGATCCTTAGCAT	*RPL16B*_mRNA_qPCR_rev
KA46	ATTAAGAAACAATGGCCCCAAACAC	*RPL22A*_mRNA_qPCR_fwd
KA47	TGGGTCGAAGACACCGTTTTCA	*RPL22A*_mRNA_qPCR_rev
KA50	CAACCACAATGGCTCCAAACAC	*RPL22B*_mRNA_qPCR_fwd
KA51	ACCTCAATGGCGTTCCCTAAGT	*RPL22B*_mRNA_qPCR_rev

KA62	AAGAGGTATTTGCTAAAGCCTCATACA	*RPL37A*_mRNA_qPCR_fwd
KA63	CGTTTACCGAATGAAGGAGTACCCTTA	*RPL37A*_mRNA_qPCR_rev
KA66	TGTGTAGATAAAGAACAAAGAGGTAAACGA	*RPL37B*_mRNA_qPCR_fwd
KA67	GCTTACCGAATGAAGGAGTACCCTTA	*RPL37B*_mRNA_qPCR_rev
KA122	ACTTAGGTGCTAGAAACGTTCAAGTTC	*RPS0A*_mRNA_qPCR_fwd
KA123	GTGGGCAGCGAACTTCAAAACA	*RPS0A*_mRNA_qPCR_rev
KA124	AGGTGCTAGAAACGTTCAAGTCC	*RPS0B*_mRNA_qPCR_fwd
KA125	GCACCAGTGTGAGCAGCAAA	*RPS0B*_mRNA_qPCR_rev
KA126	ACTAGTGAACGTATACACAAGAGCGG	*RPS18A*_mRNA_qPCR_fwd
KA127	GTAAACGATCTTAATGTTACCGTCAACGTTA	*RPS18A*_mRNA_qPCR_rev
KA128	AGCCAATAGAGCAGAAAGTGGTAAAG	*RPS18B*_mRNA_qPCR_fwd
KA129	CGACATTGGTGTTCAACAAACGT	*RPS18B*_mRNA_qPCR_rev
KA134	AACCATTAGATCAATAAGCAATGGGTAGA	*RPL2A*_mRNA_qPCR_fwd
KA135	GTTGTGACCGATGATAATAACGTAGTTACCG	*RPL2A*_mRNA_qPCR_rev
KA136	ACCACAAAGTTATTGAACAATGGGTAGA	*RPL2B*_mRNA_qPCR_fwd
KA137	TTGTGACCAATGATGATAACGTAGTTACCA	*RPL2B*_mRNA_qPCR_rev
KA130	CAAGTTTTGGACCACCAAAGAGCTATTCCT	*RPL17A*_mRNA_qPCR_fwd
KA131	TTTAGTAGCATCCAAACCTTTAGCTTCAGCG	*RPL17A*_mRNA_qPCR_rev
KA132	GGACCACCAAAGAGCCATCCCA	*RPL17B*_mRNA_qPCR_fwd
KA133	CTTGGTAGCATCTAGACCCTTAGCTTCAGCA	*RPL17B*_mRNA_qPCR_rev
KA104	CTCAAAGCTGGCCAGTAGAA	*SPT15*_qPCR_fwd
KA105	CGTCACACGAACCGACAATA	*SPT15*_qPCR_rev
YAC06	GGCACTCATGACCTTC	*CUP1*-reporter_primer-extension
YU14	ACGATGGGTTCGTAAGCGTACTCCTACCGTGG	U14-snoRNA_primer-extension
FN12	CCACTCCCGCCATGGCCCCAAACACTTCCA	*RPL22A*-CDS_cloning-pACT2_fwd
FN13	TGCTTGGATCCTTATTCTTCGTCTTCTTCTTCGTCT	*RPL22A*-CDS_cloning-pACT2_rev
FN14	CCACTCCCGCCATGGCTCCAAACACTTCCAGAA	*RPL22B*-CDS_cloning-pACT2_fwd
FN15	TGCTTGGATCCTTATTCGTCATCCTCTTCTTCGTCA	*RPL22B*-CDS_cloning-pACT2_rev
FN20	ATATGCATGCTTTCGTTCCTATGTCACAATTAG	*RPL22B*_I1_cloning-p3HR2_fwd
FN21	ACATGCATGCGAATCCACTAGTTCGCTGT	*RPL22B*_I1_cloning-p3HR2_rev
FN22	ATATGCATGCTTTAAAAATTCACCCCTTATAGC	*RPL22B*_I2_cloning-p3HR2_fwd

FN23	ACATGCATGCATTAACAATCACTTCATATAGCTAG	*RPL22B*_I2_cloning-p3HR2_rev
FN24	ATATGCATGCTTTCCTCGTCCAAAC	*RPL22B*_I3_cloning-p3HR2_fwd
FN25	ACATGCATGCCTGTTACAGTTTTATGTTAG	*RPL22B*_I3_cloning-p3HR2_rev
FN26	ACATGCATGCGTACGTTAATTTTCGTTCCTAT	*RPL22B*_I_cloning-p3HR2_fwd
FN27	ACATGCATGCCTGTTACAGTTTTATGTTAGTAATC	*RPL22B*_I_cloning-p3HR2_rev
FN48	GTTCCAGATTACGCTAGCTT	pACT2_sequencing-primer
FN34	CCACTCCCGCCATGGCTCCAAATACTGCTA	*RPL22*-CDS_*K.lactis*_cloning-pACT2_fwd
FN35	TGCTTGGATCCTTATTCTTCGTCTTCTTCTTCTTCT	*RPL22*-CDS_*K.lactis*_cloning-pACT2_rev
JL443	GGTCCATGGTTAAAAAGAACACTAAGGTTA	*RPL22*-CDS_*S.pombe*_cloning-pACT2_fwd
JL444	GTTGGCAATGACGAAGAGGAGCAATAAGGATCC	*RPL22*-CDS_*S.pombe*_cloning-pACT2_rev
FN36	ATATGCATGCAGGATGAAGGACTGTAAACCA	*RPL22_K.lactis*_I1.1_cloning-p3HR2_fwd
FN37	ACATGCATGCCAGAATAGCCACCAAGTTGAGT	*RPL22_K.lactis*_I1.1_cloning-p3HR2_rev
FN38	ATATGCATGCAGAAGTGAATTGGTTACTATTTGCTAG	*RPL22_K.lactis*_I1.2_cloning-p3HR2_fwd
FN39	ACATGCATGCTAAACCAGCCTACTGCTATTAACAA	*RPL22_K.lactis*_I1.2_cloning-p3HR2_rev
FN40	ATATGCATGCCAAGAGATTGTGTGGACTGCAT	*RPL22_K.lactis*_I2_cloning-p3HR2_fwd
FN41	ACATGCATGCGAACATTCGAACGTTCAATTTGA	*RPL22_K.lactis*_I2_cloning-p3HR2_rev

*forward primer = fwd, reverse primer = rev

[Table 6] Thermal cycling conditions

	Routine PCR		**Cloning PCR**		
Step	**Temp (°C)**	**Time (sec)**	**Temp (°C)**	**Time (sec)**	**Cycles**
Denaturation	95	180	98	30	1
Denaturation	95	30	98	10	25-30
Annealing	Tm (primers) -3	30	*	20	
Extension	72	60/kb	72	20/kb	
Extension	72	120	72	120	1
Cooling	4	∞	4	∞	1

* NEB Tm Calculator was used to calculate annealing temperature with respective primers

3.2.4 Purification of PCR products

PCR products were purified (e.g. prior cloning) using NucleoSpin® Gel and PCR Clean-up kit.

- The volume of reaction was extended to 100 µl by adding deionized H_2O.
- Solution was mixed with 200 µl of Buffer NTI, loaded on a NucleoSpin column and centrifuged at 11000g for 30 sec. Flow-through in the collection tube was discarded after centrifugation.
- Column was washed with 700 µl of Buffer NT3 and centrifuged (11000g, 30 sec). Flow-through in the collection tube was discarded.
- Column was dried out by centrifugation (11000g, 1 min).
- Column was transferred to a new microtube and DNA eluted by adding 20 µl deionized water. Column was centrifuged (11000g, 1 min) after one minute incubation.

3.2.5 Agarose gel electrophoresis

BlueMarine™ 100 (7x10 cm gel format, Serva) or BlueMarine™ 200 (15x20 cm gel format, Serva) gel electrophoresis system was used for separation of DNA molecules by their size. SeaKem® LE Agarose (Lonza) was used to prepare 0.8 – 2% agarose gels in the 1x TAE buffer (40 mM Tris, 20 mM acetate, 2 mM EDTA, pH 8.5), depending on the size of DNA fragments. DNA samples (5 – 50 µl) were mixed with 6x Orange DNA loading dye (Thermo Scientific) and loaded into wells of a gel. GeneRuler™ 1 kb DNA Ladder (Thermo Scientific), GeneRuler™ 50 bp DNA Ladder (Thermo Scientific) or GeneRuler™ DNA Ladder Mix (Thermo Scientific) of the amount of 6 µl was used as DNA marker. Gel electrophoresis was performed under the constant voltage of 50 – 120 V, depending on application and size of a gel. Gels with separated DNA fragments were submerged in the staining solution (0.5 µg/ml ethidium bromide) for 20 min, then washed in deionized water. Gels were visualized using FOTO/UV 21 transilluminator (Fotodyne) and photographed using DMC-F27 camera with red/UV filter (Panasonic).

3.2.6 DNA extraction from agarose gels

DNA fragments were extracted from agarose gels (e.g. prior cloning) using NucleoSpin® Gel and PCR Clean-up kit.

- After electrophoresis with <2% agarose gel, DNA fragment of interest was excised using ethanol-cleaned scalpel and weighted on an analytical scale (with pre-weighted clean microtube).
- 200 µl of Buffer NTI per 100 mg gel was added and the sample was incubated at 50°C for 10 min with shaking.
- Dissolved sample was loaded on a NucleoSpin column (placed in a collection tube) and centrifuged at 11000g for 30 sec. Flow-through in a collection tube was discarded after centrifugation.
- Column was washed with 700 µl of Buffer NT3, centrifuged (11000g, 30 sec) and flow-through in a collection tube was discarded.
- Column was dried out by centrifugation (11000 g, 1 min).
- Column was transferred to a new microtube and DNA eluted by adding 20 µl deionized water. Column was centrifuged (11000g, 1 min) after one minute incubation.

3.2.7 Plasmid cloning

3.2.7.1 Restriction enzyme digestion

Restriction reaction was performed in a microtube using restriction enzymes from the Thermo Fisher with protocol according to the manufacturer's instructions. The double-digest reactions were performed in the buffer suggested by the *Double Digest Calculator* (https://goo.gl/h8q2uz). The composition of a typical restriction reaction was as follows:

0.1 - 4 µg	DNA
2 µl	10x restriction buffer
0.2 µl	restriction enzyme (10u/µl)
up to 20 µl	deionized water

The reaction was typically run for 1-3 hours at 37°C and then inactivated as recommended by the manufacturer. The successful restriction enzyme reaction was verified using agarose gel electrophoresis. The list of all used restriction enzymes with the specification of their use is provided in the Table 7.

[Table 7] List of restriction enzymes and their use in this study

Name	Buffer	Incubation temperature	Inactivation
PaeI	10x Buffer B	37°C	65°C for 15 min
NcoI + BamHI	2x Tango (2-fold excess of BamHI)	37°C	65°C for 15 min

3.2.7.2 Phosphatase treatment of DNA fragments

Plasmid backbone was dephosphorylated after restriction enzyme digestion using FastAP phosphatase (Thermo Scientific). The enzyme of the amount of 1 µl was added to the reaction and incubated for 15 minutes at 37°C. The reaction was stopped by a heat inactivation at 65°C for 15 minutes.

3.2.7.3 Ligation

Ligation reaction was performed using T4 DNA ligase (5u/µl, Thermo Fisher) with the 1:3 molar ratio vector:insert. The composition of a typical ligation reaction was as follows:

100 ng	dephosphorylated plasmid backbone
x ng	insert
2 µl	10x T4 DNA Ligase Buffer
0.2 µl	T4 DNA Ligase
up to 20 µl	deionized water

The ligation was typically run overnight (16 hours) at room temperature and then stopped by a heat inactivation at 65°C for 15 minutes. The amount of 1 µl of reaction was used for the electroporation of electrocompetent *E.coli* cells.

3.2.8 RNA isolation and DNase treatment

Total RNA was isolated using MasterPureTM Yeast RNA Purification Kit (Epicentre). RNase-free water was prepared by treatment of deionized water with 0,1% v/v diethyl pyrocarbonate (Sigma) overnight and then being autoclaved at 119°C for 20 minutes. All plasticware was autoclaved 3-times before use (autoclave Tuttnauer 2840EL-D).

- Yeast culture was grown until it reached mid-exponential phase. Volume equivalent to 1 ml of OD600 = 1 was harvested by centrifugation and stored in -80°C.
- Pellet was resuspended in 300 µl of Extraction Reagent containing 1 µl of 50 µg/µl Proteinase K and incubated at 70°C for 15 minutes (vortexing 10 sec every 5 min). Then, 175 µl of MPC Protein Precipitation Reagent was added to a lysed sample and mixed by vortexing for 10 sec. Sample was chilled on ice for 5 min and pelleted (20000g, 10 min, 4°C).
- Supernatant was transferred to a new microtube. Nucleic acids were precipitated by adding 500 µl of isopropanol and mixed by inverting tubes 40 times. Precipitated sample was centrifuged (20000g, 10 min, 4°C) and supernatant precisely discarded.
- Pellet containing nucleic acids was resuspended in 200 µl of DNase I solution (175 µl RNase-free H2O, 20 µl of 10x DNase Buffer and 5 µl of RNase-free DNase I) and incubated for 30 min at 37°C.
- 200 µl of 2x T and C lysis solution was added, vortexed and proteins precipitated by adding 200 µl of MPC Protein Precipitation Reagent. Solution was mixed by vortexing for 10 sec. Samples were chilled on ice for 5 min and pelleted (20000g, 10 min, 4°C).
- Supernatant was transferred to a new microtube. RNA was precipitated by adding 500 µl of isopropanol and mixed by inverting tubes 40 times. Precipitated sample was centrifuged (20000g, 10 min, 4°C) and supernatant precisely discarded.

- Pellet was rinsed twice with 70% ethanol and then dried on air. Dried RNA was resuspended in 35 µl of RNase-free water. Concentration and purity of purified RNA was determined using NanoDrop 2000 (Thermo Scientific).

3.2.9 Reverse transcription

Total RNA was reversely transcribed using RevertAid™ First Strand cDNA Synthesis Kit (Thermo Scientific). Non-reverse transcriptase and non-template control were always included.

- A mixture of RNA (2 µg) and 1 µl of random hexamer primer was filled to a total volume of 12,5 µl with RNase-free water and vortexed, shortly spun down and incubated for 5 min at 65°C. Then, sample was cooled on ice.
- A reverse-transcription premix (below) was added to the sample, mixed by pipetting, incubated for 5 min at room temperature and then for 1 h at 42°C.

4 µl	5x Reaction Buffer
0.5 µl	RiboLockTM RNase Inhibitor (40u/µl)
2 µl	dNTP Mix (10 mM)
1 µl	RevertAid™ M-MuLV Reverse Transcriptase (200u/µl)

- Reaction was terminated by incubation of samples for 5 min at 70°C and stored at -80°C.

3.2.10 Quantitative PCR (qPCR)

3.2.10.1 Performing qPCR experiment

qPCR was performed using MESA GREEN qPCR MasterMix Plus for SYBR Assay No ROX (Eurogentec). Reaction was set up as premix in a microtube on ice. The composition of single reaction was as follows:

6.25 µl	MESA GREEN qPCR MasterMix Plus
0.375 + 0.375 µl	forward + reverse primer (10 µM each)
4 µl	deionized water

Premix was pipetted into wells of a LightCycler Multiwell Plate 384 (Roche), 11 µl per well. Then, template DNA (usually 100-times diluted cDNA) was added in the amount of 1.5 µl per well. Plates were sealed with a LightCycler 480 Sealing Foil (Roche), samples mixed by vortexing and then spun down (500g, 3 min).

The reaction was performed on the LightCycler 480 II machine (Roche) with program described in the Table 8. All samples were pipetted in triplicates and every measurement had included non-reverse transcriptase, non-template control (see 2.2.9) and water as negative controls.

[Table 8] Typical qPCR program

Step	Temperature (°C)	Time (sec)	Number of cycles
Denaturation	95	300	1
Denaturation	95	15	40
Annealing	Tm (primers) -3*	30	
Extension	72	30	
Fluorescence read			
Melting analysis	95	300	1
	50	60	
	+1 (read)	60	

3.2.10.2 Analysis of qPCR data

Initial analysis was performed using LightCycler 480 Software (version 1.5) from Roche. The software calls mean threshold-cycles (C_T) with the standard deviation (s.d.) for each measured sample (always measured as three technical replicates). These data were used for the relative quantification normalized to the *SPT15* reference gene using $\Delta\Delta C_T$ method (Livak and Schmittgen 2001) as follows:

- Mean C_T values of gene of interest (C_T[gene of interest]) were normalized to the C_T value of *SPT15* gene (C_T[*SPT15*]), getting ΔC_T values.
- ΔC_T values of manipulated genes (i.e. with intron deletion) were normalized to the ΔC_T value of gene in its *wild type* state, getting $\Delta\Delta C_T$ values.
- The expression ratio (e.g. fold change) was calculated as $2^{-\Delta\Delta CT}$ value and plotted.

Specificity of primers was determined by melting analysis, when the melting curve was calculated using LightCycler 480 Software, version 1.5. Presence of a single peak when plotted the first negative derivative of fluorescence as a function of temperature confirmed the specificity of primer pairs.

3.2.10.3 Validation of primers for a qPCR experiment

Potential primers were used in qPCR validation experiment with a suitable template, e.g. containing binding sites for tested primers. Template cDNA was prepared as in 3.2.9. Three-times diluted cDNA was used as initial template (T1), as well as for making series of five ⅕ dilutions (T2-T6). Each template was measured in triplicates in accordance with a standard qPCR experiment described above. Efficiency of amplification was calculated using LightCycler 480 Software (version 1.5), when plotted C_T values as function of logarithmically transformed template concentration. Slope of the function was used to calculate efficiency of amplification as $-1+10^{1/slope}$. The efficiency of tested primers was always higher than 96%.

3.2.11 Primer extension analysis

3.2.11.1 Labelling of primers and DNA marker

Primers and DNA marker were labelled on their 5' ends with γ^{32}P-ATP (6000 Ci/mmol, MP Biomedicals) using T4 Polynucleotide Kinase (PNK, Thermo Scientific) and Primer Extension System - AMV Reverse Transcriptase (Promega) commercial kit. Labelling reaction was prepared as described in the Table 9.

[Table 9] The composition of labelling reactions

Primers			DNA marker	
1 µl	primer (10 µM)		5 µl	PhiX174 HingI marker (250 ng, Promega)
1 µl	T4 PNK 10x buffer		1 µl	T4 PNK 10x buffer
3 µl	γ^{32}P-ATP (6000 Ci/mmol)		3 µl	γ^{32}P-ATP (6000 Ci/mmol)
1 µl	T4 PNK (10u/µl)		1 µl	T4 PNK
4 µl	RNase-free water			

Reaction was incubated at 37°C for 10 minutes and stopped by heat inactivation at 75°C for 10 minutes. Reaction was diluted by adding 90 and 190 µl of RNase-free water to primer and DNA marker, respectively.

Incorporation of the isotope was determined using Primer Extension System - AMV Reverse Transcriptase (Promega) kit. Briefly, 4 µl of previously diluted primer/DNA marker was further diluted with 12 µl of water. Three microliters of samples were spotted always on 4 Whatman filters (1x1 cm squares) and let dried for 1-3 minutes. Two of the filters (for the measurement of incorporated isotope) were washed for 5 minutes in a beaker with 100 ml of 0.5M sodium phosphate buffer (pH 6.8), then washed for 10 minutes in a beaker with 300 ml of 0.5M sodium phosphate buffer (pH 6.8). After drying the filters, radioactivity of unbathed and bathed filters was measured using Geiger counter and incorporation measured as a ratio between radioactivity of washed (incorporated) and unwashed (total) filters. Incorporation of the isotope was in the range of 20-34%.

3.2.11.2 Primer extension reaction

Reaction was performed using RevertAid™ First Strand cDNA Synthesis Kit (Thermo Scientific). Reverse transcription was always performed with two gene-specific primers, YAC06 (against the *CUP1* reporter) and YU14 (against the U14 snoRNA, serving as a loading control).

- A mixture of RNA (5 µg), 1 µl of radioactivity-labelled YAC06 and 1 µl of YU14 primer was filled to a total volume of 12.5 µl with water and vortexed, spun down and incubated at 65°C for 5 min. Samples were cooled on ice.
- A reverse-transcription premix (below) was added to sample, mixed by pipetting, incubated for 5 min at room temperature and then for 1 h at 42°C.

  4 µl 5x Reaction Buffer

  0.5 µl RiboLockTM RNase Inhibitor (40u/µl)

  2 µl dNTP Mix (10 mM)

  1 µl RevertAid^{TM} M-MuLV Reverse Transcriptase (200u/µl)
- Reaction was terminated by adding 20 µl of loading buffer (98% formamide, 10 mM EDTA, 0.1% bromophenol blue) and stored in a lead container at -20°C.

3.2.11.3 Primer extension analysis

Samples after primer extension reaction were run on vertical polyacrylamide gel electrophoresis using model V16 system from Bethesda Research Laboratories. Composition of the polyacrylamide gels is described in the Table 10. Mix for the polyacrylamide gels can be stored at 4°C for up to one month.

[Table 10] Composition of polyacrylamide gels (per one 50 ml gel)

	Amount	Final concentration
38% Acrylamide/ 2% BIS	10 ml	8%
urea	21 g	7M
10x TBE buffer*	5 ml	1x
deionized water	17.5 ml	-l

**(1M Tris, 1M boric acid, 20mM EDTA)*

Polymerization of the gel was induced by adding 250 µl of 10% (w/v) APS and 35 µl of TEMED to 50 ml of mix prepared earlier. Electrophoresis cell was assembled and filled with 1x TBE buffer. Gel was pre-heated by running it for 20 minutes under the constant voltage of 280 V (Lightning Volt Power Supply Model OSP-4000L, OWL Separation systems).

Marker was prepared by mixing 1 µl of radioactivity-labelled DNA marker, 9 µl of TE buffer and 10 µl of loading buffer (see above). Marker and samples were denatured by incubation at 90°C for 10 minutes. Samples of the amount of 18 µl and 20 µl of the marker were loaded on gel by Hamilton pipette. Gels were run for the first 5 minutes under the constant voltage of 400 V and then reduced to 340 V.

Separated gel was wrapped into a plastic foil and incubated inside the cassette with Imaging Screen-K (Kodak) for 16 hours. Afterwards, radioactive signal was detected using External laser molecular imager FX (Bio-Rad) on Molecular Imager® PharosFX (Bio-Rad). Signal was captured and saved as a TIFF file using Quantity One 4.5.2 (Bio-Rad). Imaging Screen-K (Kodak) was restored on the Screen Eraser-K (Bio-Rad) for 2-times 15 minutes.

3.3 Protein techniques

3.3.1 Preparation of denatured protein extracts

Yeast culture was grown until it reached mid-exponential phase. Volume equivalent to 1 ml of OD600 = 3 was harvested by centrifugation (2000g, 3 min). Pellet was washed in 1 ml of deionized water, transferred to a microtube, centrifuged (11000g, 30 sec) and supernatant discarded. Cell pellet could be stored in -80°C. All subsequent procedures were performed on ice.

- Pellet was resuspended in 100 µl of freshly prepared 1,85 M NaOH with 7% β-mercaptoethanol, vortexed for 2 min and then incubated on ice for 10 min.

- Proteins were precipitated by adding 100 µl of 50% trichloroacetic acid. Samples were incubated on ice for 5 min and centrifuged (12000g, 10 min, 4°C).
- Sediment was resuspended in 500 µl of 1 M Tris and centrifuged (12000g, 10 min, 4°C).
- Supernatant was quantitatively removed, sediment resuspended in 100 µl 2x Laemmli buffer (0.112 M Tris-HCl, pH 6.8, 3.42% SDS, 12% (v/v) glycerol, 0.002% bromophenol blue) and incubated for 5 min at 95°C. Protein extracts were stored in -20°C.

3.3.2 Denaturing polyacrylamide gel electrophoresis (SDS-PAGE)

SDS-PAGE was performed using Mini-PROTEAN® Tetra handcast system (Bio-Rad) according to the manufacturer's instructions. Standard Tris-glycine polyacrylamide gel that consist of 12% separating and 4% stacking gel was prepared using plates with 0.75 mm integrated spacers with compounds described in the Table 11.

[Table 11] Composition of polyacrylamide gels (per one slab)

	4% stacking gel	**12% separating gel**
30% Acrylamide/0.8% BIS	325 µl	2.00 ml
1.5 M Tris-HCl/ 0.4% SDS, pH 8.8	-	1.25 ml
0.5 M Tris-HCl/ 0.4% SDS, pH 6.8	625 µl	-
deionized water	1.55 ml	1.75 ml
TEMED	2.5 µl	3.4 µl
10% (w/v) APS	12.5 µl	16.5 µl

- Electrophoresis cell was assembled and filled with 1x running buffer (25 mM Tris-HCl, 190 mM glycine, 0.1% SDS, pH 8.3).
- Protein samples (see above) were thawed and 20 µl of an extract was transferred to a new microtube supplied with 1 µl of 1 M dithiothreitol. Mix was denatured at 95°C for 5 min and 15 µl of denatured extracts and 5 µl of PageRuler™ Plus Prestained Protein Ladder (Thermo Scientific) were loaded on gel using Hamilton syringe.
- Electrophoresis was performed under the constant current with 10 mA/gel in stacking gel and 20 mA/gel in separating gel.

3.3.3 Western blot (wet transfer)

Proteins were transferred to a nitrocellulose membrane using the Mini Trans-Blot® cell (Bio-Rad) according to the manufacturer's instructions.

- Transfer sandwich was set up under the transfer buffer (25 mM Tris, 192 mM glycine, 20% methanol) using a foam pad, filtration paper (Whatman, 3 mm), gel, nitrocellulose membrane (Bio-Rad, 0.45 µm), filtration paper (Whatman, 3 mm) and a foam pad, respectively.
- Transfer was performed under the constant voltage of 110 V for 1.5 hours. Apparatus was cooled during the transfer by using cooling units.
- Nitrocellulose membrane was washed with TBS buffer (20 mM Tris-HCl, 500 mM NaCl, pH 7.5) and blocked in 0.1% TTBS buffer (TBS buffer containing 0.1% Tween 20) supplied with 5% nonfat dry milk for 1 hour on a rocker-shaker.

3.3.4 Immunodetection of proteins

- Staining was performed with anti-HA mouse primary antibody (HA.11, MMS-101P-500, Covance) diluted 1000 times in blocking buffer (0.1% TTBS buffer/5% nonfat dry milk). Membrane was incubated with the primary antibody at room temperature for 1 hour and then overnight at 4°C on a rocker-shaker.

- Membrane was washed 3 times for 10 minutes in 0.05% TTBS buffer on a rocker-shaker. Then, it was incubated for 1 hour on a rocker-shaker with secondary goat anti-mouse IgG (H+L) antibody, conjugated with alkaline phosphatase (GAM-AP, Bio-Rad), diluted 4000 times in 0.05% TTBS buffer/3% non-fat dry milk.
- Membrane was washed 4 times for 10 minutes in 0.05% TTBS buffer and 2 times for 5 minutes in TBS buffer on a rocker-shaker.
- AP conjugate substrate kit (Bio-Rad) was used for the development of membrane according to the manufacturer's instructions. Membrane was washed in AP buffer and transferred to the color development buffer prepared immediately before use (6.5 ml AP buffer, 65 µl color reagent A, 65 µl color reagent B). Membrane was developed in darkness until the bands appeared. Reaction was stopped by washing the membrane in deionized water.

3.3.5 Staining of polyacrylamide gels

- Gels were stained in Coomassie stain buffer (20% methanol, 0.117% (v/v) Coomassie Brilliant Blue R-250 (Bio-Rad), 0.051% (v/v) Bismarck Brown R (Sigma), 7% acetic acid) after Western blotting for 30 min on an orbital shaker.
- Gels were de-stained in destaining buffer (7% acetic acid, 5% methanol) overnight on an orbital shaker.

4 Results

4.1 Impact of intron deletion on the expression of duplicated ribosomal protein genes

Firstly, we aimed to identify candidate pairs of RP genes, in which removal of intron affects not only the expression of its own gene (*intra*genic regulation) but also its paralog *in trans* (*inter*genic regulation). We used data from (Parenteau et al., 2011), who identified 36 pairs with intron-dependent intergenic regulation. They defined the regulation as reproducible change in the mRNA level of paralog *in trans* by at least 20% relative to *wild type* (*wt*) level in the absence of intron. We selected 7 most prominent pairs, which had at least 200% change in mRNA levels of at least one of the paralogs *in trans*. As summarized in the Figure 3, all 7 chosen pairs (*RPL16*, *RPL37*, *RPL17*, *RPS0*, *RPS18*, *RPL2*, *RPL22*) were shown to display a reciprocal positive intergenic regulation, i.e. removal of either intron led to downregulation of paralogs *in trans*. Furthermore, 11 of all selected RP genes display positive intragenic regulation, i.e. removal of intron led to downregulation of the host gene. Three RP genes (*RPL16A*, *RPL22A*, *RPL22B*) have a negative intragenic regulation, i.e. removal of intron led to upregulation of the host gene.

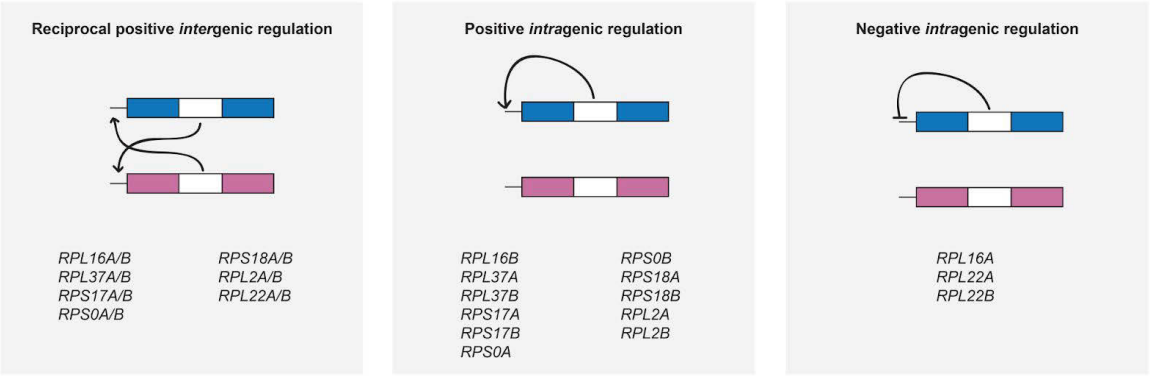

[Figure 3] Introns regulate the expression of candidate RP genes. Systematic analysis of intron deletions done by Parenteau and colleagues revealed *inter*genic regulation in all of our chosen pairs of RP genes. Moreover, all 14 genes show either positive or negative *intra*genic regulation. Figure was made based on the data from (Parenteau et al. 2011).

We systematically re-examined the impact of intron deletions on the steady-state mRNA levels of RP paralogs in all selected pairs. To replicate the finding of Parenteau and colleagues, we used same parental strains, primers and conditions as authors ((Parenteau et al. 2011) and J. Parenteau, personal communication). Diploid strains containing heterozygous intron deletion (Δi) in each RP paralog, kindly provided from Abou Elela lab, were sporulated and haploid cells selected for the presence of either *his3-ADE2* or *HIS3-ade2* auxotrophic markers (to allow for subsequent experiments). Intron deletion was confirmed by PCR genotyping (see the Supplementary Figure 1 for the example of *RPL2* strains preparation). Finally, we prepared strains lacking intron in either paralog A, paralog B or in both genes (summarized in the Figure 4A).

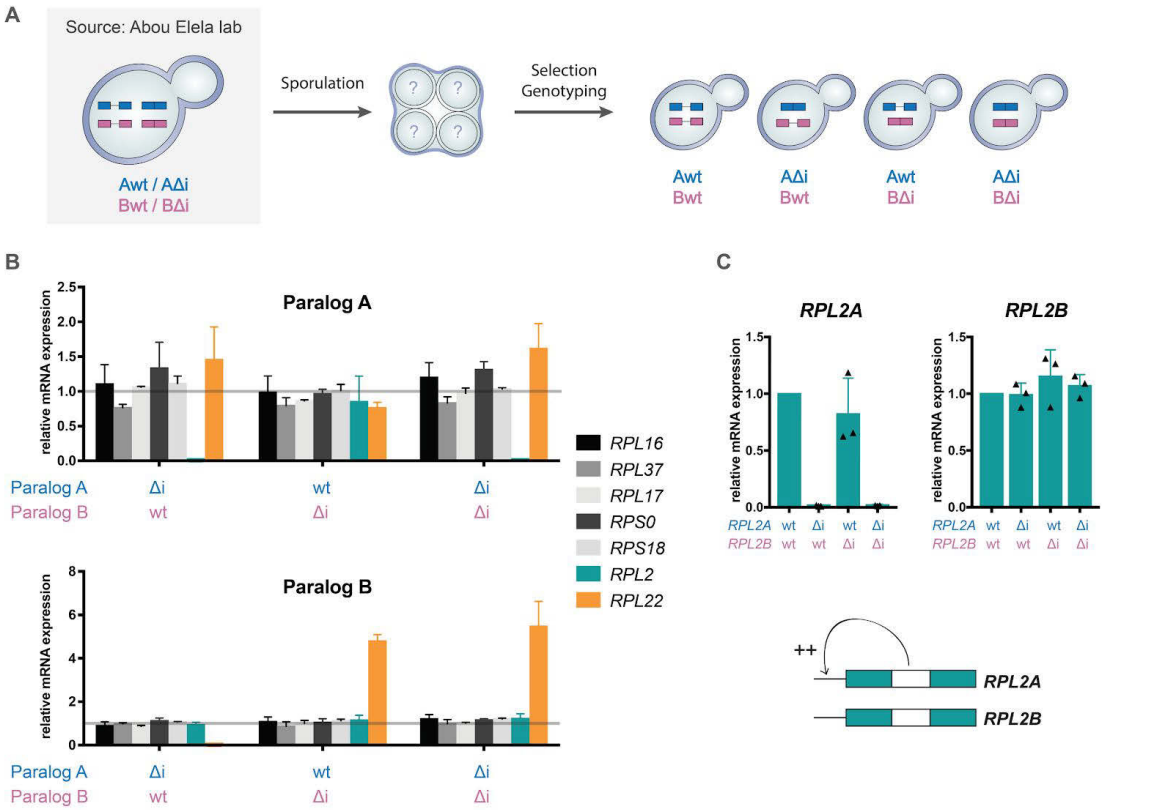

[Figure 4] Most introns can be removed with no effect on mRNA levels of duplicated RP genes. (A) Strategy to create haploid strains used for testing of candidate RP genes. (B) Shown is the mean mRNA expression of paralog A (up) and paralog B (down) in strains with deleted intron(s) (marked as Δi) relative to *wt*. Data were obtained by RT-qPCR and normalized to *SPT15* expression. Error bars represent s.d. of two (*RPL17*, *RPS0*, *RPS18*) or three (*RPL2*, *RPL16*, *RPL37*, *RPL22*) biological replicates. (C) Shown are the same expression data of *RPL2* genes as in (B), with emphasis on the *intra*genic regulation of *RPL2A* paralog. Triangles indicate values of individual replicates.

Based on the suggestions of J.Parenteau, we used freshly prepared haploid strains, i.e. made <1 month before analysis of mRNA expression (this is also why we obtained heterozygous strains instead of the same haploid strains as in (Parenteau et al. 2011)). We used long cultivation conditions in complex YPAD media by diluting pre-cultures so that cells could undergo at least 10 generations before reaching mid-exponential phase. Analysis was performed using RT-qPCR. Measured mRNA levels were normalized to *SPT15* expression and shown as relative expression to *wt* levels (Figure 4B).

We were not able to reproduce any impact of intron deletion on mRNA levels of *RPL16*, *RPL37*, *RPL17*, *RPS0* or *RPS18* pairs when repeated the experiments of (Parenteau et al. 2011) - loss of any intron had no apparent effect on the expression of neither host gene nor paralog *in trans* (Figure 4B). We tried different cultivation conditions with manipulated strains of *RPL16* and *RPL37* genes - either by using complex YPAD medium under standard cultivation conditions (2 generations before reaching mid-exponential phase, called “short”) or by using synthetic SD medium with the original, long cultivation. Nevertheless, none of the conditions replicated published findings and rather shown a mild if any effect of intron deletions (Figure 5).

On the contrary, we found a strong intron-dependent intragenic regulation of *RPL2A* gene, i.e. removal of intron in *RPL2A* gene leads to the loss of *RPL2A* expression with no effect on its paralog, *RPL2B*. Removal of *RPL2B* intron had no effect on any of the paralogs (Figure 4C).

The only pair with the reproducible intron-dependent intergenic regulation was *RPL22A/B*, which will be described later (Figure 4B). Since we aimed to identify candidate(s) with an intron-dependent intergenic regulation, the rest of this thesis is focused on the analysis of *RPL22A* and *RPL22B* paralogs.

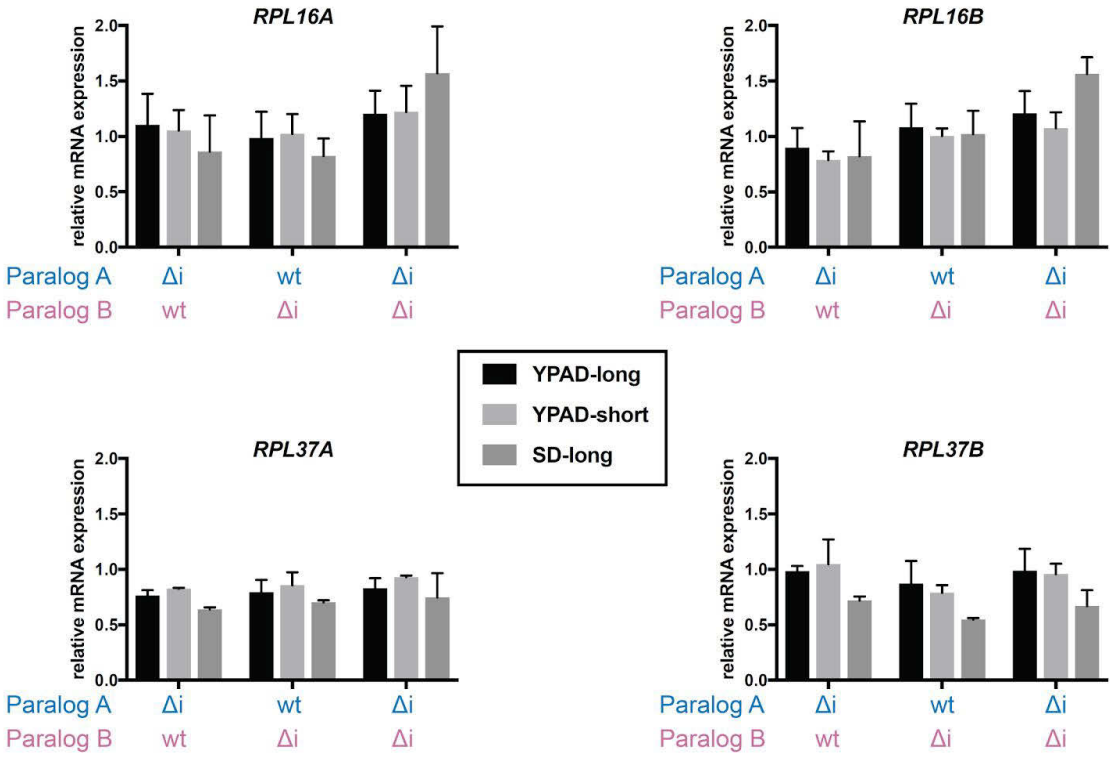

[Figure 5] Different cultivation conditions did not reveal the *inter*genic regulation between *RPL16* and *RPL37* paralogs. Plots show mean fold changes of mRNA levels of *RPL16* and *RPL37* paralogs relative to *wt* under different conditions. Data were determined by RT-qPCR and normalized to the *SPT15* expression. Error bars represent s.d. of two (YPAD-short, SD-long) or three (YPAD-long) independent biological replicates.

4.2 Intergenic regulation of *RPL22* paralogs is mediated by their introns

Since the study of Parenteau and colleagues was based on their own laboratory parental strain JPY10I (*MATa/α ura3Δ0/ura3Δ0 leu2Δ0/leu2Δ0 lys2Δ0/lys2Δ0 ADE2/ade2Δ::hisG HIS3/his3*Δ200), K.Abrhámová prepared intronless versions of *RPL22A* and *RPL22B* genes in commonly used haploid laboratory strains, BY4741 (*MATa his3Δ1 leu2Δ0 met15Δ0 ura3Δ0*) and BY4742 (*MATα his3Δ1 leu2Δ0 met15Δ0 ura3Δ0*), which were also used in the yeast ORF deletion collection (Winzeler et al. 1999). The effect of intron deletion on steady-state mRNA levels of *RPL22A* and *RPL22B* paralogs was consistent with the original tested strains and indeed confirmed the positive intron-dependent intergenic regulation between *RPL22* paralogs (compare first 4 columns in Figures 6A, 6B with the Figure 4B).

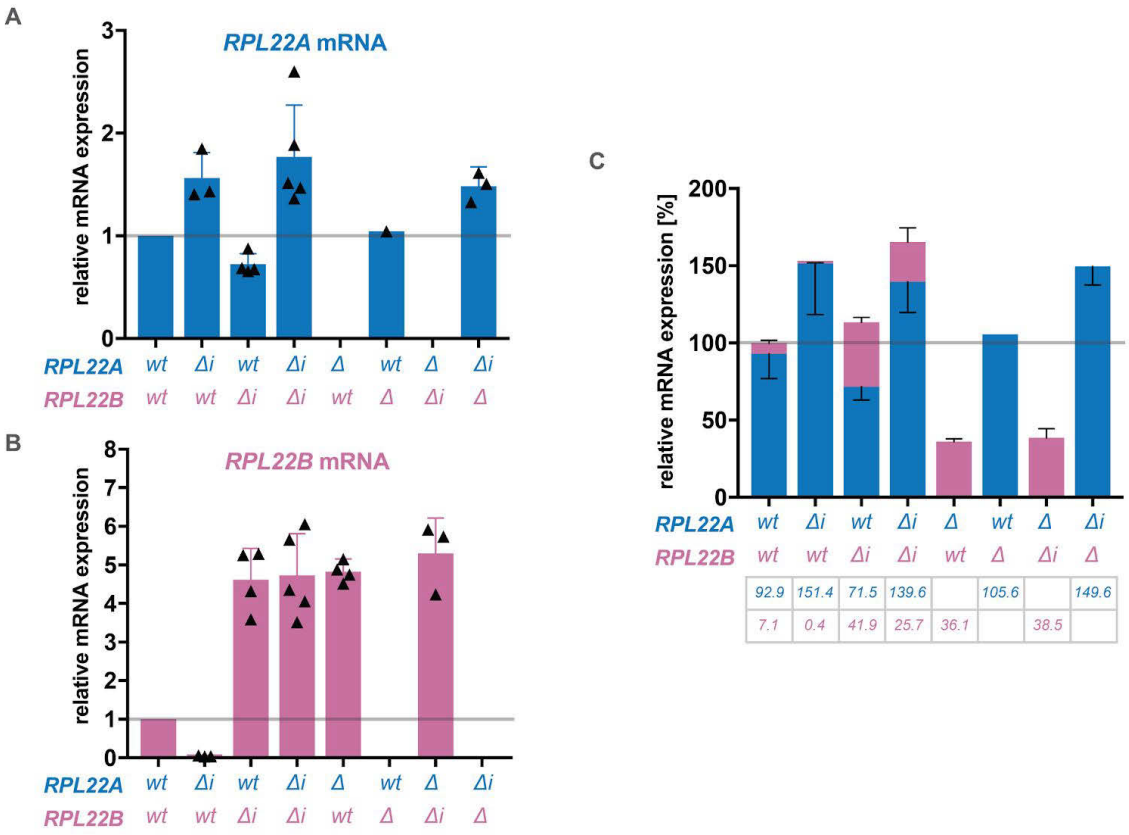

[Figure 6] Introns modulate the expression of *RPL22* paralogs. (A,B) Plots show mean fold changes of RPL22A (A) and RPL22B (B) mRNA levels relative to *wt* as determined by RT-qPCR. Data were normalized to the *SPT15* expression. Shown are individual values and error bars of s.d. from three (*AΔi-wt, AΔ-BΔi, AΔi-BΔ*), four (*wt-BΔi, AΔ-wt*) or five (*AΔi-BΔi*) biological replicates. (C) Data from (A,B) normalized to the total *RPL22* mRNA (*RPL22A* and *RPL22B*) level in *wt* cells.

To better capture the regulation, we renormalized our qPCR expression data to the total *RPL22* mRNA level (*RPL22A* and *RPL22B*) in *wild type* cells (Figure 6C). Recalculation allowed as to see that *RPL22A* paralog represents the majority (93%) of *RPL22* mRNA in cells. While the expression ratio *RPL22A/RPL22B* is 93/7 in *wt* cells, deletion of intron in the major *RPL22A* paralog resulted in the ratio of 151/0.4 (referred to the total *wt* level of *RPL22*), i.e. led to ~1.6-fold increase of *RPL22A*, complemented by the loss (~21-fold decrease) of *RPL22B* mRNA. *RPL22BΔ*i mutant showed a reciprocal phenotype with ~1.4-fold decrease in the abundance of *RPL22A* accompanied by ~4.6-fold increase in the amount of *RPL22B*, i.e. the ratio of *RPL22* paralogs was 72/42. Deletion of both introns resulted in the increase of *RPL22A* (~1.8-fold) and *RPL22B* (~4.7-fold) mRNA levels with the ratio of 140/26 (Figure 6C).

Because deletion of intron in any of the *RPL22* paralogs led to increase in the expression of its own gene (intragenic regulation) followed by decrease in the expression of paralog *in trans* (intergenic regulation), we reasoned that Rpl22 proteins have an inhibitory effect on the intron-containing gene. To test this hypothesis, we made use of *rpl22A⊿* and *rpl22B⊿* strains from the yeast ORF deletion collection (Winzeler et al. 1999). We also prepared double intron-gene deletion mutants, *rpl22A⊿ RPL22B⊿i* and *RPL22A⊿i rpl22B⊿* and verified the strains by PCR genotyping (data not shown). As hypothesized, deletion of the major *RPL22A* gene led to ~4.8-fold increase in the expression of *RPL22B*, similarly to ~5.3-fold increase in the double *rpl22A⊿ RPL22B⊿i* mutant, indicating that the Rpl22A protein might have inhibitory effect on the *RPL22B* expression, which however depends on the presence of *RPL22B* intron (e.g. compare *RPL22A⊿i* with *RPL22A⊿i RPL22B⊿i* mutant). Interestingly, while deletion of the minor *RPL22B* paralog had no effect on the expression of *RPL22A* paralog (while this was only measured once by me, K.Abrhámová measured independently the *RPL22A* expression and found similar effect), double *RPL22A⊿i rpl22B* mutant led to ~1.5-fold increase in the *RPL22A* mRNA level, similarly as in *RPL22A⊿i* mutant alone. Our experiments imply that both Rpl22A and Rpl22B proteins have an inhibitory effect on the expression of both intron-containing *RPL22A* and *RPL22B* paralogs.

4.3 Expression of *RPL22* paralogs is regulated on level of pre-mRNA splicing

Based on the observation that *RPL22A* and *RPL22B* exhibit intra- and intergenic regulations, which depend on the presence of introns, we aimed to test if the expression of *RPL22* paralogs is regulated on the level of pre-mRNA splicing. To test this hypothesis, we used primer extension analysis of pre-mRNA splicing using *RPL22*-derived reporter constructs cloned by M.Oplová. Briefly, the *RPL22A*-based reporter was made by phusion of *RPL22A* intron and flanking regions (38 bp upstream and 41 bp downstream of the intron) with the coding sequence of *CUP1*. The *RPL22B*-based reporter contains *RPL22B* intron as well as flanking regions of 56 bp upstream and 60 bp downstream of the intron. We

chemically transformed the splicing-reporter plasmids into yeast strains harbouring various deletions of *RPL22* paralog(s) and/or intron(s) and analyzed their splicing efficiency using primer extension assays (summarized in the Figure 7A).

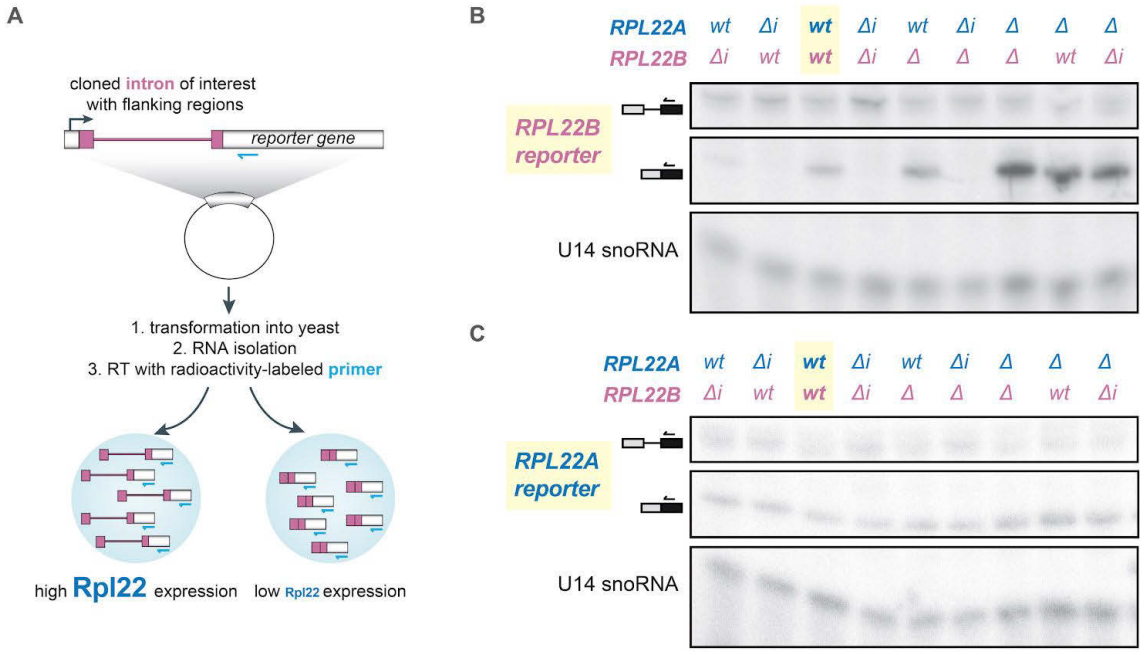

[Figure 7] Splicing of the *RPL22B* reporter is highly sensitive to the presence of Rpl22. (A) Scheme of the experiment to test splicing efficiency of *RPL22*-based reporters. (B,C) Shown are gels after primer extension analysis with radioactivity-labelled primers against constant part of the *RPL22B*- (B) and *RPL22A*-splicing reporter (C). Signal of the U14 snoRNA serves as a loading control. Shown are representative gels from three independent experiments.

We observed splicing of both reporters in *wt* cells, confirming the functionality of constructs (Figures 7B and 7C). Overproduction of *RPL22* (e.g. in the *RPL22AΔi* strain) blocked the splicing of *RPL22B*-based reporter, while both decrease (e.g. in the *rpl22AΔ* strain) and the complete loss of Rpl22 protein (*rpl22AΔrpl22BΔ* strain) led to higher signal of spliced *RPL22B*-derived reporter compared to *wt* levels. Blockage of the splicing did not lead to the accumulation of lariat-intermediate, but rather to increased levels of pre-mRNA species (Figure 7B). On the other hand, the splicing of *RPL22A*-based reporter was insensitive to different levels of *RPL22* and did not recapitulate endogenous levels of *RPL22A* mRNA (Figure 7C).

4.4 Rpl22 protein interacts with the stem-loop of *RPL22B* intron

Since the described regulation of Rpl22 depends on the presence of introns and Rpl22 protein itself, we speculated that interaction Rpl22 protein-intron might play a role in the control of pre-mRNA splicing. To test this hypothesis, we used yeast three-hybrid (3-H) system developed to assess RNA-protein interactions (SenGupta et al. 1996). In brief, protein of interest was fused with the Gal4 activation domain, while RNA of interest was fused with two MS2 loops. Interactions were tested in the strain expressing MS2 coat protein (which recognizes MS2 loops) fused with the LexA domain, which recognizes LexA motives, present upstream of the *HIS3* reporter gene. If interactions occur, Gal4 activation domain is brought to the proximity of *HIS3* reporter and activates its expression, therefore cells would grow in media without histidine (Figure 8).

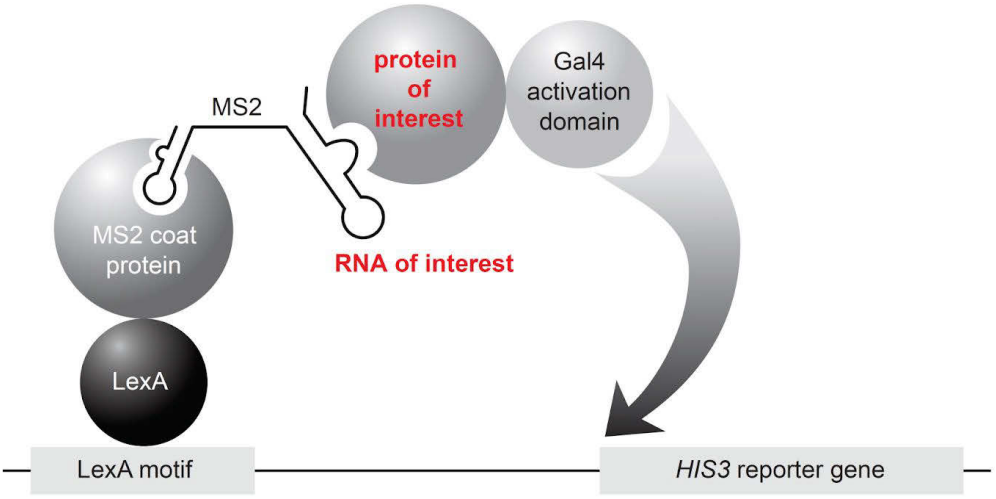

[Figure 8] Yeast three-hybrid system used to assay protein-RNA interactions. In the case of interaction between RNA and protein of interest, Gal4 activation domain is brought to the proximity of *HIS3* reporter and activates its expression. Adapted from (Stumpf et al. 2008).

We used the pair iron-responsive element (IRE) - iron regulatory protein (IRP) as positive control, which has been shown to interact in 3-H system using *HIS3* reporter, even when plated on media with 3-aminotriazole, a competitive inhibitor of the enzymatic function of the *HIS3* reporter (Klopotowski and Wiater 1965). We could recapitulate the IRE - IRP interaction in our system (growth on media without

Histidine), while empty plasmids or only one of the partners did not induce the growth (Figure 9B and data not shown).

We tested the whole *RPL22B* intron (called *I*) as well as 3 regions (called *I1-3*), which represent 3 distinct domains of the intron predicted secondary structure (Figure 9A). Even more importantly, the regions were selected to not contain more than three consecutive thymidine residues, which can terminate transcription of RNA in the 3-H system (the whole intron contains four of such regions). The regions were PCR amplified with primers introducing *PaeI* site on both 5' and 3' end, digested and cloned into p3HR2 plasmid containing two MS2 loops downstream of the cloned fragments. Plasmid maps and sequencing results confirming successful cloning are shown in the Supplementary Figure 2.

When tested the prepared constructs with both, Rpl22A and Rpl22B proteins in 3-H system, we identified the *I2* region of *RPL22B* intron interacting with Rpl22 paralogous proteins. The *I2* represents 72 bp part of *RPL22B* intron and is potentially folded to stem-loop (Figure 9). While we could see the interaction of Rpl22 with the part of *RPL22B* intron, whole-intron construct did not interact - most probably because of the presence of transcription terminator signals for RNA polymerase III, used for the expression of RNA baits (the proteins fused with HA-Gal4 activation domain were expressed in all tested combinations, see the Figure 10).

We also examined the mutated versions of Rpl22A and Rpl22B with lost ability to block pre-mRNA splicing of *RPL22* paralogs when ectopically overexpressed, prepared by K.Abrhámová (Abrhámová et al. 2018). These mutants lost their binding capacities to the *I2* stem-loop of *RPL22B* intron (Figure 9B), potentially explaining the regulatory defects.

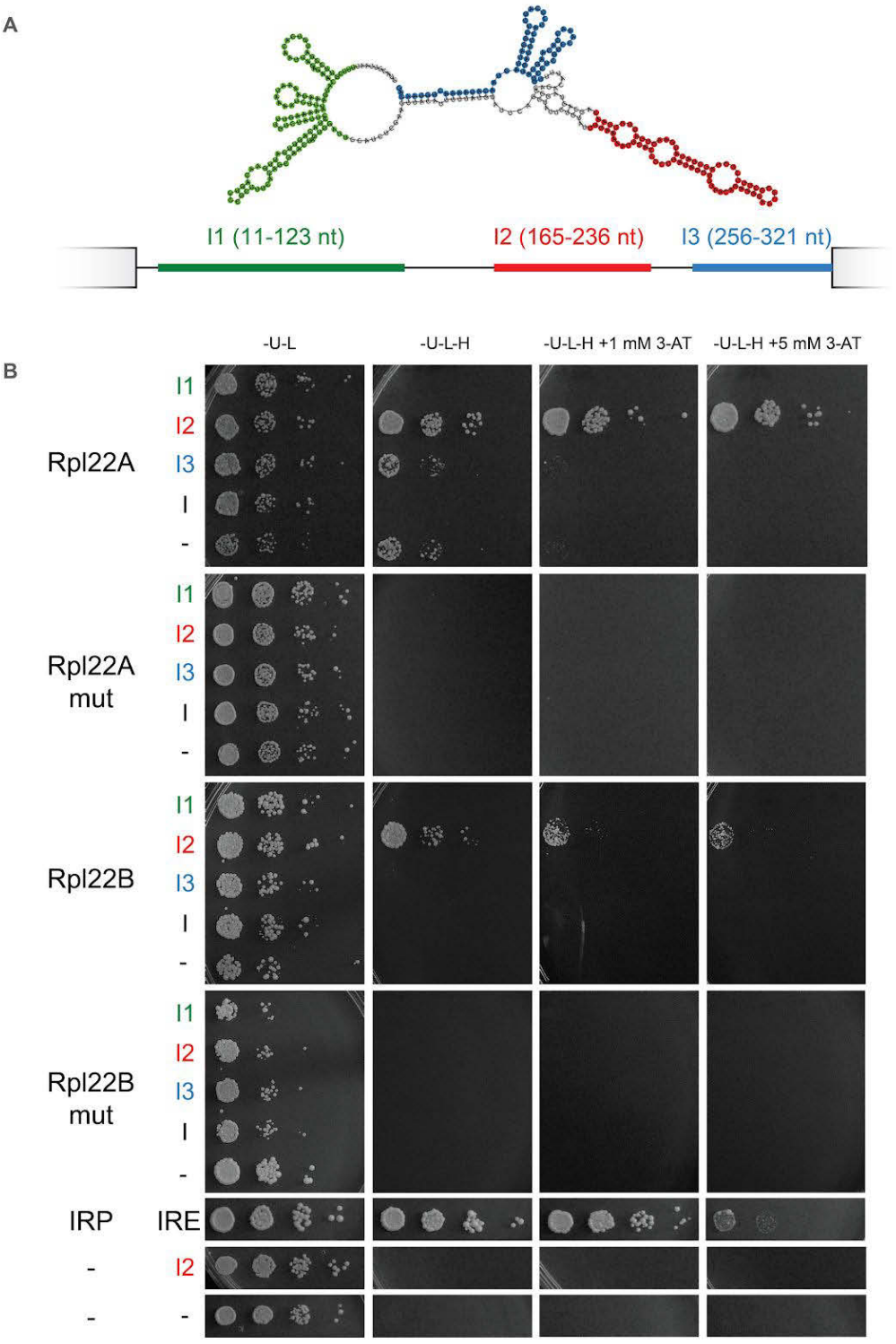

[Figure 9] Yeast three-hybrid system identified the region of *RPL22B* intron interacting with Rpl22 proteins. (A) Secondary structure prediction of the *RPL22B* intron with respective *I1-3* regions shown in color. Prediction was made on the RNAfold web server. (B) RNA-protein interactions were assayed using yeast 3-H system with the *HIS3* reporter. Cells were spotted in 10-fold serial dilutions on plates without Ura, Leu (-U-L) to confirm the presence of both plasmids, as well as on media without His (-U-L-H) or additionally in the presence of 3-aminotriazole (3-AT), to test the interactions. IRP-IRE interaction serves as positive control. "-" means the presence of empty 3-H vectors. Shown are representative plates from three independent experiments.

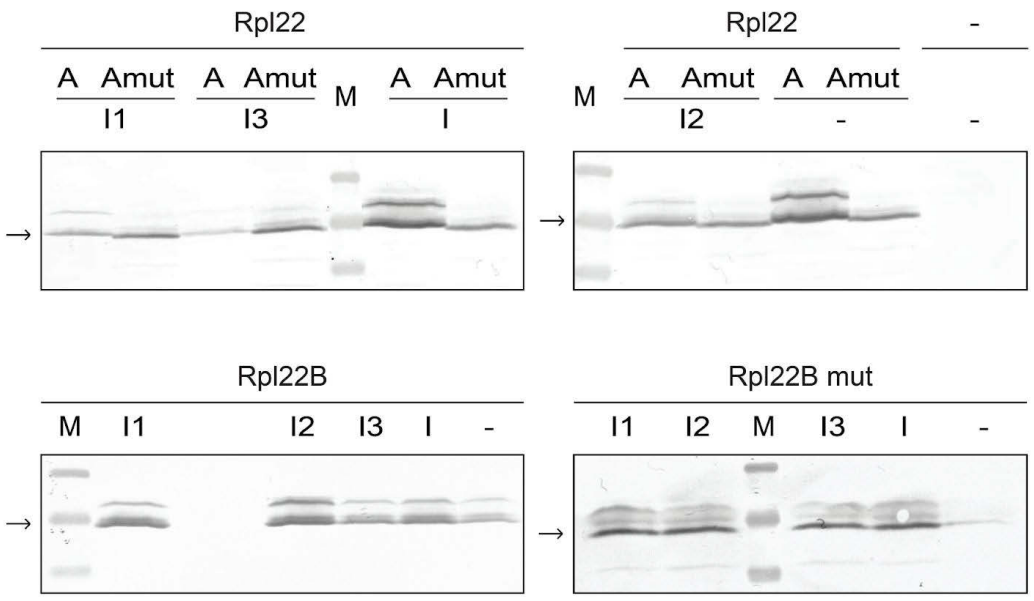

[Figure 10] All Rpl22 proteins used in the 3-H were expressed. Production of all proteins used in the 3-H system was verified using Western blot analysis with anti-HA antibody against the HA-tagged Gal4 activation domain. Hybrid proteins of 31 kDa (marked with an arrow) were detected in extracts of the strain with all tested constructs. M - size marker PageRuler™ Plus Prestained Protein Ladder (Thermo Scientific). All membranes were cut to show 25 - 40 kDa part.

4.5 Some orthologous Rpl22 proteins have preserved the regulatory function

Our laboratory has recently shown that the intergenic intron-dependent regulation of *RPL22* paralogs in *S.cerevisiae* (presented above) most probably evolved from the intron-dependent *auto*regulatory feedback loop, since the regulation is present also in yeast *Kluyveromyces lactis* with the single *RPL22* gene (see our work (Abrhámová et al. 2018)). We hypothesized that *K.lactis* Rpl22 regulates the expression of its own gene in the same manner and therefore retains the same binding capacities. Indeed, we confirmed the interaction between *K.lactis* Rpl22 and the *I2* stem-loop of *RPL22B*, when tested by yeast 3-H system (Figure 11A and Supplementary Figure 3A).

We aimed to test more distal orthologs of *S.cerevisiae* Rpl22 proteins and possibly expand our set of *I2*-interacting partners. We assessed the binding of distal Rpl22 relatives from *Schizosaccharomyces pombe* and *Homo sapiens*. Surprisingly,

while the *S.pombe* Rpl22 does not interact with the *RPL22B* intron in 3-H system (despite being expressed, Figure 11B and Supplementary Figure 3), we observed the interaction of human Rpl22 with yeast *I2* region (Figure 11A). The mass of colonies was much smaller in the case of *H.sapiens* Rpl22, either suggesting a weaker interaction or a higher toxicity of ectopically overexpressed human protein in yeast (Tugendreich et al. 2001).

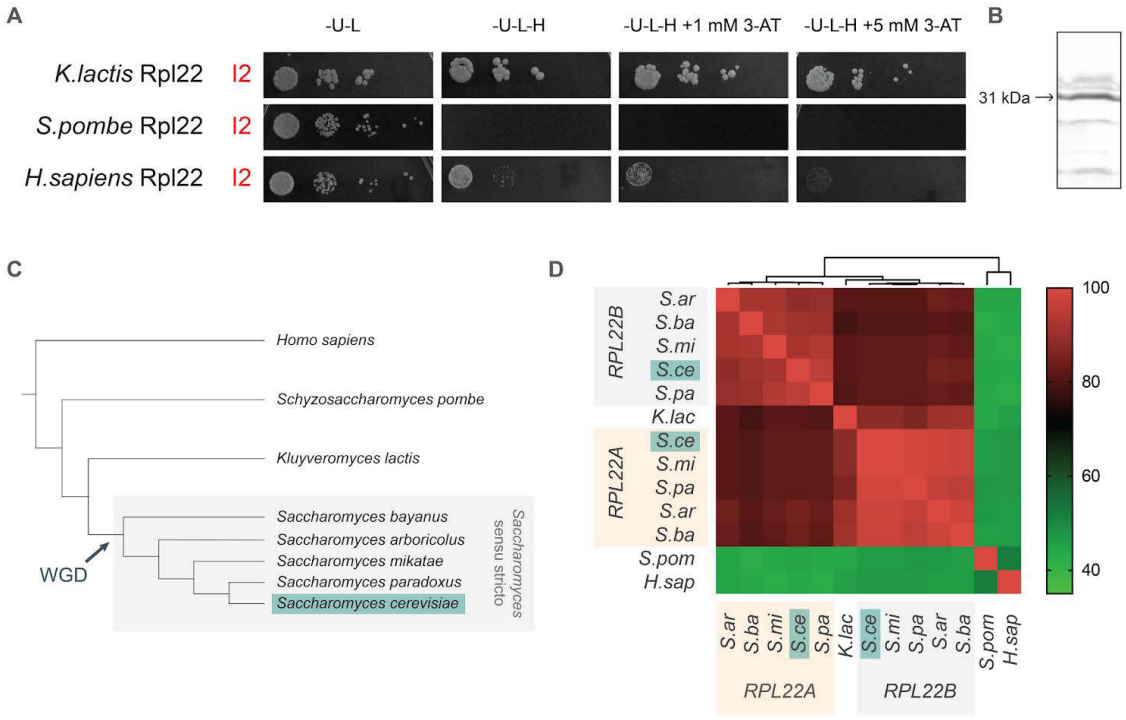

[Figure 11] *K.lactis* and *H.sapiens* Rpl22 orthologs interact with the stem-loop of *RPL22B* intron. (A) Interactions of Rpl22 orthologs with the *I2* stem-loop assayed using yeast 3-H system with the *HIS3* reporter. Cells were spotted in 10-fold serial dilutions on plates without His (-U-L-H) or additionally in the presence of 3-aminotriazole (3-AT). Shown are representative plates from at least three independent experiments. (B) Western blot analysis with anti-HA antibody against HA-tagged Gal4 activation domain. Shown is band representing hybrid *S.pombe* Rpl22 protein of 31 kDa. Membrane was cut to show 15 - 40 kDa part. For the original membrane with respective controls see Supplementary Figure 3B. (C) Schematic representation of the phylogenetic relations between species used in (D) based on the (Scannell et al. 2011). Branch lengths are not proportional to the species divergence. WGD - whole genome duplication. (D) Heatmap showing percentage of identity between Rpl22 orthologs calculated by Clustal2.1. Hierarchical clustering is based on the average linkage using Euclidean distance measurement method.

Intrigued by findings that distal Rpl22 orthologs are capable of the interaction with *I2* stem-loop of *S.cerevisiae RPL22B* intron, we intended to compare protein sequences of tested species and potentially identify conserved residues responsible for the binding. We expanded our list of orthologs by 4 *Saccharomyces sensu stricto* species - all undergone whole-genome duplication and containing two Rpl22 paralogs (Figure 11C). When compared sequences of Rpl22 orthologs by multiple sequence alignments and plotted results by their sequence identity, we recognized two distinct clusters - one containing all Rpl22B orthologs of *Saccharomyces sensu stricto* group, which share on average 91.6% sequence. Interestingly, Rpl22A orthologs and Rpl22 of *K.lactis* cluster together and have on average 94.4% identity. These two clusters differ on average in 18.4% of protein sequence. On the contrary, both *S.pombe* and human Rpl22 orthologs show no apparent conservation and share only around 45% of protein sequence compared to Saccharomycetaceae species (Figure 11D).

4.6 Structured region of *K.lactis RPL22* intron interacts with Rpl22 proteins

K.lactis Rpl22 shares a high similarity with *S.cerevisiae* Rpl22 orthologs and is capable to interact with the I2 region of *RPL22B* intron as well as to ensure the intron-dependent regulation in both *Kluyveromyces lactis* and *S.cerevisiae* (see above and (Abrhámová et al. 2018)). We reasoned that similar structured region of *RPL22* intron might be responsible for the binding of Rpl22 in *K.lactis*. We selected 3 regions (with 2 overlapping subregions) of *K.lactis RPL22* intron, which represent 2 distinct domains of intron predicted secondary structure (Figure 12A). Regions I1.1 and I2 were selected to not contain more than three consecutive thymidine residues, which can terminate transcription of RNA in the 3-H system. I1.2 region (containing also I1.1) covers larger part of predicted stem-loop and was tested despite containing six consecutive thymidine residues. The regions were PCR amplified with primers introducing *PaeI* site on both 5’ and 3’ end, digested and cloned into p3HR2 plasmid containing two MS2 loops downstream of the cloned fragments (see the Supplementary Figure 4 with sequencing results confirming successful cloning).

We identified I2 structural region of the *K. actis RPL22* intron, which interacts with both Rpl22A of *S.cerevisiae* and Rpl22 of *K.lactis* in the 3-H system (Figure 12B). The mass of colonies was much smaller compared to *S.cerevisiae* 3-H screen (Figure 9B) and might indicate weaker interactions compared to the I2 region of *RPL22B* intron. We found that both I2 of *S.cerevisiae RPL22B* and I2 of *K.lactis RPL22* consist of highly similar parts, as seen on the sequence alignment (Figure 12C). The conserved parts also potentially form the same secondary substructure as predicted by the exact sequence-structure matching (Figure 12D).

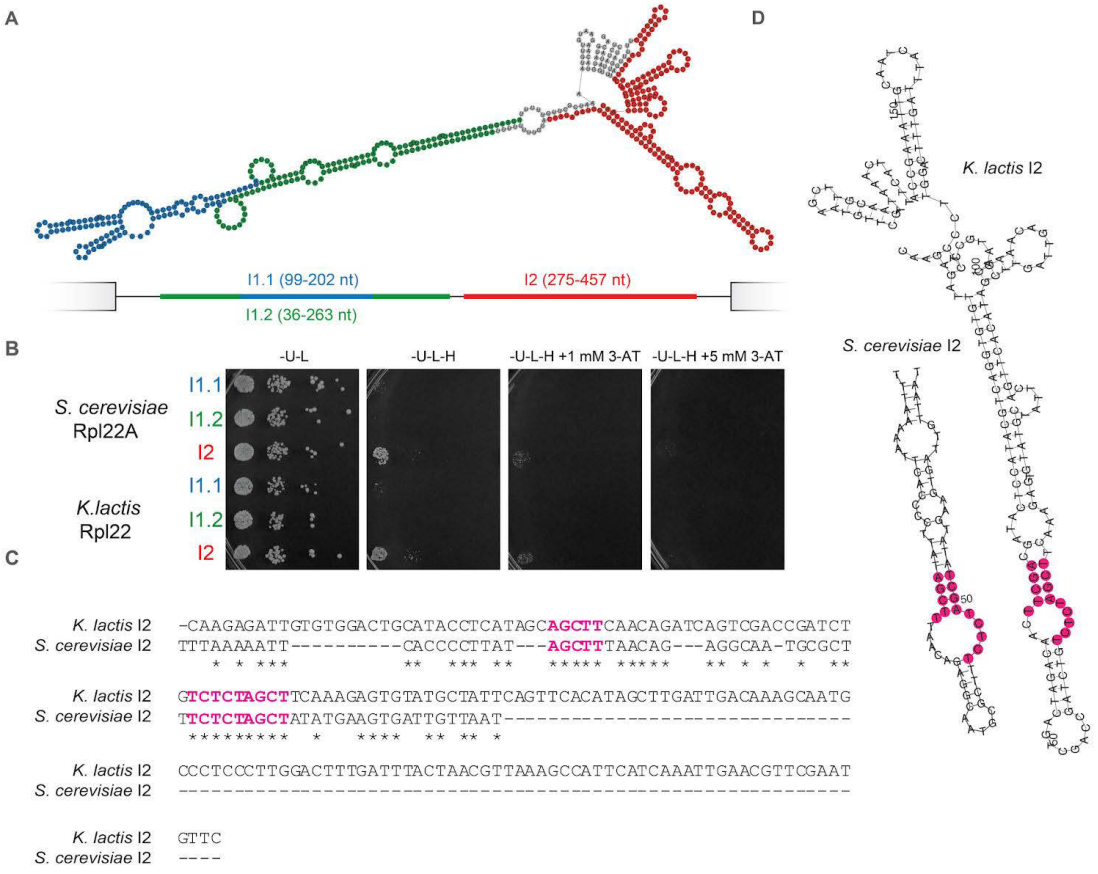

[Figure 12] Identification of Rpl22 binding site in the *RPL22* intron of *K.lactis*. (A) Secondary structure prediction of *K.lactis RPL22* intron with respective *I1.1, I1.2* and *I2* regions shown in color. Prediction was made on the RNAfold web server. (B) RNA-protein interactions assayed using yeast 3-H system with the *HIS3* reporter. Cells were spotted in 10-fold serial dilutions on plates without His (-U-L-H) or additionally in the presence of 3-aminotriazole (3-AT). Shown are representative plates from three independent experiments. (C) Alignment of *K.lactis RPL22* I2 and *S.cerevisiae RPL22B* I2 DNA sequences made in CLUSTAL multiple sequence alignment by MUSCLE (3.8). (D) Comparison of predicted secondary structures of I2 regions identified shared local sequence-structure patterns based on exact matching of at least 7 nucleotides using ExpaRNA (1.0.0). Found substructure is highlighted by magenta in (C) and (D).

4.7 Study of *RPL22* introns identified conserved regions

Excited by the finding of shared substructure in Rpl22-interacting intronic regions by 3-H system, we aimed to analyze intron sequences and to find potential regulatory elements. We expanded our list by *Saccharomyces sensu stricto RPL22A* and *RPL22B* orthologs, since they most probably retained the Rpl22 regulatory circuit described above, which evolved before the *RPL22* duplication (Abrhámová et al. 2018).

While different yeast species share on average 84.5% of *RPL22* coding sequence, introns have higher evolvability with overall 64.3% identity. Interestingly, *K.lactis RPL22* shares higher similarity with *RPL22A* orthologs on both protein (Figure 11D) and coding sequence (Figure 13A). Additionally, comparison of introns based on their identity reveals slightly higher similarity of *K.lactis RPL22* with *RPL22A* orthologs (Figure 13B).

We found several conserved regions present in *RPL22* introns from the sequence alignment of introns (Figure 13C). Three of them - 5' splice site, branch site, and 3' splice site - were expected to be conserved and represent essential elements for the pre-mRNA splicing. The other two conserved regions are *RPL22*-specific and are located upstream of the branch site - the upstream conserved element of 24 nt (GCTATTCTGTATTTTAAAAATTCA in *RPL22B* of *S.cerevisiae*), which contains 3 non-conserved nucleotides, and the downstream conserved elements of 20 nt (TGATTGTTAATAGCAGTAGG) identical in all testes orthologs. While the *S.cerevisiae RPL22B* I2 region partially overlap with both conserved elements, the *K.lactis RPL22* I2 region does not. However, when compared the parts shared by both I2 (Figure 12C), we found conserved elements in the *K.lactis* intron, which are either overlapping or are in the close proximity of conserved regions present in the *RPL22B* intron of *S.cerevisiae* (Figure 13C).

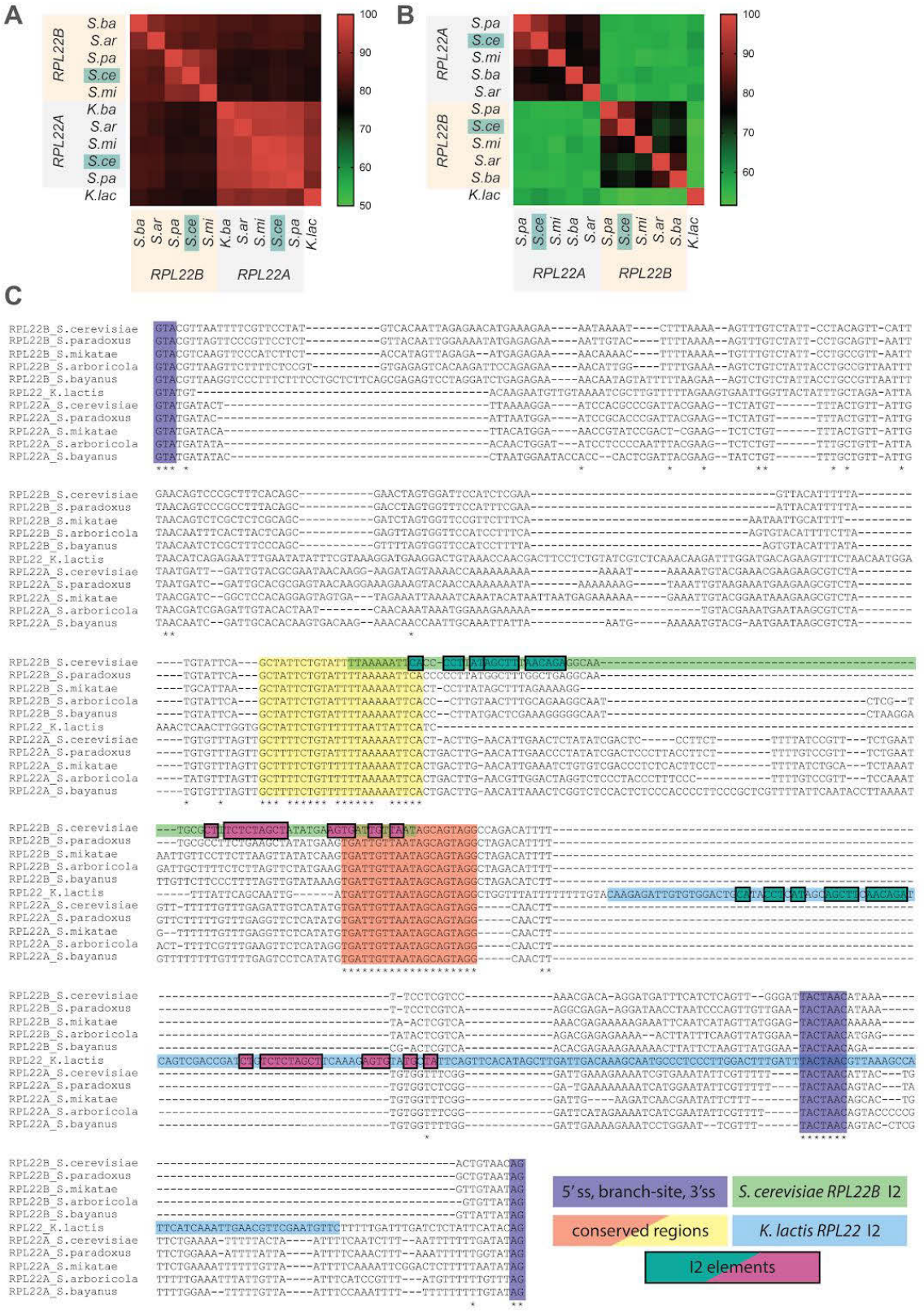

[Figure 13] Conservation of orthologous *RPL22* introns. (A,B) Heatmap showing the percentage of identity between coding sequences (A) and introns (B) of *RPL22* orthologs calculated by Clustal2.1. (C) Sequence alignment of orthologous *RPL22* introns made in CLUSTAL multiple sequence alignment by MUSCLE (3.8) and manually re-aligned using Jalview 2.10.

We then focused on the predicted secondary structures of introns (Figure 14A). While both conserved regions in *RPL22B* intron are predicted to interact with each other and therefore make the stem-loop responsible for interaction with Rpl22 proteins, conserved regions in *RPL22A* and *RPL22* of *K.lactis* do not (Figure 14B). The part between two conserved regions (which is responsible for the interaction in 3-H system) is very short (18 nt) in *K.lactis RPL22* intron. Nevertheless, the *K.lactis* I2 interacting part is outside of part flanked by the conserved regions. Interestingly, when marked I2 elements as found in the alignment (see Figure 12C) with the same color in both I2 regions of *RPL22B* and *RPL22* of *K.lactis*, we can see a larger homology than by only comparing the exact sequence-structure matching (compare Figure 12D and 14C).

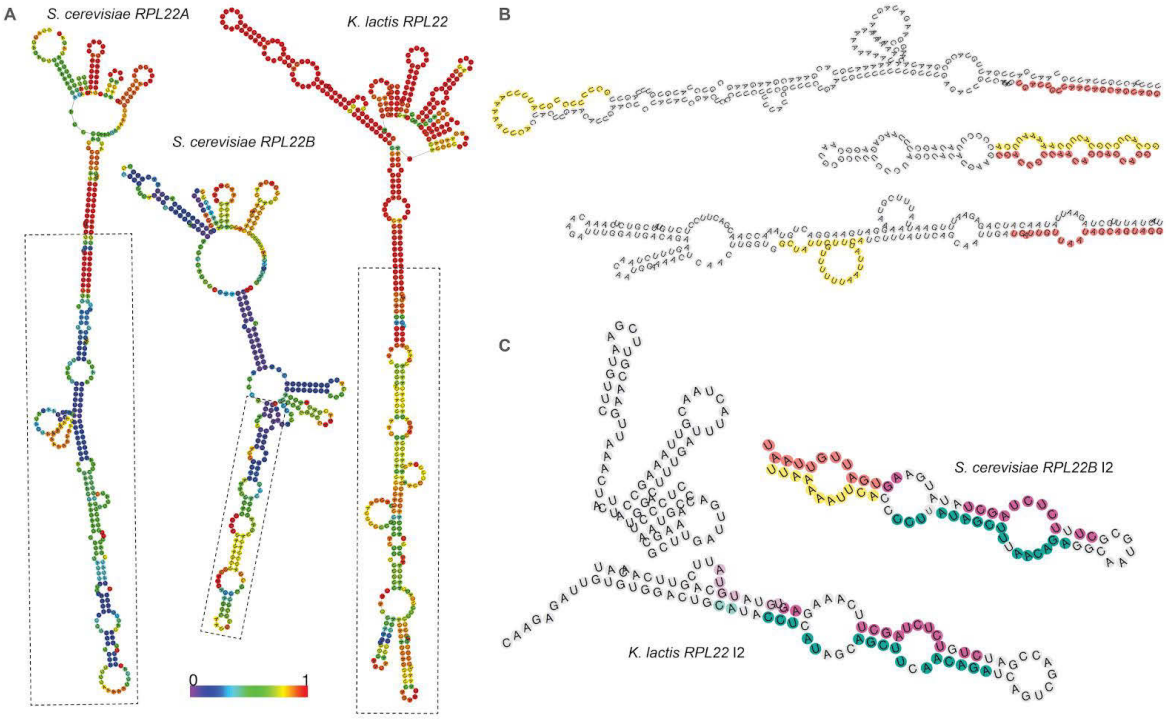

[Figure 14] Predictions of secondary structures of studied introns. (A) Secondary structure prediction of introns made on the RNAfold web server. Drawn are minimal-free-energy structures with color coded base-pair probabilities. (B) Shown are indicated regions from (A) with the colored conserved elements as in the Figure 13C. (C) Shown are predicted secondary structures of I2 regions with highlighted I2 elements found in the Figure 13C.

4.8 Limited production of Rpl22 leads to growth defects in yeast

RPL22 paralogs are not essential in yeast *S.cerevisiae* (Costanzo et al. 2010). However, we noticed a reduced growth of strains with deletion of either major *RPL22A* paralog (therefore having only 36% of *wt* levels of *RPL22* mRNA, see the Figure 6C) or with double-deletion *rpl22AΔrpl22BΔ*. We intended to measure growth parameters of strains used in this study. We used two different cultivation conditions. The strains were either cultivated in complex YPAD medium and the optical density of biomass was measured every 10 minutes using Varioskan Flash reader (Thermo Fisher). Independently, the strains were cultured in synthetic SD medium and the density was manually measured every 120 minutes using CO8000 Cell Density Meter. While the growth of strains with intron(s) deletions and *RPL22B* deletion was comparable to *wild type* strain, strains with either *rpl22AΔ* or *rpl22AΔrpl22BΔ* genotype have on average 1.5 and 1.6-times longer doubling time, respectively (Figure 15).

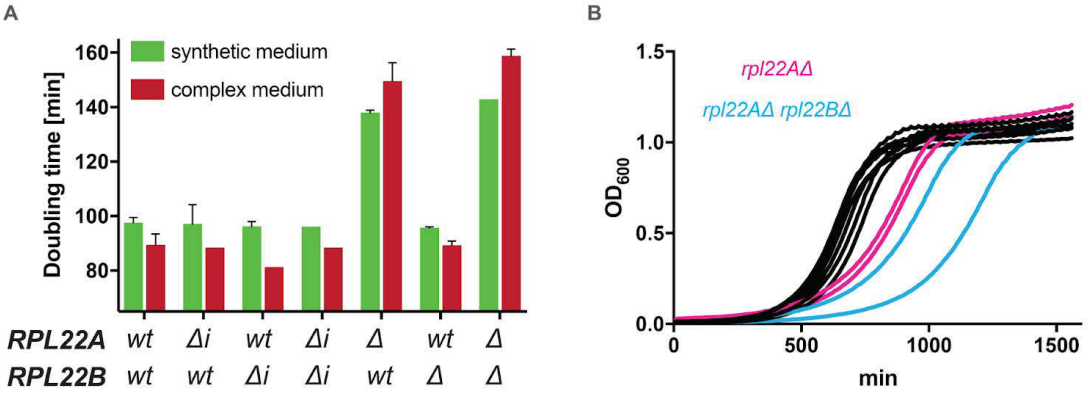

[Figure 15] Slow growth phenotype is a result of limited Rpl22 production. (A) Shown is doubling time calculated from the slope of logarithmically transformed exponential phase growth data. Optical density was measured either every 10 min using Varioskan Flash reader (complex medium) or every 120 min using CO8000 Cell Density Meter (synthetic medium). Error bars represent s.d. of two independent replicates (strains *AΔi-wt, wt-BΔi, AΔi-BΔi* in the complex medium and *AΔ-BΔ* in the synthetic medium were measured only once). (B) Shown are growth curves of all measured cultures in the complex medium with the emphasis on strains with the growth phenotype.

5 Discussion

5.1 Effects of intron deletion on duplicated ribosomal protein genes

Our replication study of effects of intron removal on the RP genes expression, in which we were using the same strains and primers as authors (Parenteau et al. 2011, and J. Parenteau, personal communication), did not recapitulate the findings of authors. They observed that removal of introns in duplicated *RPL16*, *RPL37*, *RPL17*, *RPS0*, *RPS18*, *RPL2*, *RPL22* genes affects not only the expression of their own genes (intragenic regulation) but also their paralogs *in trans* (intergenic regulation). In contrast, we found that the expression of 5 out of 7 pairs of RP genes was not altered, when tested effects of intron deletions (Table 12).

[Table 12] Effect of intron removal on RP genes. Shown is relative mRNA expression of paralog A (A) and paralog B (A) in strains with deleted intron(s) (marked as Δi) relative to *wt*. "This study" shows mean values with s.d. from two (*RPL17*, *RPS0*, *RPS18*) or three (*RPL2*, *RPL16*, *RPL37*, *RPL22*) biological replicates. (Parenteau et al., 2011) data are shown as published mean values for the comparison. Red color indicates at least 200% decrease, while green color marks at least 200% increase in the expression of paralog as a consequence of intron removal.

A

Paralog A	AΔi / Bwt		Awt / BΔi		AΔi / BΔi	
	this study	Parenteau et al., 2011	this study	Parenteau et al., 2011	this study	Parenteau et al., 2011
RPL16	1.10 ± 0.28	1.21	0.99 ± 0.24	0.56	1.20 ± 0.21	0.97
RPL37	0.76 ± 0.05	0.39	0.79 ± 0.11	0.78	0.83 ± 0.09	0.23
RPL17	1.06 ± 0.01	0.35	0.86 ± 0.01	0.2	0.97 ± 0.07	0.45
RPS0	1.33 ± 0.38	0.49	0.97 ± 0.07	0.29	1.32 ± 0.11	0.54
RPS18	1.11 ± 0.11	0.35	1.01 ± 0.09	0.37	1.04 ± 0.02	0.42
RPL2	0.02 ± 0.01	0.07	0.85 ± 0.37	0.34	0.02 ± 0.01	0.04
RPL22	1.46 ± 0.47	1.75	0.76 ± 0.08	0.83	1.62 ± 0.36	2.14

B

Paralog B	AΔi / Bwt		Awt / BΔi		AΔi / BΔi	
	this study	Parenteau et al., 2011	this study	Parenteau et al., 2011	this study	Parenteau et al., 2011
RPL16	0.90 ± 0.18	0.41	1.08 ± 0.21	0.49	1.21 ± 0.20	0.5
RPL37	0.98 ± 0.05	0.14	0.87 ± 0.20	0.26	0.99 ± 0.20	0.07
RPL17	0.86 ± 0.05	0.33	1.01 ± 0.14	0.35	1.02 ± 0.03	0.48
RPS0	1.12 ± 0.13	0.28	1.05 ± 0.16	0.31	1.17 ± 0.05	0.39
RPS18	1.08 ± 0.02	0.33	1.13 ± 0.08	0.44	1.21 ± 0.03	0.44
RPL2	0.94 ± 0.12	0.30	1.15 ± 0.23	0.3	1.22 ± 0.23	0.32
RPL22	0.05 ± 0.00	0.08	4.80 ± 0.30	6.42	5.48 ± 1.15	8.02

Although we tried to repeat the experiments as accurately as possible, we were not able to reproduce their findings. We used haploid strains prepared less than 1 month before the analysis, since some ribosomal protein genes seem to adapt with time and relatively quickly lose their intron dependencies (J.Parenteau, personal communication). We also tried different cultivation conditions. While it is true that we did not use exactly same conditions (e.g. different batches of media, kits for RNA isolation and qPCR), we expected that such strong changes in mRNA levels would not be lost. Intrigued by the discrepancy, we tried to find out where the problem was. We noticed that primers specifically designed to detect mRNA levels of *RPL18A* do not span the exon-exon junction, thus detect total RNA of *RPL18A*. Therefore, we looked closer on all primers, which we and the authors were using. The primers supposedly able to distinguish between RP paralogs often differed only in few nucleotides. We therefore made use of yeast ORF deletion collection (Winzeler et al. 1999) present in our lab and tested the specificity of primers for mRNA detection of *RPL2, RPS0* and *RPL17* paralogs in strains with their deletions. While primers for *RPL2A, RPS0A, RPS0B* and *RPL17A* were paralog-specific, the primers for *RPL2B* and *RPL17B* detected mRNA levels also in strains with *RPL2B* and *RPL17B* deletion, respectively (data not shown). Note that Ct values differed by less than 1.5 cycle compared to *wild type* strains. Although this means that some of our results are incorrect (and maybe authors have used special conditions, which allowed them to specifically detect paralogs of their choice), the fact that we do not see any effects of intron removal on paralogs with the specific primers suggests that there is simply no regulation present.

Interestingly, study focused on the intergenic regulation between *RPS9* paralogs done as the follow-up of same lab (Petibon et al. 2016) as well as independent study done by Guthrie lab (Plocik and Guthrie 2012) show effects of *RPS9* intron deletions, which are not in agreement with the original study (Parenteau et al. 2011). Similarly, the expression changes of *RPS14* paralogs deviate from the earlier findings (Li et al. 1995).

Therefore, we must disagree with authors and rather put their findings of widespread intron-dependent intergenic regulation (in fact 36 identified pairs of RP genes) as questionable.

5.2 Intragenic regulation of *RPL2A*

Rpl2 protein is one of the most conserved ribosomal proteins (e.g. human or archaebacterial Rpl2 orthologs can replace *E.coli* Rpl2 protein and still being functional). It is present in the core of large ribosomal subunit, interacting with different domains of rRNA and ribosomal proteins (Uhlein et al. 1998, Ben-Shem et al. 2010). It has been believed for many years that Rpl2 is a major component of peptidyl transferase centre of ribosome (Schulze and Nierhaus 1982, Cooperman et al. 1995). While we now know that ribosome is ribozyme (Nissen et al. 2000, Schmeing et al. 2005), the role of Rpl2 in supporting ribosome function remain to be essential (Diedrich et al. 2000; Meskauskas et al. 2008).

In yeast, both *RPL2A* and *RPL2B* paralogs encode identical Rpl2 protein (their coding sequence differs in 28 out of 765 bp). Their expression is asymmetrical, with ~1.59 times higher mRNA level of *RPL2B* paralog (based on RNA-seq data, Abrhámová et al. 2018). Both paralogs contain one intron. Interestingly, while the length of *RPL2A* intron is only 147 bp, *RPL2B* intron is 400 bp long -a length more typical for introns of RP genes (see the Introduction).

Testing effects of intron removal on the expression of *RPL2* paralogs revealed an intron-dependent intragenic regulation of *RPL2A* paralog. *RPL2A* intron serves as an expression enhancer - its deletion is followed by the lost of *RPL2A* mRNA. The downregulation of *RPL2A* has no effect on the mRNA expression of its paralog, *RPL2B*. This findings deviate from the study of (Parenteau et al. 2011).

Although our results are very limited and we have no evidence for any proposed models, we might speculate that the *RPL2A* regulation operates on the level of transcription. It is well known that intron-containing genes are significantly more

expressed than non-intron-containing in *S.cerevisiae* (Ares et al. 1999, Juneau et al. 2006). Moreover, run-on experiments on *DYN2* and *ASC1* genes showed that removal of introns (in the case of a gene with two introns it is the promoter-proximal intron) leads to the reduced transcription of respective genes (Furger 2002). These intron-mediated enhancements of transcription are not fully understood and are probably involved in many different steps of transcription (e.g. reviewed in Chorev and Carmel 2012). It was shown in yeast that introns might induce physical interaction of promoter and terminator regions (i.e. gene looping) and therefore stimulate transcription reinitiation of respective genes (Moabbi et al. 2012). Later on, authors proposed that intron-dependent gene looping might confer directionality to otherwise bidirectional promoters (Agarwal and Ansari 2016). Alternatively in higher eukaryotes, binding of U1 snRNA to 5' splice site of promoter-proximal introns can stimulate transcription reinitiation by recruitment of TFIIH, TFIIB and/or TFIID general transcription factors to respective promoters (Tian 2001, Kwek et al. 2002, Damgaard et al. 2008).

While these studies claim that presence of introns lead to higher expression, our experiments showed that deletion of introns in 12 different ribosomal protein genes (including *RPL2B* paralog) have no significant effect on the expression of respective genes (see the Table 12). This is in agreement with other studies showing that introduction of introns does not always mean an increased expression of host genes (Yofe et al. 2014). Therefore, it is not the presence of introns or pre-mRNA splicing in general, but rather specific properties of introns, which boost expression of some genes (e.g. *RPL2A*, but not *RPL2B*).

5.3 Intergenic regulation between *RPL22* paralogs

Testing the effects of intron deletion on expression of *RPL22* paralogs in two different genetic backgrounds (Figures 4, 6) revealed the *RPL22* intron-dependent intergenic regulation. This results are in agreement with earlier finding (Parenteau et al. 2011) as well as work of Gabunilas and Chanfreau, who independently described the splicing-mediated autoregulation in *RPL22B* paralog, while this work was still in progress (Gabunilas and Chanfreau 2016).

Briefly, deletion of intron in any of *RPL22* paralogs leads to an increase in the expression of its own gene (intragenic regulation) followed by a decrease in the expression of paralog *in trans* (intergenic regulation). In other words, *RPL22A* and *RPL22B* introns have inhibitory effects on the expression of their host genes. Interestingly, deletion of intron in both paralogs abolished the intergenic regulation, i.e. both paralogs were upregulated (Figure 6). Note, that all measurement done in this work were on the level of mRNA. To confirm that observed changes at the mRNA level are reflected also at the protein levels, K.Abrhámová did the proteomic analysis of manipulated strains and found that Rpl22 protein levels match *RPL22* mRNA levels (Abrhámová et al. 2018).

5.3.1 Focus on the RPL22B regulation

We hypothesized that it is the final product of expression, Rpl22 protein, which have an inhibitory effect on *RPL22* paralogs, however, only in the presence of their introns. Indeed, deletion of *RPL22A* paralog (*rpl22A⊿*) had the same effect on *RPL22B* expression as deletion of *RPL22B* intron (*RPL22B⊿i*) alone or the double deletion (*rpl22A⊿ RPL22B⊿i*). Hence, Rpl22A protein blocks the expression of intron-containing *RPL22B* paralog in *wild type* cells, which is reflected also at the amount of Rpl22B protein. Unlocking of *RPL22B* expression, either by removing the *RPL22B* intron or Rpl22A protein, leads to ~4.85-fold increase of its expression (Figure 6B).

To test if this intron-dependent regulation operates on the level of pre-mRNA splicing, we cloned *RPL22B* intron (together with short flanking regions) into the reporter gene and measured its splicing using primer extension assays. While the reporter was spliced in *wild type* background, its splicing was inhibited in the background with higher level of Rpl22A protein (e.g. *RPL22A⊿i* strain). Vice versa, deletion of major *RPL22A* paralog leads to the more efficient splicing compared to *wt* (Figure 7B). Interestingly, deletion of intron in the *RPL22B* gene, which unlocks its expression and therefore leads to the upregulation of *RPL22* mRNA in cells (113% of *wt* mRNA level) leads to less efficient splicing of *RPL22B* reporter compared to *wt*, arguing that Rpl22B protein has also a potential to inhibit its own expression (Figure 7B).

K.Abrhámová and J.Libus additionally showed that the ectopic overexpression of either *RPL22A* or *RPL22B* leads to the downregulation of endogenous *RPL22B* mRNA as well as to the inhibition of splicing of *RPL22B*-derived reporter (Abrhámová et al. 2018). The inhibition did not lead to the accumulation of lariat-intermediate, suggesting that the early steps of spliceosome assembly are blocked by Rpl22 proteins.

5.3.2 Focus on the RPL22A regulation

Similarly as *RPL22B*, we found that the expression of *RPL22A* is regulated on the level of introns. Removal of *RPL22A* intron leads to the upregulation of *RPL22A*. In contrast to the *RPL22B* regulation, deletion of paralog *in trans* - in this case of the minor *RPL22B* paralog, does not change the *RPL22A* mRNA levels. This is most probably because the *RPL22B* deletion does not significantly change Rpl22 level in cells (~105% of the *wt* level of *RPL22* mRNA). Deletion of both, the *RPL22B* paralog and the *RPL22A* intron leads to upregulation similar to single *RPL22A* intron deletion, arguing that it is mostly the Rpl22A protein which regulates its own expression. Interestingly, the deletion of *RPL22B* intron, which leads to upregulation of Rpl22B (roughly to 113% of *wild type* level of *RPL22* mRNA) results in approximately 1.4-fold downregulation of *RPL22A* mRNA (Figure 6A).

K.Abrhámová and J.Libus showed that the ectopic overexpression of either *RPL22A* or *RPL22B* leads to the downregulation of *RPL22A* mRNA as well as *RPL22B* (Abrhámová et al. 2018).

In contrast to *RPL22B*, *RPL22A*-derived splicing reporter did not respond to different levels of Rpl22 (Figure 7C). While this might argue that *RPL22A* intron alone is not responding and requires additional regulatory regions (present either in the exon or untranslated regions), J.Libus showed that transplantation of *RPL22A* intron to the *RPL22B* locus leads to regulation of same range as in the *RPL22A* locus, showing that *RPL22A* intron alone maintains its regulatory potential (Abrhámová et al. 2018). Furthermore, K.Abrhámová demonstrated that the downregulation of *RPL22A* mRNA is followed by an increase in the amount of *RPL22A* pre-mRNA, when used strains with inactivated nonsense-mediated decay, e.g. in *RPL22BΔi/upf1Δ* strain (Abrhámová et al. 2018). This supports the hypothesis that *RPL22A* is regulated on the level of pre-mRNA splicing, similarly as *RPL22B*.

5.3.3 Focus on the mechanism

To better understand how the regulation works, we tested if Rpl22 protein can physically interact with the *RPL22B* intron. Using yeast 3-H system, we found that Rpl22 proteins expressed from both paralogs bind to the stem-loop (165-236 nt) of *RPL22B* intron (Figure 9). Interestingly, using site-directed mutagenesis, others found that the region of 153-225 bp is necessary for the *RPL22B* regulation (Gabunilas and Chanfreau 2016).

Despite having only 84% sequence identity, both Rpl22 protein paralogs are capable of binding the stem-loop of *RPL22B* intron and regulating the pre-mRNA splicing of *RPL22B* paralog (Figure 16). We also tested the mutants of Rpl22A and Rpl22B prepared by K.Abrhámová. She made use of known RNA-binding site of human Rpl22, which interacts with the 28S rRNA (Houmani and Ruf 2009) and mutated the cluster of basic amino acids (Lysines) in yeast orthologs as shown in

the Figure 16. These mutants lost their ability to inhibit the pre-mRNA splicing of both *RPL22* paralogs (Abrhámová et al. 2018). In this work we demonstrated that the loss-of-function mutation is due to the disruption of binding to the stem-loop of *RPL22B* intron (Figure 9). We might speculate that the same happens for the *RPL22A* intron, which was not tested because of the incompatibility of intron sequence with the yeast 3-H system - presence of at least 9 sequences, which can terminate transcription of RNA polymerase III used in our system (Geiduschek 1988).

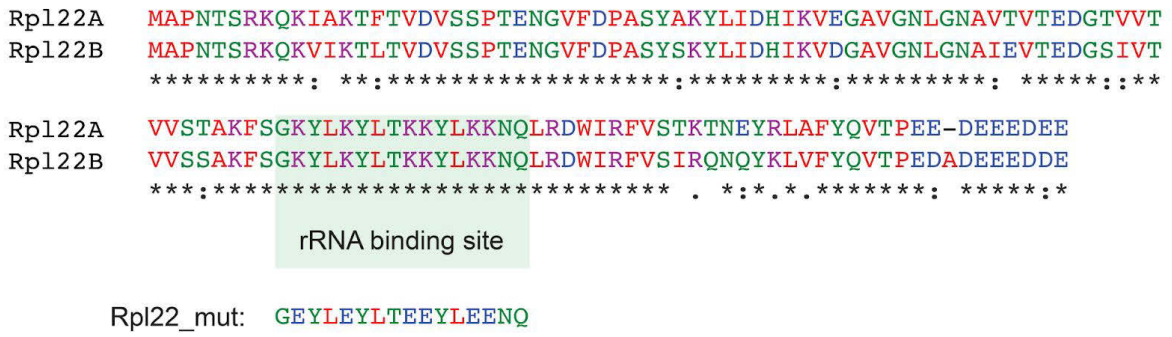

[Figure 16] Alignment of Rpl22A and Rpl22B proteins. The alignment was made in CLUSTAL multiple sequence alignment by MUSCLE (3.8). rRNA-binding site as defined in (Houmani and Ruf 2009) is marked with the green window. The sequence replacing binding site in Rpl22 mutant proteins is shown.

Overall, we propose a model, in which both *RPL22A* and *RPL22B* paralogs contribute to the pool of Rpl22 proteins in cells. Under normal conditions, the expression is in favor of *RPL22A* paralog - it represents 93% of total *RPL22* mRNA and 96% of total Rpl22 protein. When in excess, both Rpl22A and Rpl22B proteins auto-regulate their own expression by blocking the pre-mRNA splicing of their own transcripts. The regulation operates on both *RPL22A* and *RPL22B* transcripts, with more relative changes in *RPL22B*. This (together with its high transcription) makes the Rpl22A paralog a major protein/isoform present in ribosomes under normal conditions (Figure 17).

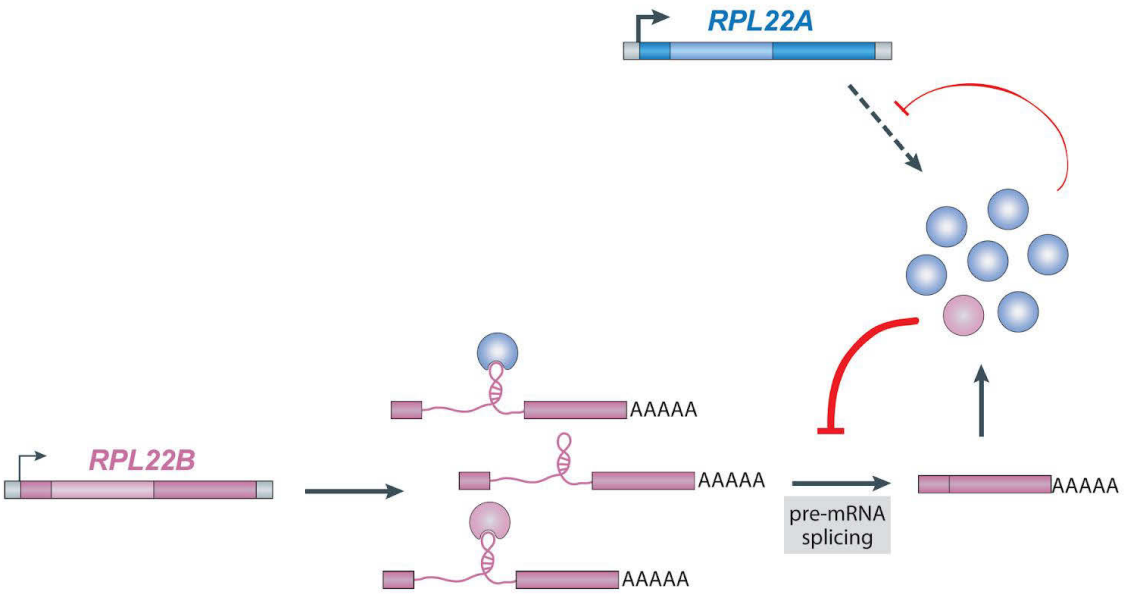

[Figure 17] Model summarizing the intergenic regulation between *RPL22* paralogs.

5.4 Evolutionary study of *RPL22* regulation

Using the yeast 3-H system, we showed that *S.cerevisiae* Rpl22A and Rpl22B, *K.lactis* Rpl22 and human Rpl22 proteins interact with the stem-loop of *RPL22B* intron (Figures 9 and 11). *Schizosaccharomyces pombe* Rpl22 most probably lost the ability to interact. On the contrary, J.Libus and A.Dědková demonstrated that all tested Rpl22 orthologs (including *S.pombe* Rpl22) interact with the 25S rRNA of *S.cerevisiae* (unpublished results). Rpl22 proteins might therefore recognise the stem-loop of *RPL22B* intron through the other than rRNA-binding site. However, mutagenesis of rRNA-binding sites abrogated the regulatory potential of Rpl22A and Rpl22B (Figure 9). Comparison of sequences between all Rpl22 orthologs did not reveal any apparent bifurcation between interacting and noninteracting Rpl22 proteins (Figure 18C). Moreover, overexpression of *S.pombe* Rpl22 in yeast leads to the downregulation of *RPL22B* expression, indicating that *S.pombe* might still retain the regulatory potential (unpublished results).

A similar situation seems to happen to the RNA targets. While intronic elements present in *S.cerevisiae RPL22B* and *K.lactis RPL22* share lots of similarities, they do share only marginal similarities with helices 57 and 59 of 25S rRNA known to be interacting with Rpl22 (compare blue parts in the Figure 18A and 18B). Note that most of the interaction in ribosome happens on the helix 57 (de la Cruz et al. 2015). Examples here as well as others, such as the identification of RNA-binding site of human Rpl22 using systematic evolution of ligands by exponential enrichment (SELEX) or the analysis of yeast ribosome structure revealed that the interaction of Rpl22 with its RNA targets is rather nonspecific and based on shape and charge complementarities (Dobbelstein and Shenk 1995, Ben-Shem et al. 2010, Klinge et al. 2011). Overall, we were not able to define the Rpl22 binding site required for the *RPL22* regulation with our simple evolutionary study and would need a functional study instead.

J.Libus recently demonstrated that despite having only one copy of *RPL22*, *K.lactis* has the preserved intron-dependent regulation (Abrhámová et al. 2018). Therefore we hypothesize that the simple intron-dependent autoregulation of Rpl22 expression was present before the split (and genome duplication) of *S.cerevisiae* and *K.lactis* ancestors. Only after the genome duplication of *S.cerevisiae* ancestor, the simple auto-regulation evolved into the intergenic regulation, which asymmetrically regulates the production of Rpl22 from two paralogs and sets up the expression ratio in favor of Rpl22A under normal conditions. As we discussed in the Introduction, *RPL22A* and *RPL22B* paralogs have distinct functions in yeast, therefore the control of their expression is crucial for cells. We might speculate that the regulation described here is capable of changing the ratio under other conditions, the phenomenon shown for other pairs of ribosomal protein genes (Parenteau et al. 2011, Petibon et al. 2016).

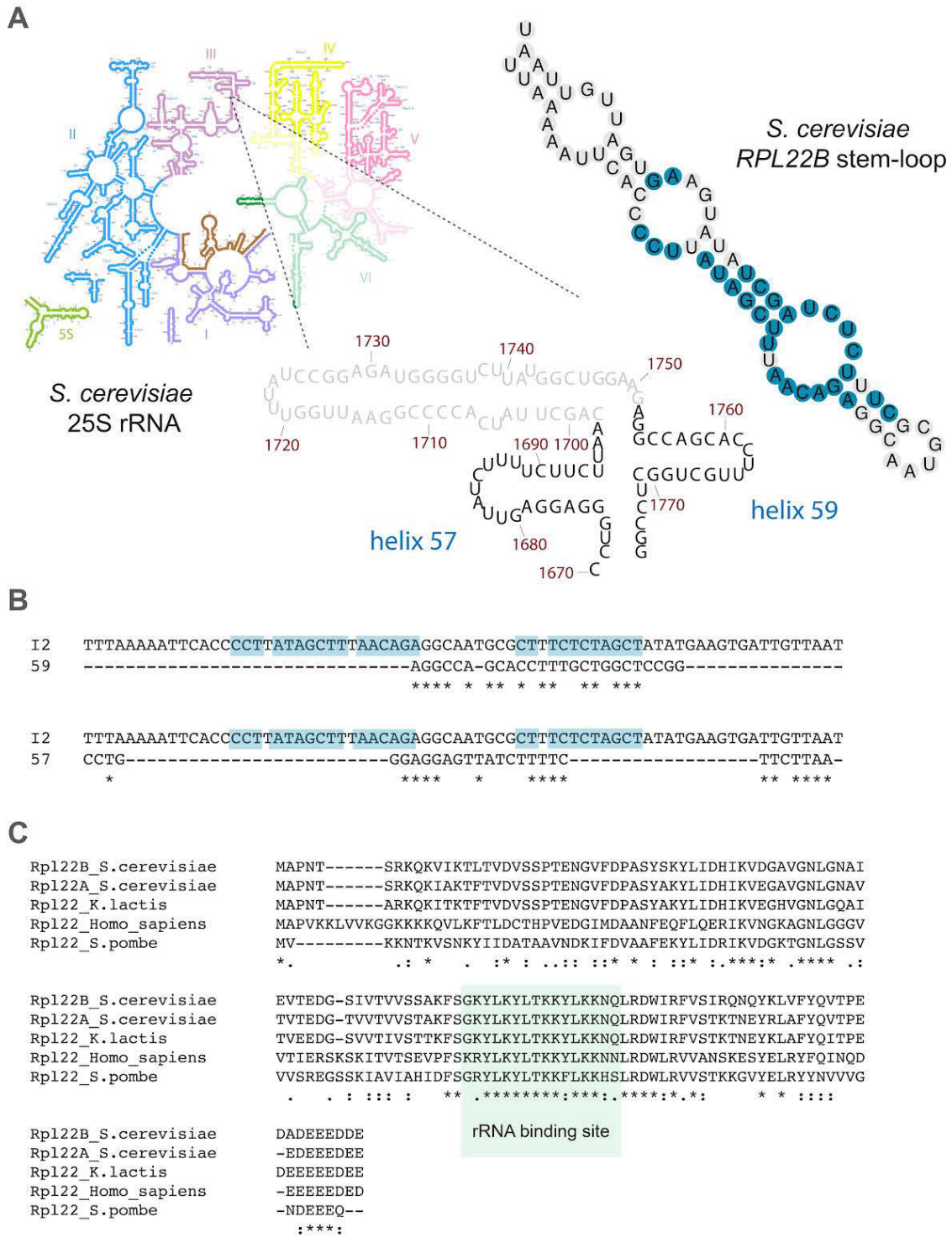

[Figure 18] Comparison between rRNA and the stem-loop of *RPL22B* intron. (A) Shown is the 25S rRNA structure with focus on helices 57 and 58. Schemes were adapted from (Bernier et al. 2014). Additionally, the *S.cerevisiae RPL22B* stem-loop structure is shown with highlighted conserved I2 elements. (B,C) The alignments made in CLUSTAL multiple sequence alignment by MUSCLE (3.8). (B) Conserved I2 elements are highlighted. (C) The rRNA binding site is highlighted in all tested Rpl22 orthologs.

We identified the region of *K.lactis RPL22* intron, which interacts with both *K.lactis* Rpl22 and *S.cerevisiae* Rpl22A (Figure 12). This suggests that both structures are orthologous, e.g. appeared already in their ancestor. Therefore, we tried to find the shared elements which would possibly reveal the RNA binding sites. We identified short elements shared between two yeast, which are 100% conserved and are predicted to make the same secondary structure (Figures 12B and 12C). We even expanded the potential regions (called I2 elements), when compared sequence and structural alignments (Figures 13 and 14). Interestingly though, the two ultra-conserved regions present in all *Saccharomyces sensu stricto RPL22A/B* introns as well as the *RPL22* intron of *K.lactis* seem not be part of interactions, since they are only partially present in the *RPL22B* region and are completely missing in the *K.lactis RPL22* region. They surround the stem-loop of *RPL22B* intron, but not of *K.lactis RPL22*. Validations of these elements still remain to be done.

Overall, all the presented results in this project lead to better understanding of intergenic regulation, which adjusts the expression ratio between functionally different *RPL22* paralogs. Part of these results was published as the co-first author publication (see the Supplements):

> Abrhámová K, Nemčko F, Libus J, Převorovský M, Hálová M, Půta F & Folk P (2018) Introns provide a platform for intergenic regulatory feedback of RPL22 paralogs in yeast. PLoS One 13: e0190685.

6 Conclusions

- The expression of 5 out of 7 tested pairs of ribosomal protein genes was not altered upon intron deletion in any of paralogs.

- Introns modulate the expression of *RPL22A* and *RPL22B* paralogs.

- Rpl22 protein regulates the pre-mRNA splicing of *RPL22B* paralog.

- Rpl22 protein interacts with the stem-loop of *RPL22B* intron.

- While orthologous Rpl22 proteins from *Kluyveromyces lactis* and human are capable of binding to the stem-loop of *RPL22B*, *Schizosaccharomyces pombe* Rpl22 seems not to interact.

- The stem-loop structure is preserved in the intron of single-copy *RPL22* gene from *Kluyveromyces lactis*. It can be bound and regulated by Rpl22 proteins from both *K.lactis* and *S.cerevisiae*.

7 References

Abrhámová K, Nemčko F, Libus J, Převorovský M, Hálová M, Půta F & Folk P (2018) Introns provide a platform for intergenic regulatory feedback of RPL22 paralogs in yeast. *PLoS One* **13:** e0190685

An J, Kwon H, Kim E, Lee YM, Ko HJ, Park H, Choi IG, Kim S, Kim KH, Kim W & Choi W (2015) Tolerance to acetic acid is improved by mutations of the TATA-binding protein gene. *Environ. Microbiol.* **17:** 656–669

Anderson SJ, Lauritsen JPH, Hartman MG, Foushee AMD, Lefebvre JM, Shinton SA, Gerhardt B, Hardy RR, Oravecz T & Wiest DL (2007) Ablation of Ribosomal Protein L22 Selectively Impairs alpha-beta T Cell Development by Activation of a p53-Dependent Checkpoint. *Immunity* **26:** 759–772

Ares M, Grate L & Pauling MH (1999) A handful of intron-containing genes produces the lion's share of yeast mRNA. *RNA* **5:** 1138–9

Aslanzadeh V, Huang Y, Sanguinetti G & Beggs JD (2018) Transcription rate strongly affects splicing fidelity and cotranscriptionality in budding yeast. *Genome Res.* **28:** 203–213

Ban N, Beckmann R, Cate JHD, Dinman JD, Dragon F, Ellis SR, Lafontaine DLJ, Lindahl L, Liljas A, Lipton JM, McAlear MA, Moore PB, Noller HF, Ortega J, Panse VG, Ramakrishnan V, Spahn CMT, Steitz TA, Tchorzewski M, Tollervey D, et al (2014) A new system for naming ribosomal proteins. *Curr. Opin. Struct. Biol.* **24:** 165–169

Beaupere C, Wasko BM, Lorusso J, Kennedy BK, Kaeberlein M & Labunskyy VM (2017) CAN1 Arginine Permease Deficiency Extends Yeast Replicative Lifespan via Translational Activation of Stress Response Genes. *Cell Rep.* **18:** 1884–1892

Ben-Shem A, Garreau de Loubresse N, Melnikov S, Jenner L, Yusupova G & Yusupov M (2011) The Structure of the Eukaryotic Ribosome at 3.0 A Resolution. *Science.* **334:** 1524–1529

Berget SM, Moore C & Sharp PA (1977) Spliced segments at the 5' terminus of adenovirus 2 late mRNA. *Proc. Natl. Acad. Sci. U. S. A.* **74:** 3171–5

Bergkessel M, Whitworth GB & Guthrie C (2011) Diverse environmental stresses elicit distinct responses at the level of pre-mRNA processing in yeast. *RNA* **17:** 1461–78

Bernier CR, Petrov AS, Waterbury CC, Jett J, Li F, Freil LE, Xiong X, Wang L, Migliozzi BLR, Hershkovits E, Xue Y, Hsiao C, Bowman JC, Harvey SC, Grover MA, Wartell ZJ & Williams LD (2014) RiboVision suite for visualization and analysis of ribosomes. *Faraday Discuss.* **169:** 195–207

Boyle EI, Weng S, Gollub J, Jin H, Botstein D, Cherry JM & Sherlock G (2004) GO::TermFinder--open source software for accessing Gene Ontology information and

finding significantly enriched Gene Ontology terms associated with a list of genes. *Bioinformatics* **20:** 3710–5

Byrne KP & Wolfe KH (2005) The Yeast Gene Order Browser: Combining curated homology and syntenic context reveals gene fate in polyploid species. *Genome Res.* **15:** 1456–1461

Chan CTY, Pang YLJ, Deng W, Babu IR, Dyavaiah M, Begley TJ & Dedon PC (2012) Reprogramming of tRNA modifications controls the oxidative stress response by codon-biased translation of proteins. *Nat. Commun.* **3:** 937

Chorev M & Carmel L (2012) The function of introns. *Front. Genet.* **3:** 55

Chow LT, Gelinas RE, Broker TR & Roberts RJ (1977) An amazing sequence arrangement at the 5′ ends of adenovirus 2 messenger RNA. *Cell* **12:** 1–8

Collins L & Penny D (2005) Complex spliceosomal organization ancestral to extant eukaryotes. *Mol. Biol. Evol.* **22:** 1053–1066

Cooperman BS, Wooten T, Romero DP & Traut RR Histidine 229 in protein L2 is apparently essential for 50S peptidyl transferase activity. *Biochem. Cell Biol.* **73:** 1087–94

Costanzo M, Baryshnikova A, Bellay J, Kim Y, Spear ED, Sevier CS, Ding H, Koh JLY, Toufighi K, Mostafavi S, Prinz J, St. Onge RP, VanderSluis B, Makhnevych T, Vizeacoumar FJ, Alizadeh S, Bahr S, Brost RL, Chen Y, Cokol M, et al (2010) The Genetic Landscape of a Cell. *Science.* **327:** 425–431

Damgaard CK, Kahns S, Lykke-Andersen S, Nielsen AL, Jensen TH & Kjems J (2008) A 5′ Splice Site Enhances the Recruitment of Basal Transcription Initiation Factors In Vivo. *Mol. Cell* **29:** 271–278

Davis CA, Grate L, Spingola M & Ares M (2000) Test of intron predictions reveals novel splice sites, alternatively spliced mRNAs and new introns in meiotically regulated genes of yeast. *Nucleic Acids Res.* **28:** 1700–6

Diedrich G, Spahn CM, Stelzl U, Schäfer MA, Wooten T, Bochkariov DE, Cooperman BS, Traut RR & Nierhaus KH (2000) Ribosomal protein L2 is involved in the association of the ribosomal subunits, tRNA binding to A and P sites and peptidyl transfer. *EMBO J.* **19:** 5241–50

Dobbelstein M & Shenk T (1995) In vitro selection of RNA ligands for the ribosomal L22 protein associated with Epstein-Barr virus-expressed RNA by using randomized and cDNA-derived RNA libraries. *J. Virol.* **69:** 8027–8034

Engebrecht JA, Voelkel-Meiman K & Roeder GS (1991) Meiosis-specific RNA splicing in yeast. *Cell* **66:** 1257–68

Evangelisti AM & Conant GC (2010) Nonrandom survival of gene conversions among yeast ribosomal proteins duplicated through genome doubling. *Genome Biol. Evol.* **2:** 826–834

Fahl SP, Harris B, Coffey F & Wiest DL (2015) Rpl22 Loss Impairs the Development of B Lymphocytes by Activating a p53-Dependent Checkpoint. *J. Immunol.* **194:** 200–209

Fewell SW & Woolford JL (1999) Ribosomal protein S14 of Saccharomyces cerevisiae regulates its expression by binding to RPS14B pre-mRNA and to 18S rRNA. *Mol. Cell. Biol.* **19:** 826–34

Fink GR (1987) Pseudogenes in yeast? *Cell* **49:** 5–6

Fok V, Mitton-Fry RM, Grech A & Steitz JA (2006) Multiple domains of EBER 1, an Epstein-Barr virus noncoding RNA, recruit human ribosomal protein L22. *RNA* **12:** 872–882

Furger A, O'Sullivan JM, Binnie A, Lee BA & Proudfoot NJ (2002) Promoter proximal splice sites enhance transcription. *Genes Dev.* **16:** 2792–2799

Gabunilas J & Chanfreau G (2016) Splicing-Mediated Autoregulation Modulates Rpl22p Expression in Saccharomyces cerevisiae. *PLoS Genet.* **12:** e1005999

Geiduschek EP & Tocchini-Valentini GP (1988) Transcription by RNA Polymerase III. *Annu. Rev. Biochem.* **57:** 873–914

Gerstein MB, Bruce C, Rozowsky JS, Zheng D, Du J, Korbel JO, Emanuelsson O, Zhang ZD, Weissman S & Snyder M (2007) What is a gene, post-ENCODE? History and updated definition. *Genome Res.* **17:** 669–681

Gilbert W (1978) Why genes in pieces? *Nature* **271:** 501

Harlen KM, Trotta KL, Smith EE, Mosaheb MM, Fuchs SM & Churchman LS (2016) Comprehensive RNA Polymerase II Interactomes Reveal Distinct and Varied Roles for Each Phospho-CTD Residue. *Cell Rep.* **15:** 2147–2158

HOOK B, Bernstein D, Zhang B & Wickens M (2005) RNA-protein interactions in the yeast three-hybrid system: Affinity, sensitivity, and enhanced library screening. *RNA* **11:** 227–233

Hooks KB, Delneri D & Griffiths-Jones S (2014) Intron evolution in Saccharomycetaceae. *Genome Biol. Evol.* **6:** 2543–2556

Houmani JL & Ruf IK (2009) Clusters of basic amino acids contribute to RNA binding and nucleolar localization of ribosomal protein L22. *PLoS One* **4:**

Irimia M, Penny D & Roy SW (2007) Coevolution of genomic intron number and splice sites. *Trends Genet.* **23:** 321–325

Irimia M & Roy SW (2008) Evolutionary convergence on highly-conserved 3′ intron structures in intron-poor eukaryotes and insights into the ancestral eukaryotic genome. *PLoS Genet.* **4:**

Juneau K, Miranda M, Hillenmeyer ME, Nislow C & Davis RW (2006) Introns regulate RNA and protein abundance in yeast. *Genetics* **174:** 511–518

Juneau K, Palm C, Miranda M & Davis RW (2007) High-density yeast-tiling array reveals previously undiscovered introns and extensive regulation of meiotic splicing. *Proc. Natl. Acad. Sci. U. S. A.* **104:** 1522–7

Kassir Y, Granot D & Simchen G (1988) IME1, a positive regulator gene of meiosis in S. cerevisiae. *Cell* **52:** 853–62

Kim SJ & Strich R (2016) Rpl22 is required for IME1 mRNA translation and meiotic induction in S. cerevisiae. *Cell Div.* **11:** 10

Klinge S, Voigts-Hoffmann F, Leibundgut M, Arpagaus S & Ban N (2011) Crystal Structure of the Eukaryotic 60S Ribosomal Subunit in Complex with Initiation Factor 6. *Science* **334:** 941–948

Klopotowski T & Wiater A (1965) Synergism of aminotriazole and phosphate on the inhibition of yeast imidazole glycerol phosphate dehydratase. *Arch. Biochem. Biophys.* **112:** 562–6

Komili S, Farny NG, Roth FP & Silver PA (2007) Functional Specificity among Ribosomal Proteins Regulates Gene Expression. *Cell* **131:** 557–571

Kwek KY, Murphy S, Furger A, Thomas B, O'Gorman W, Kimura H, Proudfoot NJ & Akoulitchev A (2002) U1 snRNA associates with TFIIH and regulates transcriptional initiation. *Nat. Struct. Biol.* **9:** 800–5

de la Cruz J, Karbstein K & Woolford JL (2015) Functions of Ribosomal Proteins in Assembly of Eukaryotic Ribosomes In Vivo. *Annu. Rev. Biochem.* **84:** 93–129

Lander ES, Linton LM, Birren B, Nusbaum C, Zody MC, Baldwin J, Devon K, Dewar K, Doyle M, FitzHugh W, Funke R, Gage D, Harris K, Heaford A, Howland J, Kann L, Lehoczky J, LeVine R, McEwan P, McKernan K, et al (2001) Initial sequencing and analysis of the human genome. *Nature* **409:** 860–921

Le S, Sternglanz R & Greider CW (2000) Identification of two RNA-binding proteins associated with human telomerase RNA. *Mol. Biol. Cell* **11:** 999–1010

Li Z, Paulovich AG & Woolford JL (1995) Feedback inhibition of the yeast ribosomal protein gene CRY2 is mediated by the nucleotide sequence and secondary structure of CRY2 pre-mRNA. *Mol. Cell. Biol.* **15:** 6454–64

Lin K, Kuang Y, Joseph JS & Kolatkar PR (2002) Conserved codon composition of ribosomal protein coding genes in Escherichia coli, Mycobacterium tuberculosis and Saccharomyces cerevisiae: lessons from supervised machine learning in functional genomics. *Nucleic Acids Res.* **30:** 2599–2607

Livak KJ & Schmittgen TD (2001) Analysis of Relative Gene Expression Data Using Real-Time Quantitative PCR and the 2−ΔΔCT Method. *Methods* **25:** 402–408

Lõoke M, Kristjuhan K & Kristjuhan A (2011) Extraction of genomic DNA from yeasts for PCR-based applications. *Biotechniques* **50:** 325–8

Lynch M (2002) Intron evolution as a population-genetic process. *Proc. Natl. Acad. Sci.* **99:** 6118–6123

Martin Schmeing T, Huang KS, Strobel SA & Steitz TA (2005) An induced-fit mechanism to promote peptide bond formation and exclude hydrolysis of peptidyl-tRNA. *Nature* **438:** 520–524

Matsuzaki M, Misumi O, Shin-i T, Maruyama S, Takahara M, Miyagishima S, Mori T, Nishida K, Yagisawa F, Nishida K, Yoshida Y, Nishimura Y, Nakao S, Kobayashi T, Momoyama Y, Higashiyama T, Minoda A, Sano M, Nomoto H, Oishi K, et al (2004) Genome sequence of the ultrasmall unicellular red alga Cyanidioschyzon merolae 10D. *Nature* **428:** 653–657

Meskauskas A, Russ JR & Dinman JD (2008) Structure/function analysis of yeast ribosomal protein L2. *Nucleic Acids Res.* **36:** 1826–1835

Moabbi a. M, Agarwal N, El Kaderi B & Ansari a. (2012) Role for gene looping in intron-mediated enhancement of transcription. *Proc. Natl. Acad. Sci.* **109:** 8505–8510

Mourier T & Jeffares DC (2003) Eukaryotic intron loss. *Science* **300:** 1393

Neuvéglise C, Marck C & Gaillardin C (2011) The intronome of budding yeasts. *Comptes Rendus - Biol.* **334:** 662–670

Ng R, Domdey H, Larson G, Rossi JJ & Abelson J (1985) A test for intron function in the yeast actin gene. *Nature* **314:** 183–4

Ni J-Q, Liu L-P, Hess D, Rietdorf J & Sun F-L (2006) Drosophila ribosomal proteins are associated with linker histone H1 and suppress gene transcription. *Genes Dev.* **20:** 1959–73

Nissen P, Hansen J, Ban N, Moore PB & Steitz TA (2000) The structural basis of ribosome activity in peptide bond synthesis. *Science* **289:** 920–30

Nowoshilow S, Schloissnig S, Fei J-F, Dahl A, Pang AWC, Pippel M, Winkler S, Hastie AR, Young G, Roscito JG, Falcon F, Knapp D, Powell S, Cruz A, Cao H, Habermann B, Hiller M, Tanaka EM & Myers EW (2018) The axolotl genome and the evolution of key tissue formation regulators. *Nature* **554:** 50–55

O'Leary MN, Schreiber KH, Zhang Y, Duc ACE, Rao S, Hale JS, Academia EC, Shah SR, Morton JF, Holstein CA, Martin DB, Kaeberlein M, Ladiges WC, Fink PJ, MacKay VL, Wiest DL & Kennedy BK (2013) The Ribosomal Protein Rpl22 Controls Ribosome Composition by Directly Repressing Expression of Its Own Paralog, Rpl22l1. *PLoS Genet.* **9:**

Parenteau J, Durand M, Morin G, Gagnon J, Lucier JF, Wellinger RJ, Chabot B & Elela SA (2011) Introns within ribosomal protein genes regulate the production and function of yeast ribosomes. *Cell* **147:** 320–331

Parenteau J, Durand M, Véronneau S, Lacombe A-A, Morin G, Guérin V, Cecez B, Gervais-Bird J, Koh C-S, Brunelle D, Wellinger RJ, Chabot B & Abou Elela S (2008) Deletion of many yeast introns reveals a minority of genes that require splicing for function. *Mol. Biol. Cell* **19:** 1932–41

Parenteau J, Lavoie M, Catala M, Malik-Ghulam M, Gagnon J & Abou Elela S (2015) Preservation of Gene Duplication Increases the Regulatory Spectrum of Ribosomal Protein Genes and Enhances Growth under Stress. *Cell Rep.* **13:** 2516–2526

Petibon C, Parenteau J, Catala M & Elela SA (2016) Introns regulate the production of ribosomal proteins by modulating splicing of duplicated ribosomal protein genes. *Nucleic Acids Res.* **44:** 3878–3891

Planta RJ & Mager WH (1998) The list of cytoplasmic ribosomal proteins of Saccharomyces cerevisiae. *Yeast* **14:** 471–477

Pleiss JA, Whitworth GB, Bergkessel M & Guthrie C (2007a) Transcript specificity in yeast pre-mRNA splicing revealed by mutations in core spliceosomal components. *PLoS Biol.* **5:** 745–757

Pleiss JA, Whitworth GB, Bergkessel M & Guthrie C (2007b) Rapid, Transcript-Specific Changes in Splicing in Response to Environmental Stress. *Mol. Cell* **27:** 928–937

Plocik AM & Guthrie C (2012) Diverse forms of RPS9 splicing are part of an evolving autoregulatory circuit. *PLoS Genet.* **8:**

Rashkovan M, Vadnais C, Ross J, Gigoux M, Suh W-K, Gu W, Kosan C & Möröy T (2014) Miz-1 regulates translation of Trp53 via ribosomal protein L22 in cells undergoing V(D)J recombination. *Proc. Natl. Acad. Sci. U. S. A.* **111:** E5411-9

Rogozin IB, Carmel L, Csuros M & Koonin E V (2012) Origin and evolution of spliceosomal introns. *Biol. Direct* **7:** 11

Scannell DR, Zill OA, Rokas A, Payen C, Dunham MJ, Eisen MB, Rine J, Johnston M & Hittinger CT (2011) The Awesome Power of Yeast Evolutionary Genetics: New Genome Sequences and Strain Resources for the Saccharomyces sensu stricto Genus. *G3 (Bethesda).* **1:** 11–25

Schreiber K, Csaba G, Haslbeck M & Zimmer R (2015) Alternative splicing in next generation sequencing data of saccharomyces cerevisiae. *PLoS One* **10:** 1–18

Schulze H & Nierhaus KH (1982) Minimal set of ribosomal components for reconstitution of the peptidyltransferase activity. *EMBO J.* **1:** 609–13

SenGupta DJ, Zhang B, Kraemer B, Pochart P, Fields S & Wickens M (1996) A three-hybrid system to detect RNA-protein interactions in vivo. *Proc. Natl. Acad. Sci. U. S. A.* **93:** 8496–501

Shen Y, Wang Y, Chen T, Gao F, Gong J, Abramczyk D, Walker R, Zhao H, Chen S, Liu W, Luo Y, Müller CA, Paul-Dubois-Taine A, Alver B, Stracquadanio G, Mitchell LA, Luo Z, Fan Y, Zhou B, Wen B, et al (2017) Deep functional analysis of synII, a 770-kilobase synthetic yeast chromosome. *Science (80-.).* **355:** eaaf4791

Shi Z & Barna M (2015) Translating the Genome in Time and Space: Specialized Ribosomes, RNA Regulons, and RNA-Binding Proteins. *Annu. Rev. Cell Dev. Biol.* **31:** 31–54

Sil A & Herskowitz I (1996) Identification of an asymmetrically localized determinant, Ash1p, required for lineage-specific transcription of the yeast HO gene. *Cell* **84:** 711–722

Slabodnick MM, Ruby JG, Reiff SB, Swart EC, Gosai S, Prabakaran S, Witkowska E, Larue GE, Fisher S, Freeman RM, Gunawardena J, Chu W, Stover NA, Gregory BD, Nowacki M, Derisi J, Roy SW, Marshall WF & Sood P (2017) The Macronuclear Genome of Stentor coeruleus Reveals Tiny Introns in a Giant Cell. *Curr. Biol.* **27:** 569–575

Solanki NR, Stadanlick JE, Zhang Y, Duc A-C, Lee S-Y, Lauritsen JPH, Zhang Z & Wiest DL (2016) Rpl22 Loss Selectively Impairs T Cell Development by Dysregulating Endoplasmic Reticulum Stress Signaling. *J. Immunol.***:** 1600815

Spingola M, Grate L, Haussler D & Ares M (1999) Genome-wide bioinformatic and molecular analysis of introns in Saccharomyces cerevisiae. *RNA* **5:** 221–234

Stajich JE, Dietrich FS & Roy SW (2007) Comparative genomic analysis of fungal genomes reveals intron-rich ancestors. *Genome Biol.* **8:** R223

Steffen KK, MacKay VL, Kerr EO, Tsuchiya M, Hu D, Fox LA, Dang N, Johnston ED, Oakes JA, Tchao BN, Pak DN, Fields S, Kennedy BK & Kaeberlein M (2008) Yeast Life Span Extension by Depletion of 60S Ribosomal Subunits Is Mediated by Gcn4. *Cell* **133:** 292–302

Steffen KK, McCormick MA, Pham KM, Mackay VL, Delaney JR, Murakami CJ, Kaeberlein M & Kennedy BK (2012) Ribosome deficiency protects against ER stress in Saccharomyces cerevisiae. *Genetics* **191:** 107–118

Stumpf CR, Kimble J & Wickens M (2008a) A Caenorhabditis elegans PUF protein family with distinct RNA binding specificity. *RNA* **14:** 1550–1557

Stumpf CR, Opperman L & Wickens M (2008b) Analysis of RNA–Protein Interactions Using a Yeast Three-Hybrid System. In *Methods in enzymology* pp 295–315.

Tardiff DF, Lacadie SA & Rosbash M (2006) A Genome-Wide Analysis Indicates that Yeast Pre-mRNA Splicing Is Predominantly Posttranscriptional. *Mol. Cell* **24:** 917–929

Tian H (2001) RNA ligands generated against complex nuclear targets indicate a role for U1 snRNP in co-ordinating transcription and RNA splicing. *FEBS Lett.* **509:** 282–6

Toczyski DP, Matera AG, Ward DC & Steitz JA (1994) The Epstein-Barr virus (EBV) small RNA EBER1 binds and relocalizes ribosomal protein L22 in EBV-infected human B lymphocytes. *Proc. Natl. Acad. Sci. U. S. A.* **91:** 3463–7

Toczyski DP & Steitz J a (1991) EAP, a highly conserved cellular protein associated with Epstein-Barr virus small RNAs (EBERs). *EMBO J.* **10:** 459–66

Tugendreich S, Perkins E, Couto J, Barthmaier P, Sun D, Tang S, Tulac S, Nguyen A, Yeh E, Mays A, Wallace E, Lila T, Shivak D, Prichard M, Andrejka L, Kim R & Melese T (2001) A streamlined process to phenotypically profile heterologous cDNAs in parallel using yeast cell-based assays. *Genome Res.* **11:** 1899–912

Uhlein M, Weglöhner W, Urlaub H & Wittmann-Liebold B (1998) Functional implications of ribosomal protein L2 in protein biosynthesis as shown by in vivo replacement studies. *Biochem. J.* **331 (Pt 2):** 423–30

Venkataramanan S, Douglass S, Galivanche AR & Johnson TL (2017) The chromatin remodeling complex Swi/Snf regulates splicing of meiotic transcripts in Saccharomyces cerevisiae. *Nucleic Acids Res.* **45:** 7708–7721

Wallace EWJ & Beggs JD (2017) Extremely fast and incredibly close: cotranscriptional splicing in budding yeast. *RNA* **23:** 601–610

Wapinski I, Pfiffner J, French C, Socha A, Thompson DA & Regev A (2010) Gene duplication and the evolution of ribosomal protein gene regulation in yeast. *Proc. Natl. Acad. Sci. U. S. A.* **107:** 5505–5510

Will CL & Lührmann R (2011) Spliceosome structure and function. *Cold Spring Harb. Perspect. Biol.* **3:** 1–2

Winzeler EA, Shoemaker DD, Astromoff A, Liang H, Anderson K, Andre B, Bangham R, Benito R, Boeke JD, Bussey H, Chu AM, Connelly C, Davis K, Dietrich F, Dow SW, El Bakkoury M, Foury F, Friend SH, Gentalen E, Giaever G, et al (1999) Functional characterization of the S. cerevisiae genome by gene deletion and parallel analysis. *Science* **285:** 901–6

Wolfe KH & Shields DC (1997) Molecular evidence for an ancient duplication of the entire yeast genome. *Nature* **387:** 708–713

Wood J, Frederickson RM & Fields S (2001) Hepatitis C Virus 3 J X Region Interacts with Human Ribosomal Proteins. *J. Virol.* **75:** 1348–1358

Yofe I, Zafrir Z, Blau R, Schuldiner M, Tuller T, Shapiro E & Ben-Yehezkel T (2014) Accurate, Model-Based Tuning of Synthetic Gene Expression Using Introns in S. cerevisiae. *PLoS Genet.* **10:** 1–10

Yu J, Yang Z, Kibukawa M, Paddock M, Passey DA & Wong GK-S (2002) Minimal Introns Are Not Junk; *Genome Res.* **12:** 1185–1189

Zeevi D, Sharon E, Lotan-Pompan M, Lubling Y, Shipony Z, Raveh-Sadka T, Keren L, Levo M, Weinberger A & Segal E (2011) Compensation for differences in gene copy number among yeast ribosomal proteins is encoded within their promoters. *Genome Res.* **21:** 2114–2128

Zhang Y, Duc ACE, Rao S, Sun XL, Bilbee AN, Rhodes M, Li Q, Kappes DJ, Rhodes J & Wiest DL (2013) Control of hematopoietic stem cell emergence by antagonistic functions of ribosomal protein paralogs. *Dev. Cell* **24:** 411–425

Zhang Y, O'Leary MN, Peri S, Wang M, Zha J, Melov S, Kappes DJ, Feng Q, Rhodes J, Amieux PS, Morris DR, Kennedy BK & Wiest DL (2017) Ribosomal Proteins Rpl22 and Rpl22l1 Control Morphogenesis by Regulating Pre-mRNA Splicing. *Cell Rep.* **18:** 545–556